UNIVERSITY OF CALIFORNIA
RIVERSIDE

The Development of Transition Metal Silylene and Germylene Complexes for Small Molecule Activation

A Dissertation submitted in partial satisfaction
of the requirements for the degree of

Doctor of Philosophy

in

Chemistry

by

Marissa Christina Barrientos

September 2019

Dissertation Committee:

Dr. Hill Harman, Chairperson
Dr. Richard Hooley
Dr. Yadong Yin

The Dissertation of Marissa Christina Barrientos is approved:

Committee Chairperson

University of California, Riverside

Acknowledgments

I first and foremost would like to thank my advisor and mentor, Dr Hill Harman. I am forever grateful for the unique experience of being one of your first graduate students. I thank you for all your support and making me the chemist I am now.

I would also like to thank the members of my committee, Dr. Richard Hooley and Dr. Yadong Yin. Thank you for all your support and the discussions throughout my time. I would also like to thank the ACIF staff for all their help and support. Thank you to Dr. Dan Borchardt for all your help especially in setting up all those difficult silicon NMR experiments. I would also like to thank Dr. Fook Tham and Dr. Charlene Tsay for their skills and expertise in helping to mount crystals and solving XRD structures. I also want to thank Dr. Richard Kondrat and Dr. Ron New for their expertise in helping to obtain LIFDI results which were invaluable. Last, but certianly not least, I would like to thank Prisciliano Saavedra for all his help in supplying our lab and many solutions to lab issues.

I would also like to thank current and former lab members: Dr. Alex McSkimming, Jordan Taylor, Amy Bartrom-Jehl, Laura Essex, Colie Sanchez, Phil Farias, Pranee Pairs, and Andrew Patalano. I would also like to thank my undergraduates that I had the pleasure of mentoring, Daniel Barragan, Joe Mejia, and James Jimenez. I wish to thank members of the Conley group as well for all their support in our joint group meeting ventures.

Special thanks to my husband, Robert, for all his support and love through this process. I especially thank him for keeping me sane through this process.

Shout-out to my high school chemistry teacher, Mrs. Hamilton, for awakening my love for chemistry

Last, I give many thanks and gratitude to my parents for their never-ending love while I have pursued a PhD.

To my parents for all the support.

ABSTRACT OF THE DISSERTATION

The Development of Transition Metal Silylene and Germylene Complexes for Small Molecule Activation

by

Marissa Christina Barrientos

Doctor of Philosophy, Graduate Program in Chemistry
University of California, Riverside, September 2019
Dr. Hill Harman, Chairperson

While N-heterocyclic carbenes (NHC) are widely recognized for their utility as catalysts and ligands for catalysts, their heavier analogues, namely N-heterocyclic silylenes and germylenes have not been as extensively explored. These divalent group-14 compounds are intriguing as they have a more accessible empty p-orbital due to decreased overlap with the nitrogen centered lone pairs. This fact results in both nucleophilic and electrophilic character, or ambiphilicity, in silylenes and germylenes. We are interested in utilizing this property to design transition metal complexes of N-heterocyclic silylenes (NHSi) and germylenes (NHGe) Herein we report the synthesis of a several diphosphine pincer frameworks anchored by silicon and germanium atoms. In the case of the silicon-based ligands, dichlorosilane, hydrochlorosilane derivatives function as proligands whereas the germanium derivative is accessible as the free germylene. Metallation of the Si-anchored pincers with the Pt group metals (Ni, Pd, and Pt) proceeds by SiCl or SiH activation of the proligands to give divalent square planar complexes featuring a chlorosilyl anchoring ligand. Two-electron reduction of the Pd derivative affords a bimetallic dipalladium(0) disilylene species with inequivalent

metal sites that are in dynamic exchange in solution. This bimetallic disilylene activates the OH bonds of both water and phenol to give the corresponding disilyl dipalladium(I) species. In contrast to the analogous dinickel system explored in our lab, it does not react with H2. CO2 reacts with the disilylene species to give CO and a bridging disilylcarbonate complex. These results highlight the viability of cooperative small molecule activation at late-metal silylene complexes. We also report a large family of bimetallic complexes of first row metals (Mn, Fe, Co, and Ni) supported by the germylene-anchored pincer. Unlike the silicon-based ligands discussed above, which bind metals in a 1:1 ratio, the germylene ligand variant typically binds two metals. These bridging germylene complexes exhibit a range of metal-metal distances and electronic interactions resulting in both diamagnetic and paramagnetic complexes. Unlike the silicon anchored species, the bimetallic germylene complexes were generally electronically and/or coordinatively saturated, and thus typically unreactive.These results highlight the substantial differences in germylene and silylene ligand owing to the larger size of Ge versus Si.

Contents

List of Figures

List of Tables

List of Schemes

Chapter 1

Introduction

Since the discovery of stable N-heterocyclic carbenes (NHCs), a great deal of research has been devoted to exploring the properties of NHC's and other stable carbenes as ligands in transition metal catalysis.These ligands have been identified as exceptionally strong σ-donating L-type ligands and have found use in a range of important catalytic transformations including olefin metathesis and cross-coupling reactions, in addition to reactions catalyzed by NHC's under metal-free conditions[1]. The broad utility of these stable singlet carbenes suggests potential applications for analogues based on the heavier group 14 elements (i.e. NHE, where E = Si, Ge, Sn, etc.); however, these molecules possess substantially different properties than their carbene counterparts. This is due in part to the poor overlap between the 2p nitrogen lone pairs and the more diffuse np orbital (n > 2) on the group 14 center.[2][3] Whereas the lowest unoccupied molecular orbital of a diaminocarbene is highly destabilized by the nitrogen lone pairs, the less extensive π-bonding present in the heavier analogues results in a group 14 element that possesses significant ambiphilic char-

acter, acting as both an electrophile and a nucleophile.[4] As a result, the group 14 center is significantly more Lewis acidic than in analogous carbenes, a feature born out in some preliminary studies of metal-silylene reactivity.[5][6] Our aim is to exploit this feature to develop transition metal-silylene and -germylene complexes capable of cooperative activation of strong bonds across the metal-E interaction.

1.1 Carbenes

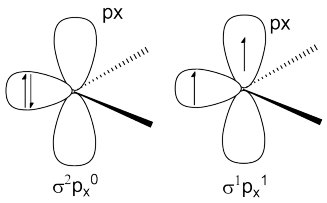

Figure 1.1: Singlet VS Triplet Carbene

Carbenes are defined as neutral compounds of divalent carbon with only six valence electrons. Carbenes are generally either in the triplet or singlet ground state. In the triplet state, one of the nonbonding electrons occupies the σ orbital and the other occupies the px orbital. In the singlet state, the two nonbonding electrons occupy the σ orbital (1.1). Since the singlet carbenes have an occupied σ orbital and empty p, they are more ambiphilic in nature than the triplet state, and are able to act as π acceptors giving rise to a linear geometry around the carbene.

The first isolated, stable carbene was in 1988 by Bertrand [7] quickly followed by the first N-heterocyclic carbene (NHC) in 1991[8].However the first carbene complex was

synthesized much earlier in 1925 by Tschugajeff, but the structure and its identity as a diaminocarbene platinum complex was not confirmed until 1970[9],[10]. Subsequently, there has been an explosion of research into this area with applications in a wide variety of areas from surface chemistry, catalytic applications such as olefin metathesis and cross-coupling, metallopharmeceuticals, and organometallic materials such as MOFs, liquid crystals, polymers, and photoactive materials.

What makes carbenes so versitile is their ability to be tuned both electronically and sterically. NHC's can be tuned though modifying the heterocyclic backbone and ring substituents. Carbenes can be tuned by modifying the HOMO-LUMO gap. The higher the HOMO energy of a ligand, the stronger σ donating it is, and conversely the lower the LUMO energy level is, the better π acceptor. NHC's futher increase this gap from the σ withdrawing and π donating effects of the nitrogen which increases the HOMO-LUMO gap resutling in the increased stability of NHC's[11],[12].

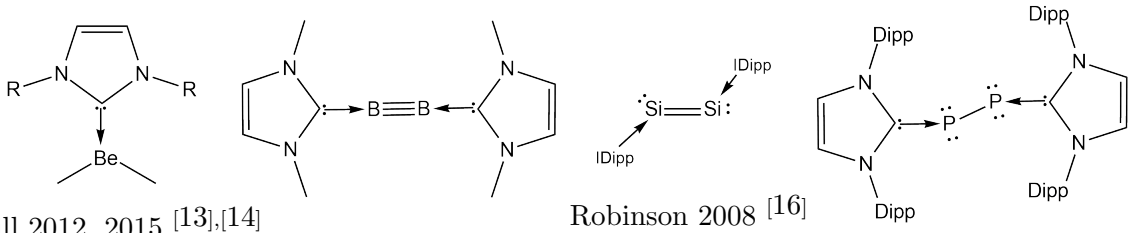

Hill 2012, 2015 [13],[14]

Braunschweig 2012 [15]

Robinson 2008 [16]

Robinson 2008 [17]

Figure 1.2: Examples of NHC's in Main Group Chemistry

The sigma donating ability of carbenes has made them good ligands for supporting low valent metal and main group compounds[18]. A very limited examples of NHC's

and main group chemistry are show in 1.2, but there are number more examples in the literature.[18]

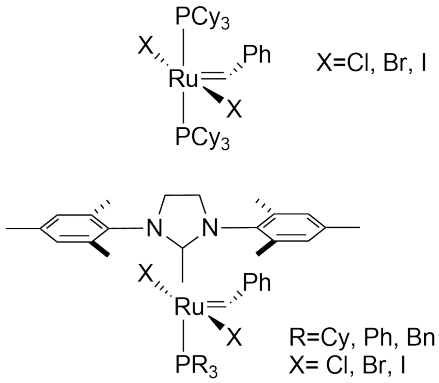

Figure 1.3: 1st and 2nd Generation Grubbs Catalysts

NHC's have also been widely explored in conjunction with metals. NHC's have been most predominately used with mid and late transition metals and with stability increasing with the heavier 5d metals due to better π bonding. The most infamous of these applications was the development of the Grubbs catalysts for olefin metathesis[19][20].

Interestingly, another class of carbenes, cyclic alkyl-amino carbenes (CAAC) which are carbenes with one nitrogen to support the carbene. This difference of a σ donating carbon and one nitrogen instead of two nitrogens causes for a smaller HOMO-LUMO gap compared to traditional NHC's. This smaller HOMO-LUMO gap leads to stronger σ donating and stronger π accepting qualities. This increase is seen in the ability of CAACs to activate H_2, CO, and NH_3. This leads us to silylenes, which also have a promise of increased reactivity due to their more ambiphilic nature.

1.2 Silylenes

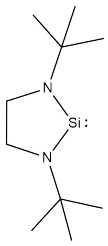

Figure 1.4: First Stable Silylene

The first stable silylene was isolated in 1994 by Denk et al[21] with 11 more isolable silylenes being reported in the subsequent 15 years. The first N-heterocyclic silylene transition metal complex was isolated in 1977 by Welz and Schmid [22].

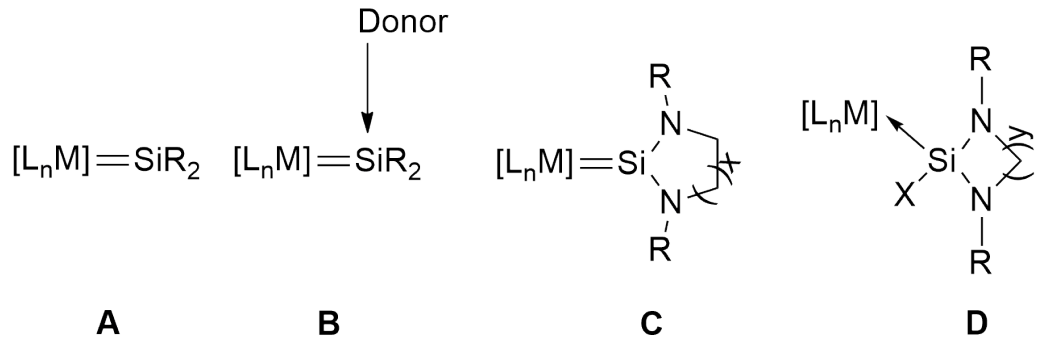

Figure 1.5: Four Types of Silylenes

There are four main types of silylene complexes. Type **A** compounds are analogues of Fischer or Schrock type carbenes (=SiR_2). Type **B** compounds are "base stabilized" silylenes. Type **C** compounds are NHSi complexes with unsaturated backboard or differing R groups. Type **D** compounds are more specifically NHSi halide or hydride complexes.

Silylenes have seen gained attention for their participation in various transformations of organosilicon compounds[23],[24],[25],[26] from the shuffling of subsituents on silcion[27], dehydrogenative coupling of hydrosilanes[28], and silicon based catalysts for polymerization.[29],[30],[31]. The first catalytic transformation by a silylene-metal catalyst, which was effective in Suzuki cross-coupling reactions, was in 2001 by Fürstner[32].

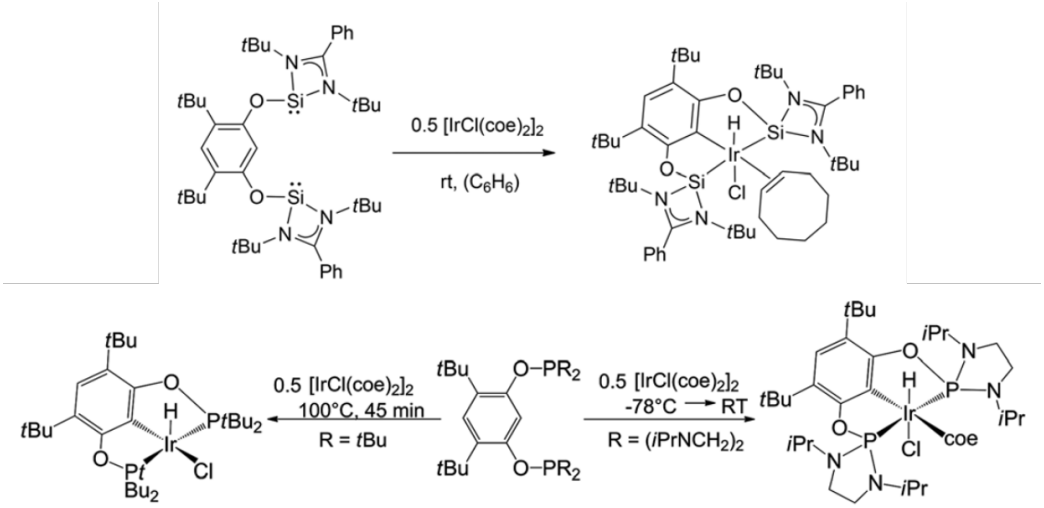

Figure 1.6: Demonstration of Si and Ge tuning Ability for C-H Borylation of Arenes

As show in Figure 1.6, Driess and co-workers [33] synthesized an iridum silylene catalyst along with the germylene analog and explored its catalyst ability for C-H borylation of arenes using pinacolborane. To explore how substantial the effects of the strong sigma donation of the silylenes and germylenes, they compared the catalytic activity to the phosphine version of the catalyst. The phosphines, while being isoelectronic to silylenes and germylenes, did not exhibit the same catalytic activity. Subsequently, the nickel version of the catalyst was synthesized, and was found to be successful as a Sonogashira cross-coupling

reaction[34].

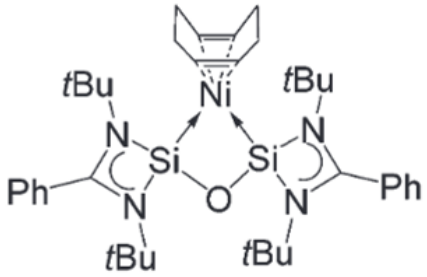

Figure 1.7: Nickel pre-catalyst for C-C cross-coupling reactions

As much interest lies in developing first row transition metal based catalysts, Inoue and coworkers developed a bis-NHSi pre-catalyst for C-C cross coupling reactions[35]. These examples demonstrate that NHSi ligands are different from NHC's; not simply isoelectronic replacements. NHSi ligands can be tuned to influence the metal center and act as a strong σ donor. We seek to continue the research to better understand the full potential of N-heterocyclic silylenes in catalysis and continue exploring first row silylene and germylene metal complexes.

Bibliography

[1] Herrmann, W. A.; Köcher, C. *Angewandte Chemie International Edition in English* **1997**,

[2] Arduengo, A. J.; Dixon, D. A.; Jones, N. L.; Bock, H.; Chen, H.; Denk, M.; West, R.; Green, J. C.; Wagner, M.; Herrmann, W. A. *Journal of the American Chemical Society* **1994**,

[3] Boehme, C.; Frenking, G. *Journal of the American Chemical Society* **1996**,

[4] Asay, M.; Jones, C.; Driess, M. *Chemical Reviews* **2011**,

[5] Petri, S. H. A.; Neumann, B.; Stammler, H.-g.; Jutzi, P.; Molybdans, S.-k.; Synthese, W. *Journal of Organometallic Chemistry* **1998**,

[6] Avent, A. G.; Gehrhus, B.; Hitchcock, P. B.; Lappert, M. F.; Maciejewski, H. *Journal of Organometallic Chemistry* **2003**,

[7] Igau, A.; Grutzmacher, H.; Baceiredo, A.; Bertrand, G. *Journal of the American Chemical Society* **1988**, *110*, 6463–6466.

[8] Arduengo, A. J.; Harlow, R. L.; Kline, M. *Journal of the American Chemical Society* **1991**, *113*, 361–363.

[9] Tschugajeff, L.; Skanawy-Grigorjewa, M.; Posnjak, A.; Skanawy-Grigorjewa, M. *Zeitschrift fr anorganische und allgemeine Chemie* **1925**, *148*, 37–42.

[10] Butler, W. M.; Enemark, J. H.; Parks, J.; Balch, A. L. *Inorganic Chemistry* **1973**, *12*, 451–457.

[11] Hahn, F. E. *Chemical Reviews* **2018**, *118*, 9455–9456.

[12] Huynh, H. V. *Chemical Reviews* **2018**, *118*, 9457–9492, PMID: 29601194.

[13] Arrowsmith, M.; Hill, M. S.; Kociok-Khn, G. *Organometallics* **2015**, *34*, 653–662.

[14] Arrowsmith, M.; Hill, M. S.; Kociok-Khn, G.; MacDougall, D. J.; Mahon, M. F. *Angewandte Chemie International Edition 51*, 2098–2100.

[15] Braunschweig, H.; Dewhurst, R. D.; Hammond, K.; Mies, J.; Radacki, K.; Vargas, A. *Science* **2012**, *336*, 1420–1422.

[16] Wang, Y.; Xie, Y.; Wei, P.; King, R. B.; Schaefer, H. F.; von R. Schleyer, P.; Robinson, G. H. *Science* **2008**, *321*, 1069–1071.

[17] Wang, Y.; Xie, Y.; Wei, P.; King, R. B.; Schaefer, H. F.; Schleyer, P. v. R.; Robinson, G. H. *Journal of the American Chemical Society* **2008**, *130*, 14970–14971, PMID: 18937460.

[18] Nesterov, V.; Reiter, D.; Bag, P.; Frisch, P.; Holzner, R.; Porzelt, A.; Inoue, S. *Chemical Reviews* **2018**, *118*, 9678–9842, PMID: 29969239.

[19] Wu, Z.; Nguyen, S. T.; Grubbs, R. H.; Ziller, J. W. *Journal of the American Chemical Society* **1995**, *117*, 5503–5511.

[20] Sanford, M. S.; Love, J. A.; Grubbs, R. H. *Journal of the American Chemical Society* **2001**, *123*, 6543–6554, PMID: 11439041.

[21] Denk, M.; Lennon, R.; Hayashi, R.; West, R.; Belyakov, A. V.; Verne, H. P.; Haaland, A.; Wagner, M.; Metzler, N. *Journal of the American Chemical Society* **1994**, *116*, 2691–2692.

[22] Schmid, G.; Welz, E. *Angewandte Chemie International Edition in English 16*, 785–786.

[23] Larson, G. *Advances in Silicon Chemistry*; Advances in Silicon Chemistry v. 2; JAI Press, 1993.

[24] Curtis, M.; Epstein, P. S. In *Redistribution Reactions on Silicon Catalyzed by Transition Metal Complexes*; Stone, F., West, R., Eds.; Advances in Organometallic Chemistry; Academic Press, 1981; Vol. 19; pp 213 – 255.

[25] Palmer, W. S.; Woerpel, K. A. *Organometallics* **1997**, *16*, 4824–4827.

[26] Ojima, I.; Inaba, S.-I.; Kogure, T.; Nagai, Y. *Journal of Organometallic Chemistry* **1973**, *55*, C7 – C8.

[27] Yamashita, H.; Tanaka, M.; Goto, M. *Organometallics* **1992**, *11*, 3227–3232.

[28] Alcaraz, G.; Sabo-Etienne, S. *Coordination Chemistry Reviews* **2008**, *252*, 2395 – 2409, Applications of NMR to Inorganic and Organometallic Chemistry.

[29] Tilley, T. D. *Accounts of Chemical Research* **1993**, *26*, 22–29.

[30] Okamoto, M.; Onodera, S.; Okano, T.; Suzuki, E.; Ono, Y. *Journal of Organometallic Chemistry* **1997**, *531*, 67 – 71.

[31] Clarke, M. P.; Davidson, I. M. *Journal of Organometallic Chemistry* **1991**, *408*, 149 – 156.

[32] Frstner, A.; Krause, H.; Lehmann, C. W. *Chem. Commun.* **2001**, 2372–2373.

[33] Brck, A.; Gallego, D.; Wang, W.; Irran, E.; Driess, M.; Hartwig, J. F. *Angewandte Chemie International Edition 51*, 11478–11482.

[34] Gallego, D.; Brck, A.; Irran, E.; Meier, F.; Kaupp, M.; Driess, M.; Hartwig, J. F. *Journal of the American Chemical Society* **2013**, *135*, 15617–15626, PMID: 24053603.

[35] Someya, C. I.; Haberberger, M.; Wang, W.; Enthaler, S.; Inoue, S. *Chemistry Letters* **2013**, *42*, 286–288.

Chapter 2

Synthesis of Bidentate Phosphine Ligands

2.1 Abstract

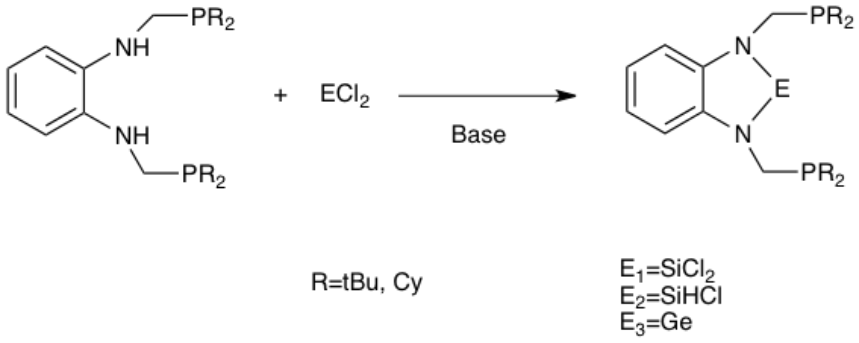

Scheme 2.1: Synthesis of Ligand Precursor

Here we report the synthesis of a family of group 14 PGeP and PSiP N-heterocyclic compounds. The phosphine pincer scaffold has proven successful in its ability to act as a

strong sigma donor to stabilize low valent metal sources. We also report attempts to isolate the free silylene ligand which we were unable to isolate in our hands. We did successfully synthesize the free germylene ligand.

2.2 Introduction

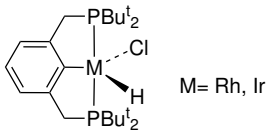

Jensen 1996 [1]

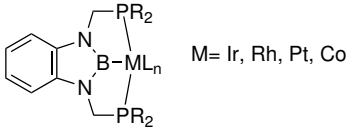

Yamashita 2014 [2]

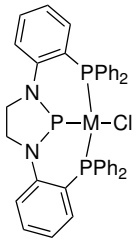

Thomas 2013 [3]

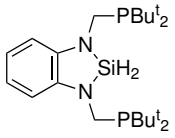

Whited 2014 [4]

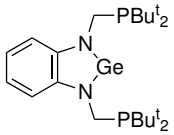

Polo 2017 [5]

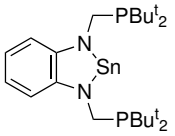

Polo 2018 [6]

Figure 2.1: Phosphine Pincer Ligands

While carbenes are ubiquitous in chemical transformations, the heavier group 14 analogs of silicon and germanium are relatively unexplored. There exists much precedence for the synthesis of various PEP and PEP N heterocyclic ligand frameworks with carbon, boron[7], and phosphorous. Furthermore, these N-heterocyclic frameworks are key to supporting carbenes and silylenes due to stabilization from π donation from the nitrogens to the central atom.[8] After we began our work, the silicon, germanium, and tin versions were

later synthesized by other groups[9]. We utilized a bidentate phosphine ligand to support various potential catalytic transformations once the ligand was bound to a metal. While attempts to synthesize the free silylene were unsuccessful, we created a novel germylene PGeP N-heterocyclic ligand framework. We also explored various silane ligand derivatives in an attempt to access a silylene metal complex.

2.3 Results and Discussion

The initial inspiration for the synthesis of a bidentate phosphine silane was derived from the diphenylphosphino and dicyclohexylphosphino boryl pincer (PBP) ligands by Nozaki[10]. However, soon after the synthesis of a dihydrosilyl ligand was reported by Whited[4] and later the dichloro and hydrochloro silyl and germylene pincer ligands were reported by Polo[11][6]. The initial base ligand $(NHCH_2P^tBu_2)_2C_6H_4$ was synthesized according to the Nozaki prep which involved the condensation of o-phenylenediamine, paraformaldehyde, and the desired phosphine. We synthesized both the ditertbutyl phos-

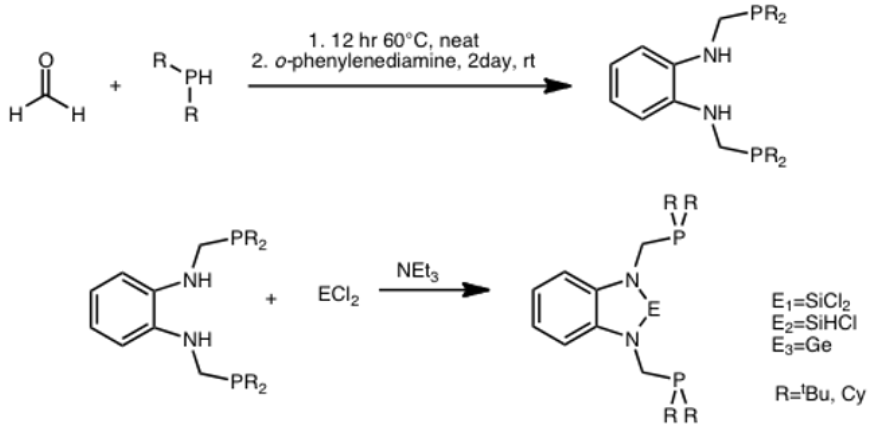

Scheme 2.2: Detailed Synthesis of Ligand Precursor

phine and dicyclohexylphosphine derivatives. While we initially synthesized the silyl derivatives using n-butyl lithium to deprotonate the bis(phosphine) diamine we later found triethylamine to be a sufficient base to mediate the insertion of the appropriate silicon or germanium electrophile. These findings are also in agreement with the aforementioned reports on this family of bidentate phosphine ligands.

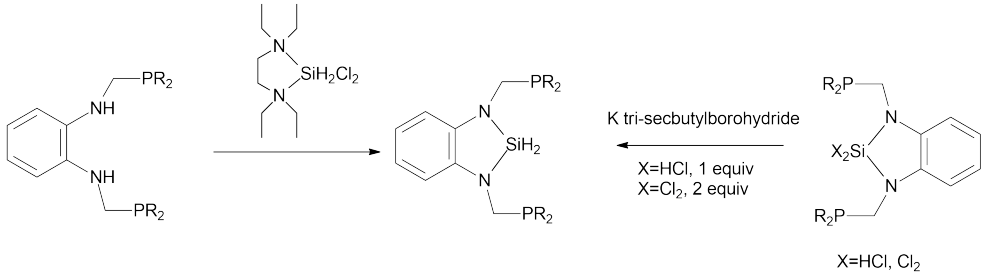

Scheme 2.3: Routes to **3**

The general synthetic approach for the targeted ligand class is outlined in 2.2. The diaminodichlorosilane $Cl_2Si(NCH_2PtBu_2)_2C_6H_4$ **1** was prepared in good yields (90%) via the addition of $SiCl_4$ to $(NHCH_2PtBu_2)_2C_6H_4$ in the presence of NEt_3 and was characterized by ^1H, ^{31}P and ^{29}Si NMR spectroscopy (^{31}P ^1H: δ 14.44; ^{29}Si: δ -27.8). and liquid injection field desorption ionization mass spectrometry (LIFDIMS). The related hydrochlorosilane **2** was prepared in analogous fashion using trichlorosilane (^{31}P $\{^1H\}$: δ 18.1 ppm, ^{29}Si: δ29.3 ppm). Dihydrosilane analogue **3** can be prepared by two different methods: 1) the reaction of 1 or 2 equivalents of K[HB(sec-butyl)$_3$] with **2** or **1**, respectively or 2) the reaction of $(NCH_2PtBu_2)_2C_6H_4$ with TEEDA(SiH_2Cl_2).

We pursued the synthesis of the free silylene in parallel as a more direct and general route to metal silylene complexes of these ligands. The free silylene has proven

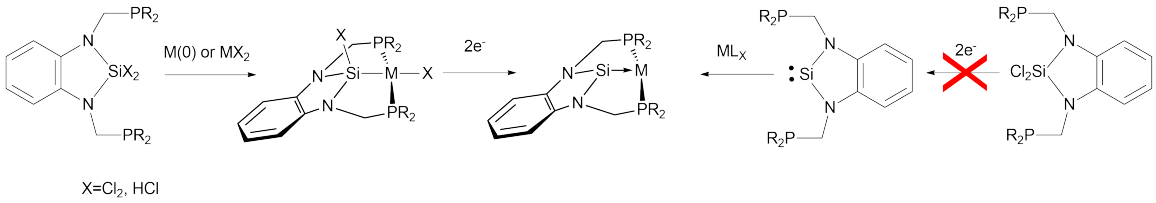

Figure 2.2: Potential Routes to a Metal Silylene Complex

challenging to isolate as reduction of either **1** and **2** using a number of conditions and reducing agents (Na, K, KC_8, etc) afforded complicated mixtures of products. As an alternative to the free silylene, we turned our attention to the germanium analogue, which, owing to the increased stability of the heavier group 14 elements in low oxidation states, could prove more synthetically tractable. The availability of a stable Ge(II) source, $GeCl_2$-dioxane, facilitated the successful synthesis of germylenes **4** ($Ge(NCH_2PC(CH_3)_3)_2C_6H_4$) and **5** ($Ge(NCH_2PCy_2)_2C_6H_4$) via NEt_3 promoted metallation of $(NHCH_2PC(CH_3)_3)_2C_6H_4$ or $(NHCH_2P(Cy)_2)_2C_6H_4$. These compounds were characterized by LIFDIMS and NMR spectroscopy and display peaks in ^{31}P NMR spectrum at δ 26.7 ppm and δ 8.10 ppm respectively. Crystals of **4** for X-ray diffraction were grown from a concentrated cold pentane solution of the complex. The Ge–N bond length is 1.883 $\mathring{A}$, roughly average for Ge–N complexes (G–N: 1.726 3.182 $\mathring{A}$).

2.4 Experimental Section

2.4.1 Synthetic Materials and Methods

Unless started otherwise, all compounds were purchased from commercial sources and used without further purification. Solvents were dried and deoxygenated by argon

sparge followed by passage through an activated alumina column and were stored over $4\mathring{A}$ molecular sieves. All manipulations were performed under an N_2 atmosphere either in a glovebox or using standard Schlenk techniques. NMR spectra were recorded at 298K using a Varian 300 MHz, 500 MHz, or Bruker 600 MHz instruments. Chemical shifts in ^{1}H NMR are referenced to deuterated solvent. Chemical shifts in ^{31}P NMR are referenced to phosphoric acid. Mass spectra were recorded using either an Agilent LCTOF mass spectrometer or a Waters GCT high-resolution mass spectrometer operating in LIFDI mode. Elemental analysis was performed by Midwest Microlab, LLC; Indianapolis, IN.

2.4.2 $\mathbf{Cl_2Si(NCH_2P^tBu_2)_2C_6H_4}$ (1)

Triethylamine was added to a stirred solution of $(NHCH_2P^tBu_2)_2C_6H_4$ in THF. To this mixture, freshly distilled silicon tetrachloride was added dropwise with stirring. Gas evolution was immediately observed. After 12 hours, the volatiles were removed in vacuo. The resulting solid was then dissolved in ether, filtered through celite and the filtrate pumped down to dryness. Recrystallization from hexanes/THF gave **1** as a white crystalline solid. Yield (90%)

^{1}H (300 MHz, C_6D_6): δ 6.95 (s, 4H), 3.50 (s, 4H), 1.09 (d, J=15 Hz, 36 H)

^{31}P: δ 14.44

^{29}Si: δ -27.8

2.4.3 $\mathbf{HClSi(NCH_2P^tBu_2)_2C_6H_4}$ (2)

Triethylamine was added to a stirred solution of $(NHCH_2P^tBu_2)_2C_6H_4$ in THF. To this mixture, freshly distilled trichlorosilane was added dropwise with stirring. Gas evolution

was immediately observed. After 12 hours, the volatiles were removed in vacuo. The resulting solid was then dissolved in ether, filtered through celite and the filtrate pumped down to dryness. Recrystallization from hexanes/THF gave **2** as a white crystalline solid. Yield (83%)

^{1}H (300 MHz, C_6D_6): δ 7.45 (t,J=12 Hz, 1H), 7.13 (dd, J=3, 6 Hz, 2H), 6.95 (dd, J=3,6 Hz, 2H), 3.69 (dd, J=3,15 Hz, 2H), 3.45 (dd, J=3,15 Hz, 2H), 1.18 (d, J=15 Hz, 36H)

^{31}P: δ 18.1

^{29}Si: δ 29.3

2.4.4 $H_2Si(NCH_2P^tBu_2)_2C_6H_4$(3)

This compound can be prepared by two general methods.

Method A: One or two equivalents of a 1.0 M solution of K[HB(sec-butyl)$_3$] in THF was added to a dissolved solution of **2** or **1** respectively in THF. After 12 hours, the volatiles were removed in vacuo and the resulting solid was redissolved in ether and filtered through celite and pumped down to dryness.

Method B: A solution of TEEDA(SiH_2Cl_2) in THF was added to a stirred solution of $(NHCH_2P^tBu_2)_2C_6H_4$ in THF.After 12 hours, the volatiles were removed in vacuo and the resulting solid was redissolved in ether and filtered through celite and pumped down to dryness. Yield (78%)

^{1}H (300 MHz, C_6D_6): δ 6.97 (dd, J=3, 6 Hz, 2H), 6.65 (dd, J=3,6 Hz, 2H), 6.56 (t,J=6 Hz, 1H), 3.28 (s, 4H), 1.04 (d, J=9 Hz, 36H)

^{31}P: δ 26.1

2.4.5 $Ge(NCH_2P^tBu_2)_2C_6H_4$ (4)

Triethylamine was added to a stirred solution of $(NHCH_2P^tBu_2)_2C_6H_4$ in THF. To this mixture, germanium chloride dioxane in a solution of THF was added dropwise with stirring. An immediate color change to orange was observed. After 12 hours, the volatiles were removed in vacuo. The resulting solid was then dissolved in ether, filtered through celite and the filtrate pumped down to dryness. Recrystallization from hexanes/THF gave **4** as a white crystalline solid. Yield (68%)

^{1}H (300 MHz, C_6D_6): δ 7.33 (dd, J=3, 6 Hz, 2H), 7.24 (dd, J=3,6 Hz, 2H), 4.12 (s, 4H), 1.08 (d, J=12 Hz, 36H)

^{31}P: δ 26.7

2.4.6 $Ge(NCH_2PCy_2)_2C_6H_4$(5)

Triethylamine was added to a stirred solution of $(NHCH_2PCy_2)_2C_6H_4$ in THF. To this mixture, germanium chloride dioxane in a solution of THF was added dropwise with stirring. An immediate color change to orange was observed. After 12 hours, the volatiles were removed in vacuo. The resulting solid was then dissolved in ether, filtered through celite and the filtrate pumped down to dryness. Recrystallization from hexanes/THF gave **5** as a pale yellow crystalline solid. Yield (56%)

^{1}HNMR:(600 MHz, C_6D_6)δ 7.36 (d, J=4.5Hz, 2H), 7.22 (d, J=4.8Hz, 2H), 4.13 (s, 4H), 1.84 (d, J=12.9 Hz, 4H), 1.73 (d, J=13.3Hz, 4H), 1.69-1.52 (m, 17H), 1.39-0.98 (m, 23H).

^{31}PNMR: δ8.10

2.5 References

Bibliography

[1] Gupta, M.; Hagen, C.; Flesher, R. J.; Kaska, W. C.; Jensen, C. M. *Chem. Commun.* **1996**, 2083–2084.

[2] Miyada, T.; Huang Kwan, E.; Yamashita, M. *Organometallics* **2014**, *33*, 6760–6770.

[3] Pan, B.; Evers-McGregor, D. A.; Bezpalko, M. W.; Foxman, B. M.; Thomas, C. M. *Inorganic Chemistry* **2013**, *52*, 9583–9589, PMID: 23923983.

[4] Whited, M. T.; Deetz, A. M.; Boerma, J. W.; Derosha, D. E.; Janzen, D. E. *Organometallics* **2014**, *33*, 5070–5073.

[5] lvarez Rodrguez, L.; Brugos, J.; Cabeza, J. A.; Garca-lvarez, P.; Prez-Carreo, E.; Polo, D. *Chem. Commun.* **2017**, *53*, 893–896.

[6] Brugos, J.; Cabeza, J. A.; Garca-lvarez, P.; Prez-Carreo, E.; Polo, D. *Dalton Trans.* **2018**, *47*, 4534–4544.

[7] Lin, T.-P.; Peters, J. C. *Journal of the American Chemical Society* **2013**, *135*, 15310–15313, PMID: 24079337.

[8] Hopkinson, M. N.; Richter, C.; Schedler, M.; Glorius, F. *Nature* **2014**, *510*, 485–496.

[9] Dixon, L. S. H.; Hill, A. F.; Sinha, A.; Ward, J. S. *Organometallics* **2014**, *33*, 653–658.

[10] Segawa, Y.; Yamashita, M.; Nozaki, K. *Organometallics* **2009**, *28*, 6234–6242.

[11] Álvarez-Rodríguez, L.; Brugos, J.; Cabeza, J. A.; García-Álvarez, P.; Pérez-Carreño, E.; Polo, D. *Chem. Commun.* **2017**,

2.6 Figures, Schemes, and Tables

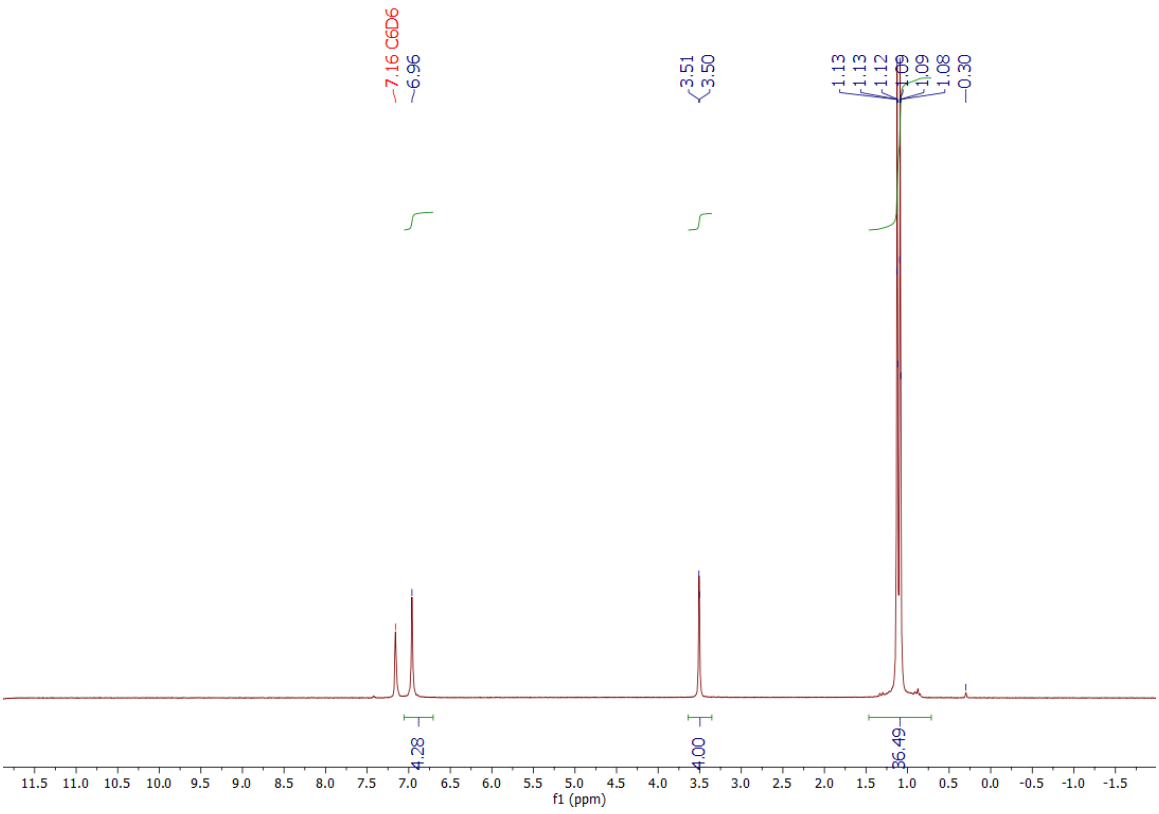

Figure 2.3: ^{1}HNMR of **1** in C_6D_6, 300MHz

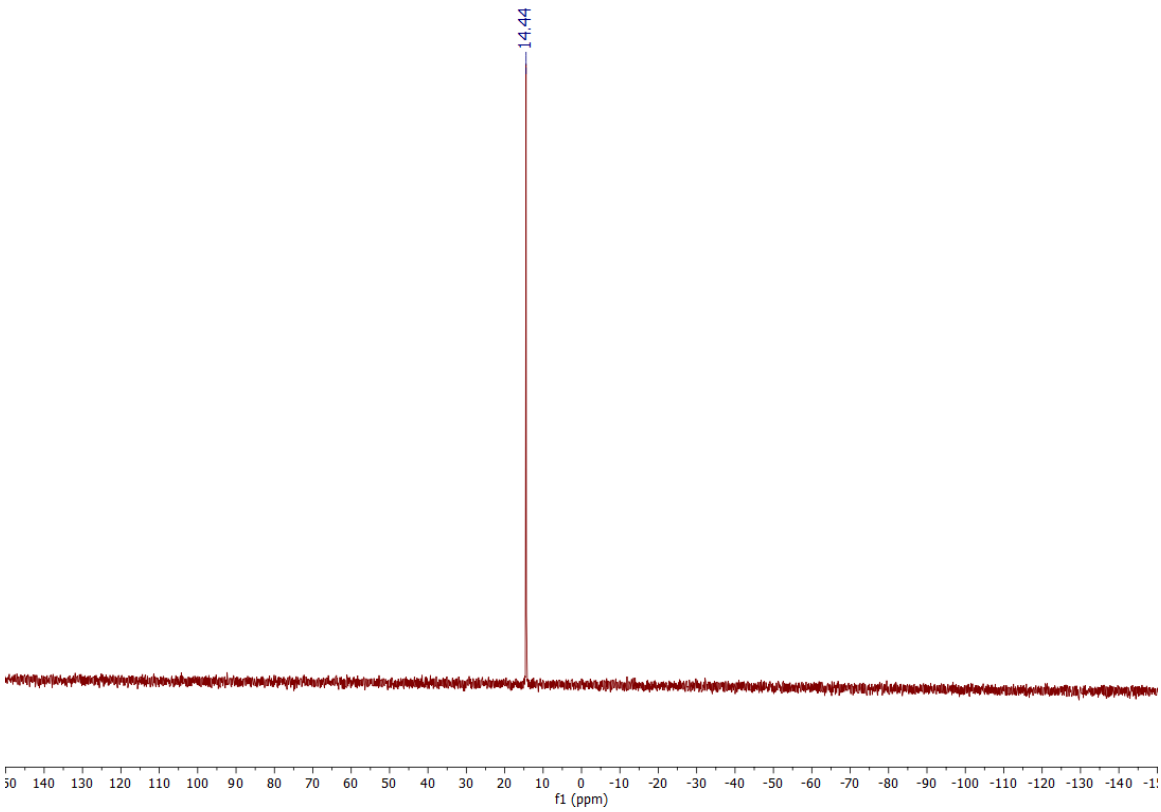

Figure 2.4: ^{31}PNMR of **1** in C_6D_6, 300MHz

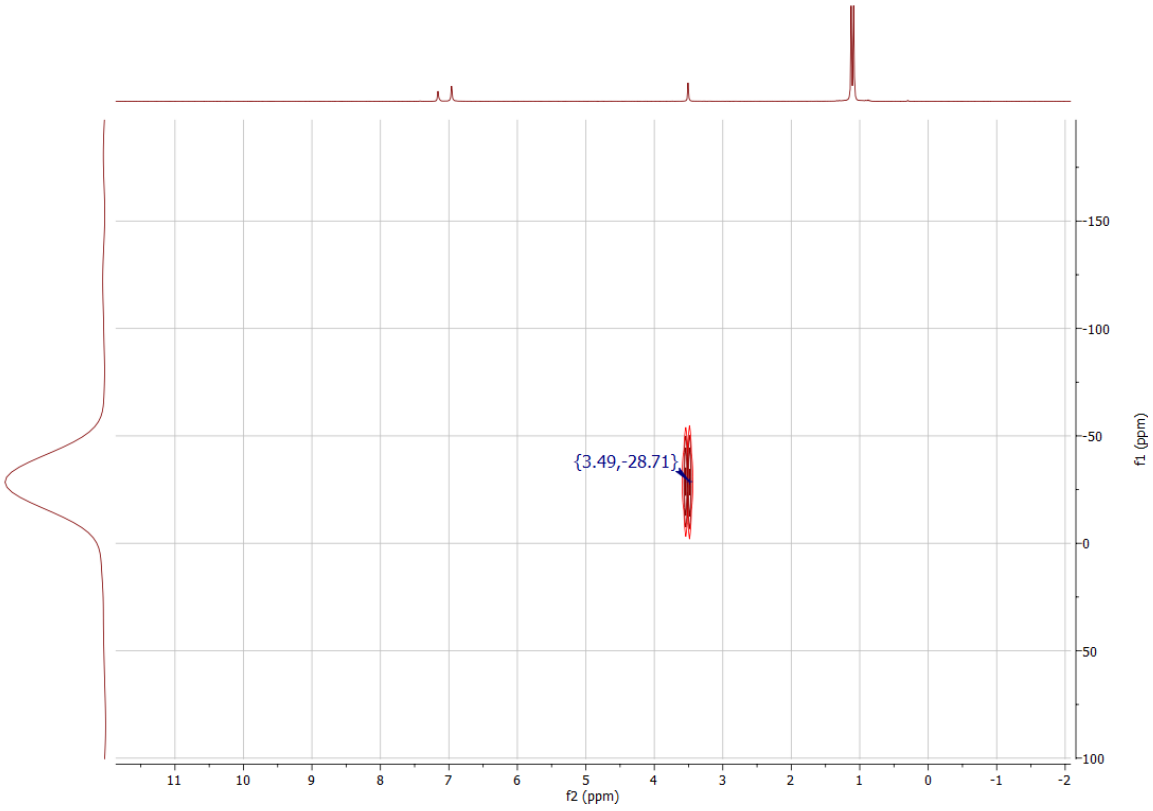

Figure 2.5: ^{29}Si{H} HSQC NMR of **1** in C_6D_6, 300MHz

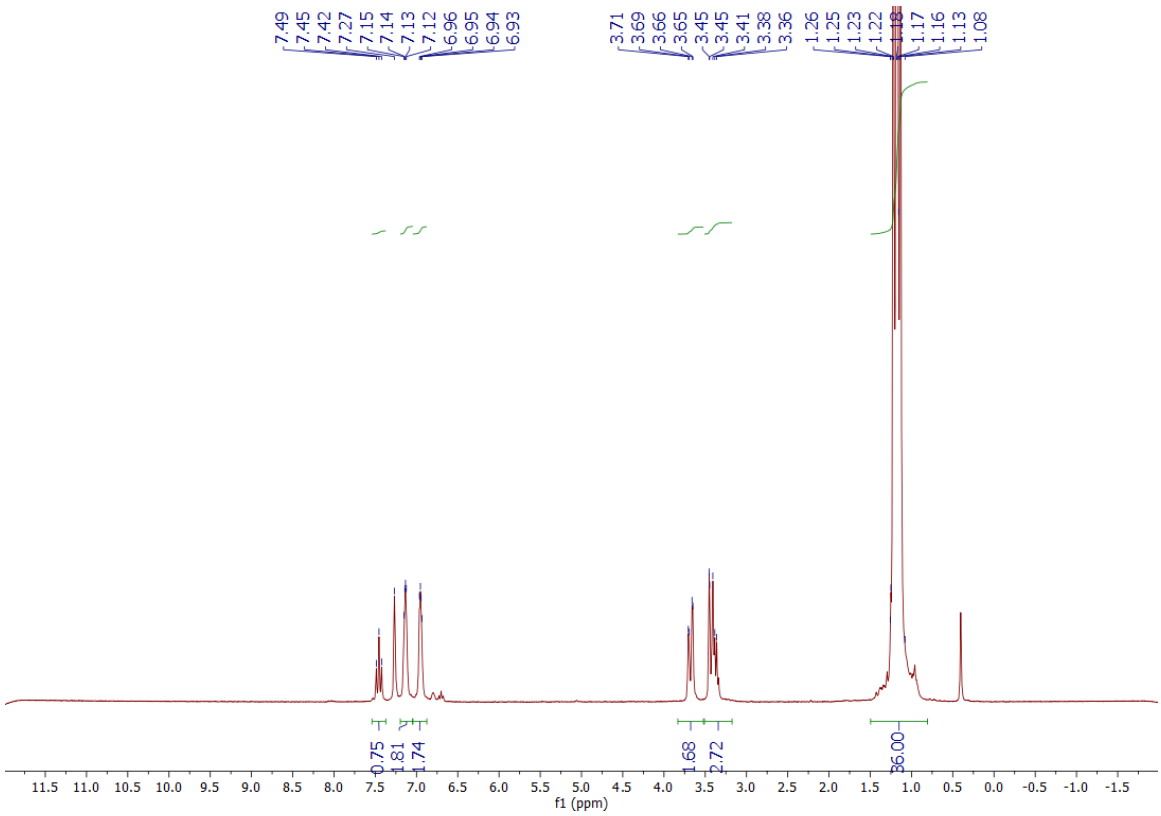

Figure 2.6: ^{1}HNMR of **2** in C_6D_6, 300MHz

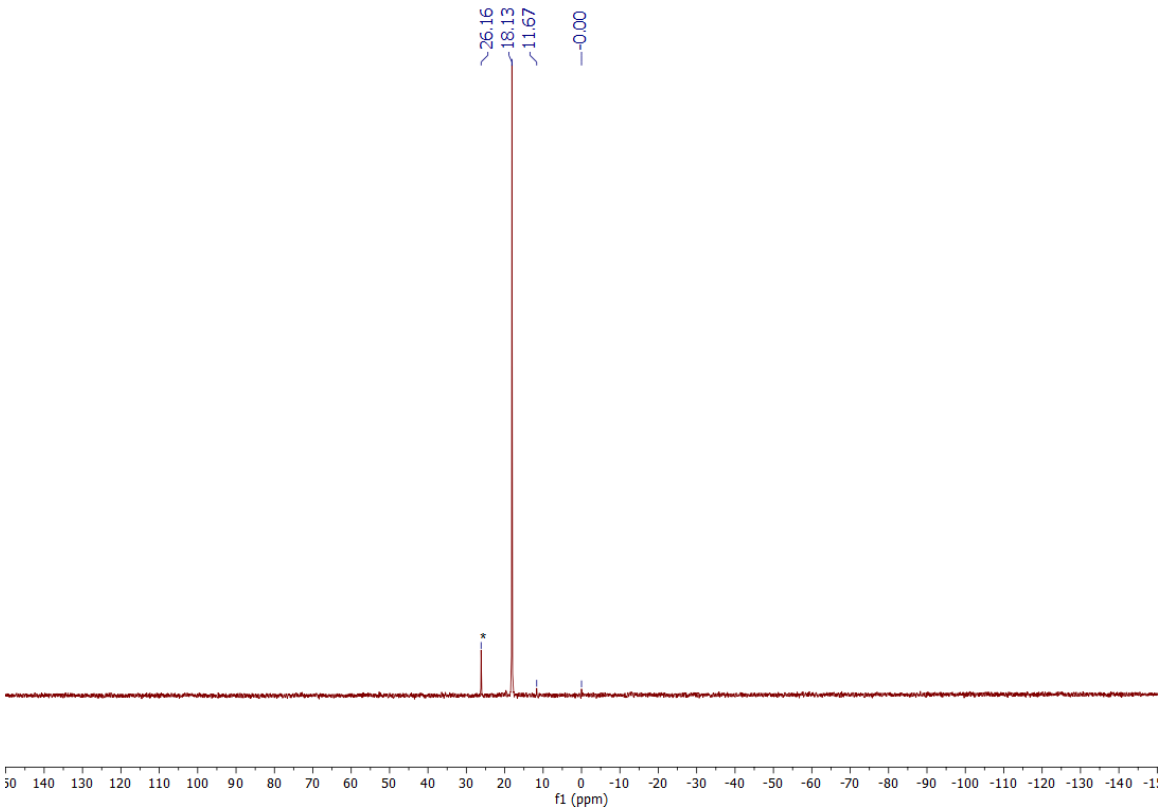

Figure 2.7: ^{31}PNMR of **2** in C_6D_6, 300MHz

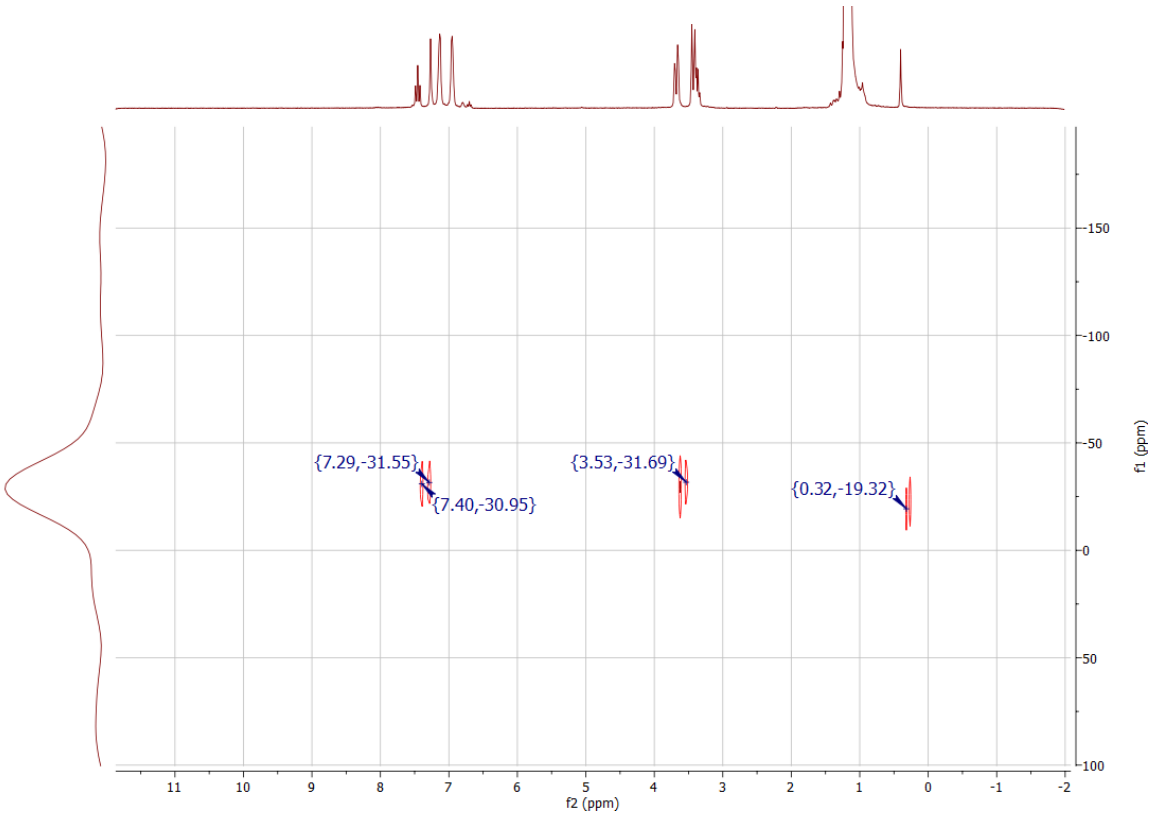

Figure 2.8: ^{29}Si{H} HSQC NMR of **2** in C_6D_6, 300MHz

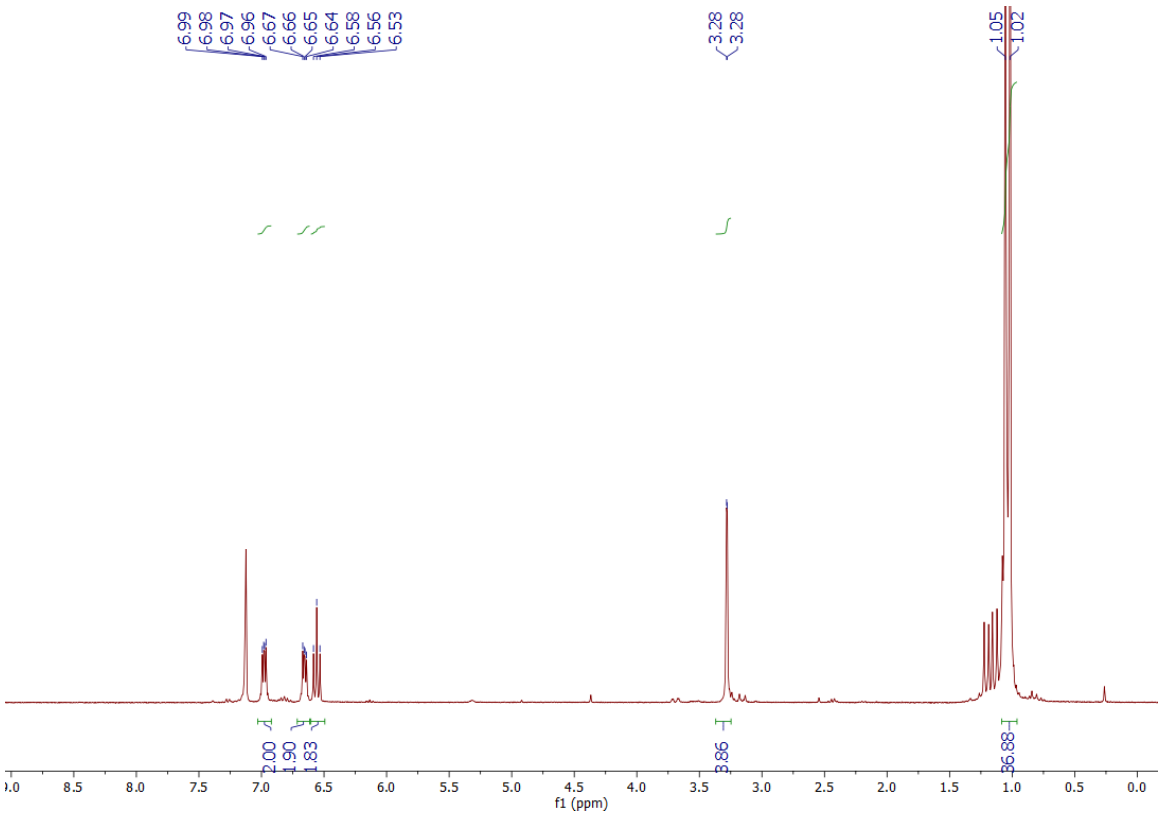

Figure 2.9: ^{1}HNMR of **3** in C_6D_6, 300MHz

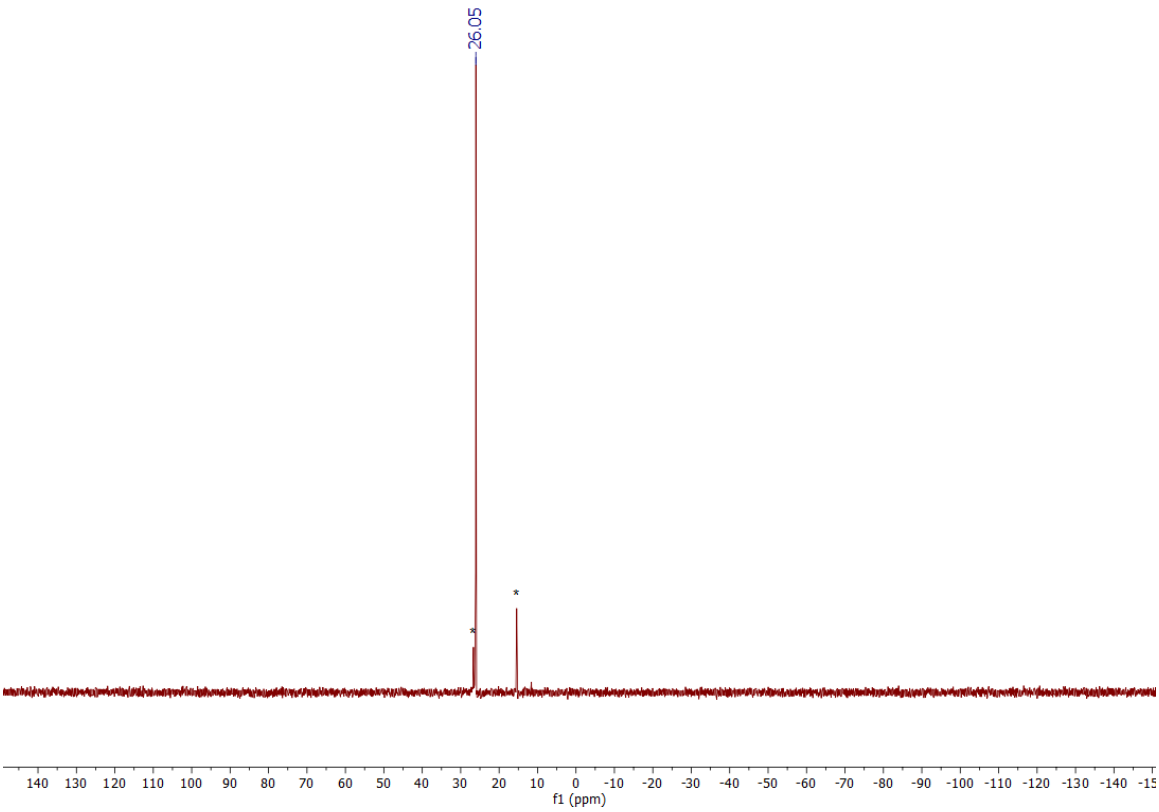

Figure 2.10: ^{31}PNMR of **3** in C_6D_6, 300MHz

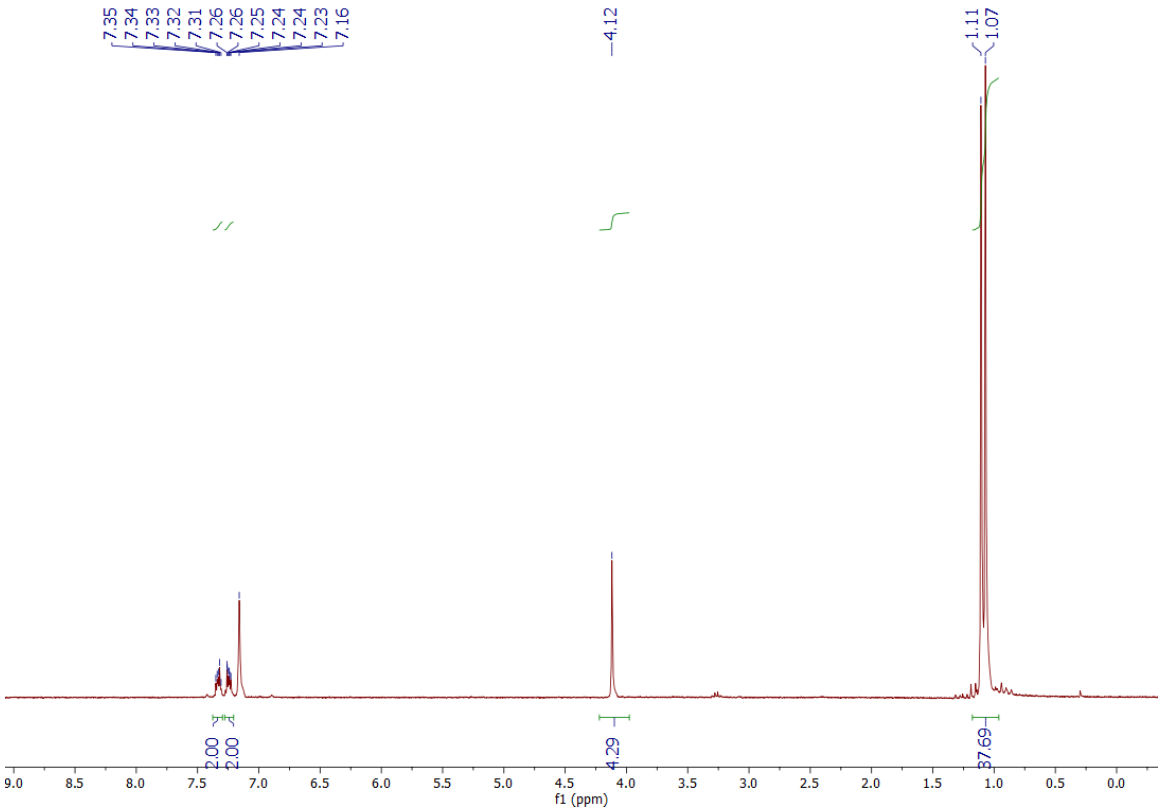

Figure 2.11: ^{1}HNMR of **4** in C_6D_6, 300MHz

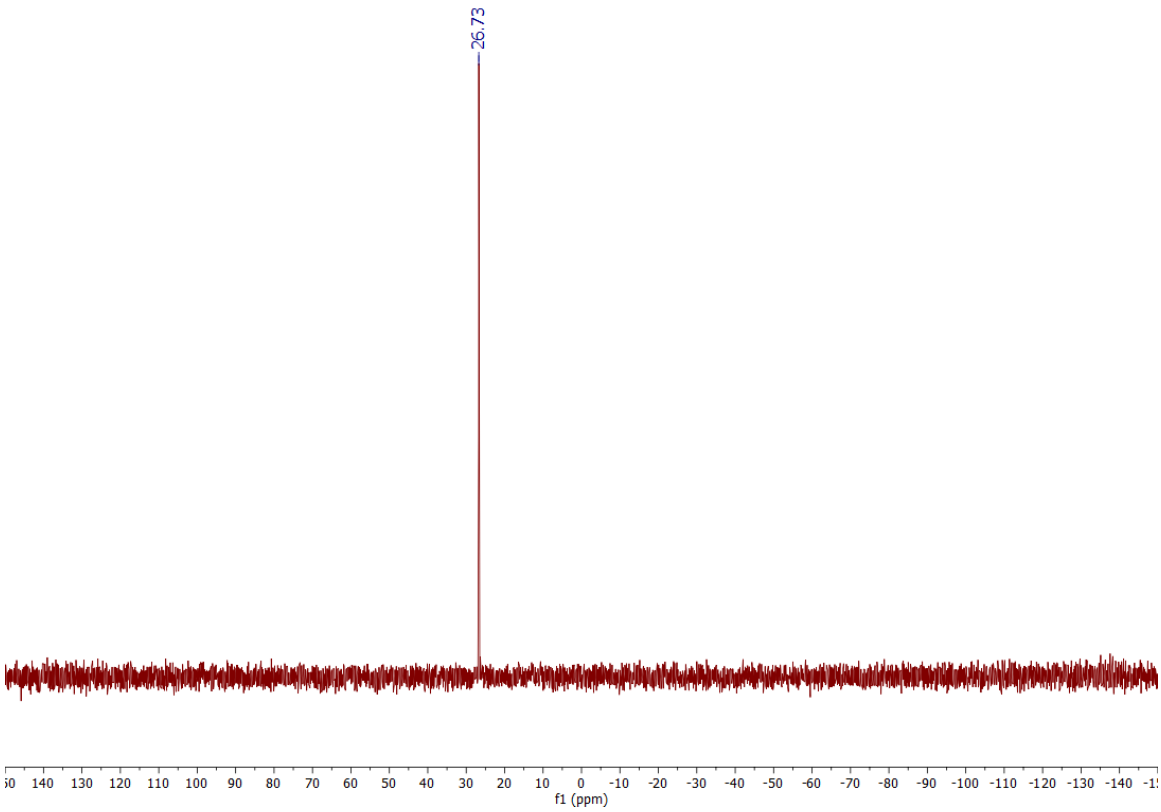

Figure 2.12: ^{31}PNMR of **4** in C_6D_6, 300MHz

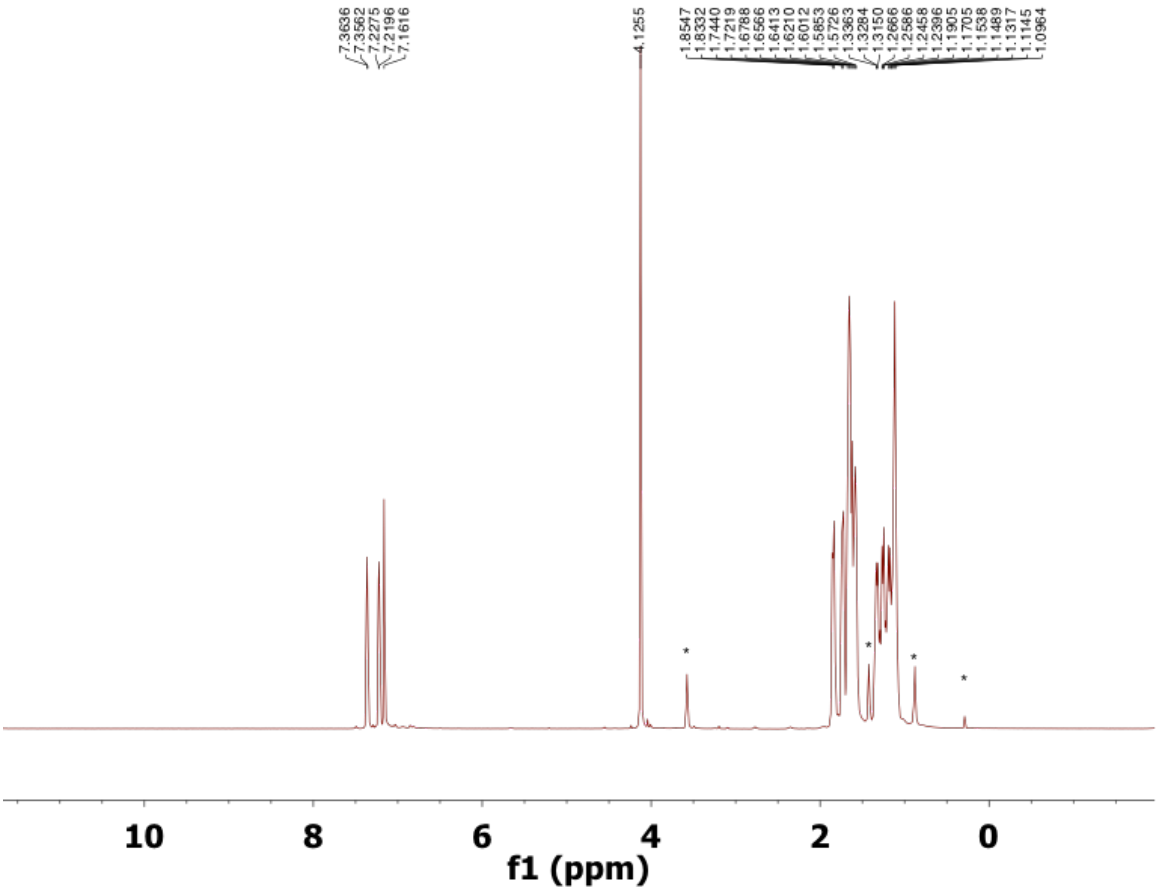

Figure 2.13: ^{1}HNMR of **5** in C_6D_6, 600MHz

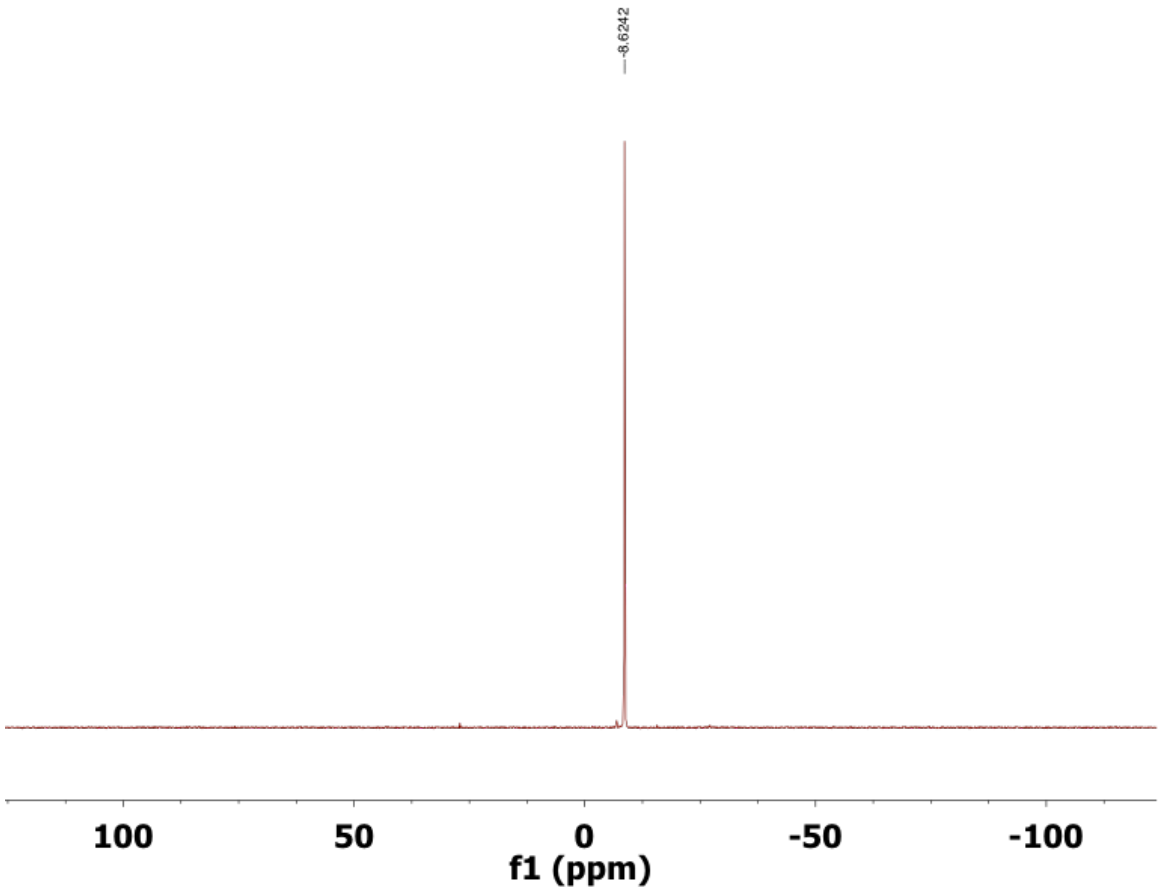

Figure 2.14: ^{31}PNMR of **5** in C_6D_6, 600MHz

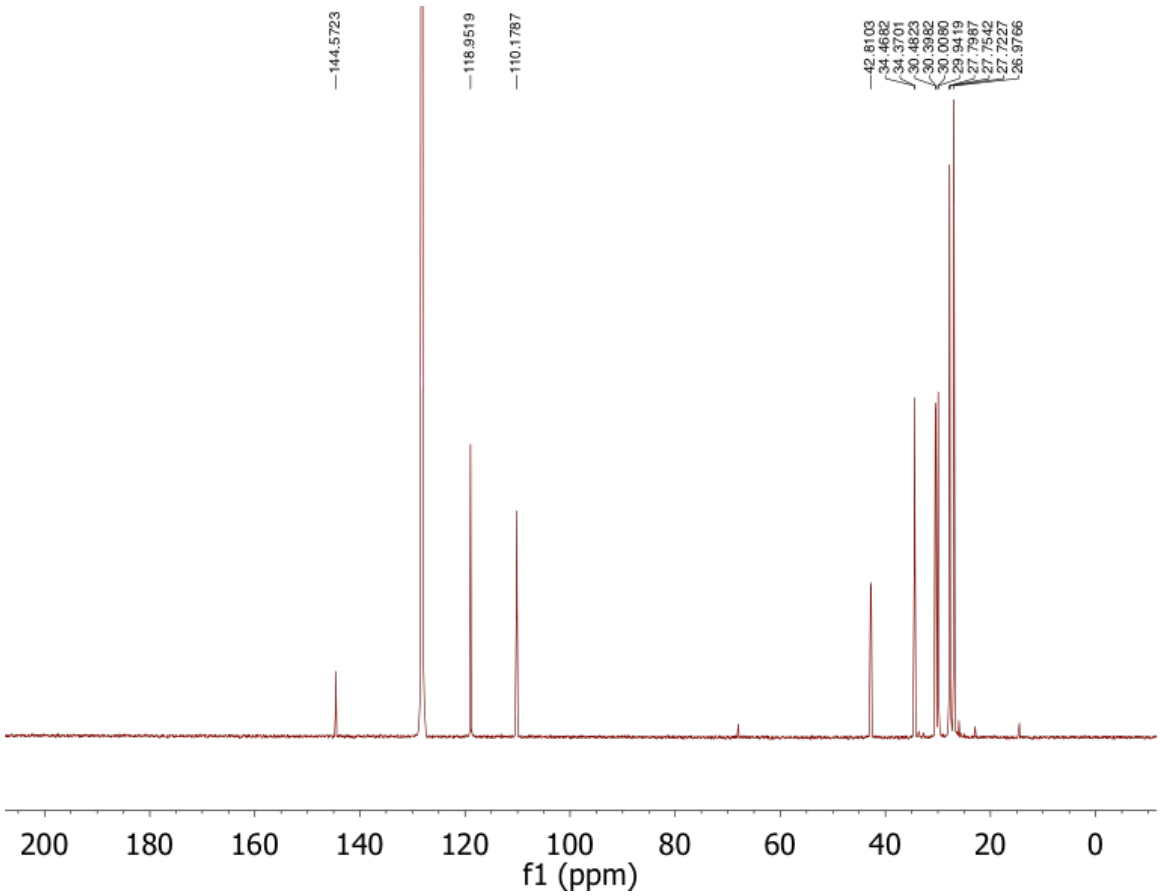

Figure 2.15: ^{13}CNMR of **5** in C_6D_6, 600MHz

	4
chemical formula	$C_{24}H_{44}GeN_2P_2$
formula weight	495.14
T (K)	100
l (Å)	0.71073
crystal system	monoclinic
space group	I 2/a(#15)
a (Å)	14.0814(4)
b (Å)	13.2784(3)
c (Å)	14.1678(6)
α **(deg)**	90
β **(deg)**	93.526(1)
γ **(deg)**	90
V (Å^3)	2644.06(15)
Z	4
$\mathbf{r}_{calcd}$ **(g/cm^3**	1.244
$\mathbf{R}_1$**,** $\mathbf{R}_W2$	0.0196, 0.0528
GOF	1.058

Table 2.1: Crystallographic Data for Complex **4**

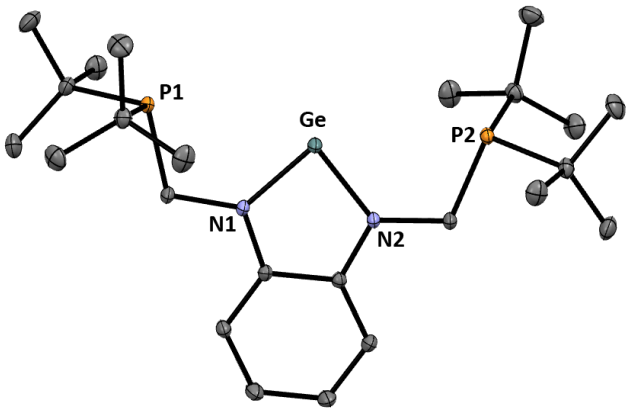

Figure 2.16: Thermal ellipsoid plot at 50% probability of the germylene complex **4**. Orange, blue, teal, and grey ellipsoids correspond to phosphine, nitrogen, germanium, and carbon atoms, respectively. Hydrogen atoms bonded to carbon have been omitted for clarity.

Chapter 3

Metallation of the Silylane Framework

3.1 Abstract

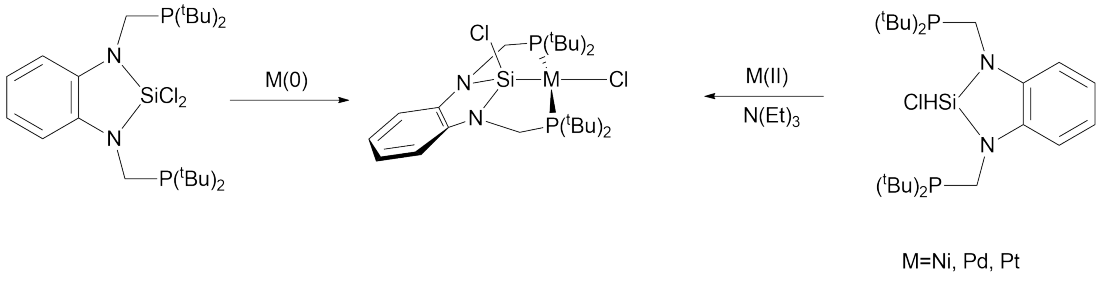

Figure 3.1: Routes to Group 10 Metal Silyl Complexes

Seeking alternate routes to a metal silylene complex, we initially explored the metallation of **1** and **2** using Group 10 metals in either the 0 or 2+ oxidation state respectively. We were successful in synthesizing a family of these complexes and explored the chemistry

of these compounds. While we were unsuccessful in reducing these complexes, we were successful in reacting the nickel silyl complex with MeMgBr to form **7**.

3.2 Introduction

The first bis-amino metal-silylene complex was synthesized in 1994 using $Ni(CO)_4$ and the N-hetercyclic tertbutyl silylene by West.[1]

In 2010, work by Hillhouse featured an unusual bridging of an H atom across nickel and silicon which gives insight into the processes occurring during Si-H activation at metals[2].

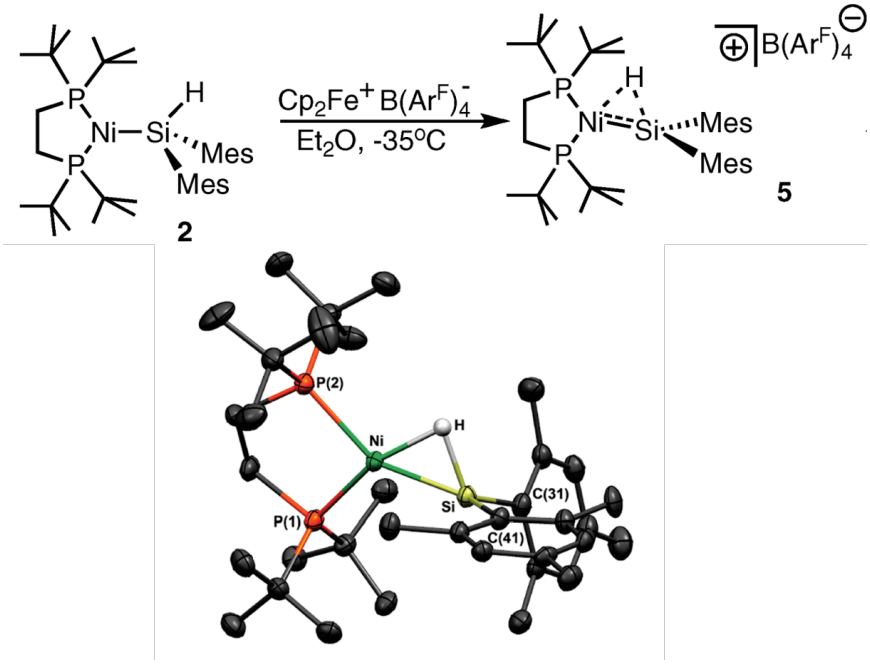

Figure 3.2: Unambiguous H atom bridging metal and silicon

After we began our work, more people found success in performing chemical trans-

formations using first row silylene complexes. One of these was a Co(III) silylene complex capable of performing Kumada cross-coupling reactions of aryl chlorides and bromides with Grignards[3]. However, we began our exploration using Group 10 metals since they have also been shown to be useful catalysts with organosilicon compounds[4]. Another advantage of using Group 10 metals is they tend to make diagmanetic complexes which understanding the results of metallations more tracktable. When we initially began, there were less examples of Group 10 silyl complexes, but since then the area has continued to explode in advances. There were initially advances in "PCP" and "PNP" pincer complexes which were able to perfrom C-H and C-C bond activations. In 2009, Turculet et al. synthesized neutral and cationioc platnium pincer complexes capable of Si-H bond activation[5],[6]. Platinum complexes have also shown other reactivity such as the oxidative addition of phenol[7]. Other notable examples are various dimers of group 10 silyl complexes[8].

3.3 Results and Discussion

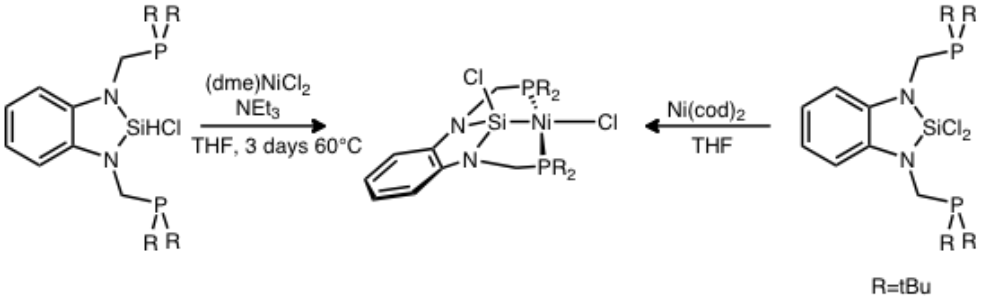

Scheme 3.1: Synthesis of **6**

Since we had little success in isolating a free silylene ligand, we sought an alterna-

tive route. We began by exploring the metallation reactions of ligand precursors **1** and **2** and focused on the Group 10 metal complexes. $NiCl_2Si(NCH_2PtBu_2)_2C_6H_4$ (**6**), an orange, air-sensitive solid, could be conveniently prepared in good yield (50%) by reaction of **2** with $NiCl_2$ and a base. Alternatively, **6** can be prepared by addition of $Ni(COD)_2$ to **1** via oxidative addition of the silicon-chloride bond. Complex **6** was characterized by LIFDIMS, NMR, spectroscopy, and X-ray crystallography. Importantly, in the ^{31}PNMR of **6** a peak is observed at δ93.22ppm, which is significantly (δ111.36ppm) downfield of the peak observed for the free ligand precursor, characteristic of a phosphine bound to a metal. Similarly, the ^{29}SiNMR spectrum shows a peak at δ52.35ppm, significantly downfield of the starting material. The ^{29}SiNMR spectrum also displays Si coupling of 53.6 Hz and the same can be seen in the ^{31}PNMR spectrum.

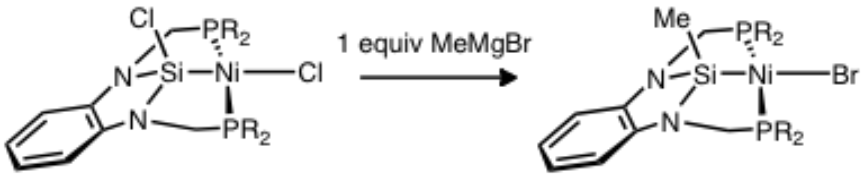

Scheme 3.2: Synthesis of **7**

Crystals suitable for X-Ray diffraction were grown from the slow evaporation of a benzene solution of **6**. The solid-state structure of **6** features a tetrahedral chlorosilyl ligand bound to a distorted square planar Ni complex. The Ni-Si bond has an average distance of 2.1388$\mathring{A}$ and is consistent with silyl ligand ligation to Ni(II) (avg Ni-Si distance 2.0376$\mathring{A}$)

The reactivity of **6** was explored. Addition of excess MeMgBr to **6** yielded a new product with was identified as **7**. A new peak in the ^{1}HNMR of **7** at δ0.7 of rela-

tive integration of 3 was assigned to a methyl group not present in the starting complex. Crystals of **7** suitable for X-ray diffraction were grown from slow evaporation of a benzene-hexamethyldisiloxane (HMDSO) solution. The structure confirmed the substitution of chloride for methyl at silicon as well as halogen exchange at Ni, with MeMgBr the likely source of bromide.

Reduction of **6** was attempted under a wide range of conditions (i.e, hydride reagents, alkali metals, etc) in order to access a low valent species capable of interesting reactivity. Unfortunately, despite all efforts, no one product could be obtained cleanly. Given that the cyclcohexyl variation of **6** and **8** can be reduced to form silylene-metal dimers, it suggests the tert-butyl groups are too bulky and prevent dimerization of **6** upon reduction. The ^{1}HNMR spectra of the crude reaction mixtures of reduction attempts with **6** invariably showed peaks below δO, consistent with the presence of metal hydride(s). Formation of a highly unstable species which undergoes C-H activaiton may explain this observation.

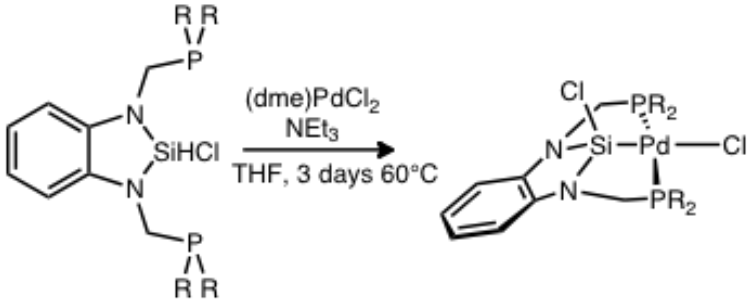

Scheme 3.3: Synthesis of **8**

We next sought to explore the rest of the group 10 elements. We found that we could prepare the palladium and platinum complexes by similar methods. Using **2** and $PdCl_2$ in the precense of a base while stirring for three days, we noticed a color change to a

dark orange solution. A new peak in the ^{31}PNMR confirmed the presence of a new metals species.

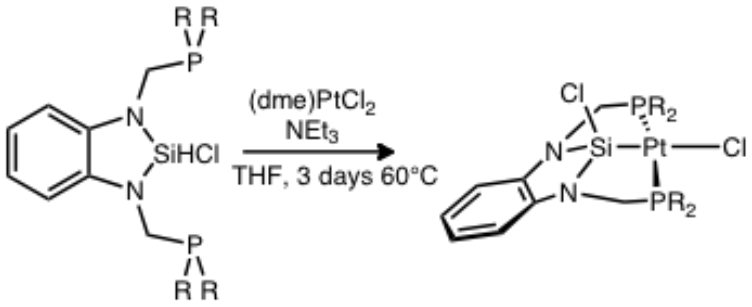

Scheme 3.4: Synthesis of **9**

Next to complete the series we prepared the platinum complex, **9** using $PtCl_2$ and the **2** in the precense of a base. A light yellow compound was formed. The ^{29}Si NMR revealed an interesting spectrum since Pt has an NMR active nuclei at 33% abundance. Looking at **??** shows a central triplet peak from Si-P coupling (9.54 Hz) then two smaller peaks from the Si-Pt coupling (1662 Hz). The ^{31}PNMR reveals a similar pattern with the Pt-P coupling being 3,053 Hz.

3.4 Experimental Section

3.4.1 $NiCl_2Si(NCH_2P^tBu_2)_2C_6H_4$ (6)

The compound can be prepared by the following two methods.

Method A: **1** was dissolved in minimal THF. To this stirring solution, a solution of $Ni(COD)_2$ in THF was added. An immediate color change to burnt orange was observed. The solution was then filtered, concentrated, and dissolved in minimal benzene to yield orange crystals.

Method B: **2** was dissolved in minimal THF. Excess triethylamine was also added to the solution. Anhydrous $NiCl_2$ was then added as a suspension in THF. The reaction was allowed to go overnight after which the solution appeared a darker orange. The reaction mixture was filtered through celite and concentrated and diluted with hexanes to yield crystals.

^{1}HNMR:(600 MHz, C_6D_6)δ 6.94 (d, J=6.0, 2H), 6.64(d, J=6.0Hz, 2H), 3.15 (s, 4H), 1.42 (d, J=6.0 Hz, 18), 1.13 (d,J=6.0Hz, 18H)

^{31}PNMR (243 MHz, C_6D_6): δ 93.22 (s).

^{13}CNMR (151 MHz, C_6D_6): δ 141.44 (s), 118.76 (s), 109.91 (s), 41.35 (s), 36.54 (s), 30.28 (s), 29.76(s).

^{29}SiNMR (119 MHz, C_6D_6): δ 52.34 (t, J=52.36Hz).

3.4.2 NiMeBrSi(NCH$_2$P^{t}Bu$_2$)$_2$C$_6$H$_4$ (7)

6 was dissolved in THF and cooled to -78°C. To this was added a 3.1M solution of MeMgBr in THF in excess. The solution was slowly warmed and became a dark brown solution. The volatiles were removed in vacuo. The solid was then redissolved in minimal benzene and the product crashed out with ether. The compound was then dissolved in minimal THF/hexanes to give dark orange crystals. ^{31}PNMR (243 MHz, C_6D_6): δ 100.8 (s).

3.4.3 PdCl$_2$Si(NCH$_2$P^{t}Bu$_2$)$_2$C$_6$H$_4$ (8)

The compound can be prepared by the following two methods.

Method A: **1** was dissolved in minimal THF. A solution of $Pd(PPh_3)_4$ dissolved in THF

was added to the ligand. A color change to dark yellow was immediately observed. After several hours, the solution was diluted with hexanes. The solution was cooled to -35°C and crystals formed. The crystals were isolated as a light orange-yellow solid.

Method B: **2** was dissolved in THF. To this was added excess triethylamine. Then a suspension of anhydrous $PdCl_2$ in THF was added. The mixture was allowed to stir overnight. The reaction was then filtered through celite and the volatiles were removed in vacuo. The mixture was then recrystalized from minimal DCM/ether. ^{1}HNMR:(400 MHz, C_6D_6) 6.91 (dd, J = 5.6, 3.3 Hz, 2H), 6.61 (dd, J = 5.6, 3.3 Hz, 2H), 3.32 (dt, J = 5.8, 3.0 Hz, 4H), 1.32 (t, J=5.6Hz 18H), 1.12 (t, J=5.6 Hz, 18H).

^{31}PNMR (243 MHz, C_6D_6): δ 103.37 (s).

^{29}SiNMR (119 MHz, C_6D_6): δ 59.07 (t, J=59.07Hz).

3.4.4 $PtCl_2Si(NCH_2P^tBu_2)_2C_6H_4$ (9)

The compound can be prepared by the following two methods.

Method A: **1** was dissolved in minimal THF. A suspension of $Pt(PPh_3)_4$ in THF was added. The reaction was allowed to stir overnight resulting in a light yellow solution. The mixture was concentrated and to this was added hexanes. The solution was then cooled and allowed to stand in a -35°C fridge until crystals formed.

Method B: **2** was dissolved in THF. To this was added excess triethylamine. Then a suspension of anhydrous $PtBr_2$ in THF was added. The solution was allowed to stir overnight resulting in a brown/yellow solution. The volatiles were removed in vacuo. The mixture was recrystallized from DCM/ether to give yellow crystals.

^{31}PNMR (243 MHz, C_6D_6): δ 97.01 (s/d, textitJ_{Pt-P}= 3053Hz).

^{29}SiNMR (119 MHz, C_6D_6): δ 53.91 (t/dt, J_{Si-P}=9.54Hz,J_{Si-Pt}=1661Hz).

3.5 References

Bibliography

[1] Denk, M.; Hayashi, R. K.; West, R. *J. Chem. Soc., Chem. Commun.* **1994**, 33–34.

[2] Iluc, V. M.; Hillhouse, G. L. *Journal of the American Chemical Society* **2010**, *132*, 11890–11892, PMID: 20690602.

[3] Xiong, Z.; Li, X.; Zhang, S.; Shi, Y.; Sun, H. *Organometallics* **2016**, *35*, 357–363.

[4] Horn, K. A. *Chemical Reviews* **1995**, *95*, 1317–1350.

[5] Mitton, S. J.; McDonald, R.; Turculet, L. *Organometallics* **2009**, *28*, 5122–5136.

[6] Korshin, E. E.; Leitus, G.; Shimon, L. J. W.; Konstantinovski, L.; Milstein, D. *Inorganic Chemistry* **2008**, *47*, 7177–7189, PMID: 18637675.

[7] Sun, S.-S.; Guo, J.-F.; Wang, S.; Huang, C.; Zhu, J.-Y.; Li, Y.-H.; Huang, W. *Inorganica Chimica Acta* **2016**, *451*, 157 – 161.

[8] Evers-McGregor, D. A.; Bezpalko, M. W.; Foxman, B. M.; Thomas, C. M. *Dalton Trans.* **2016**, *45*, 1918–1929.

3.6 Figures, Schemes, and Tables

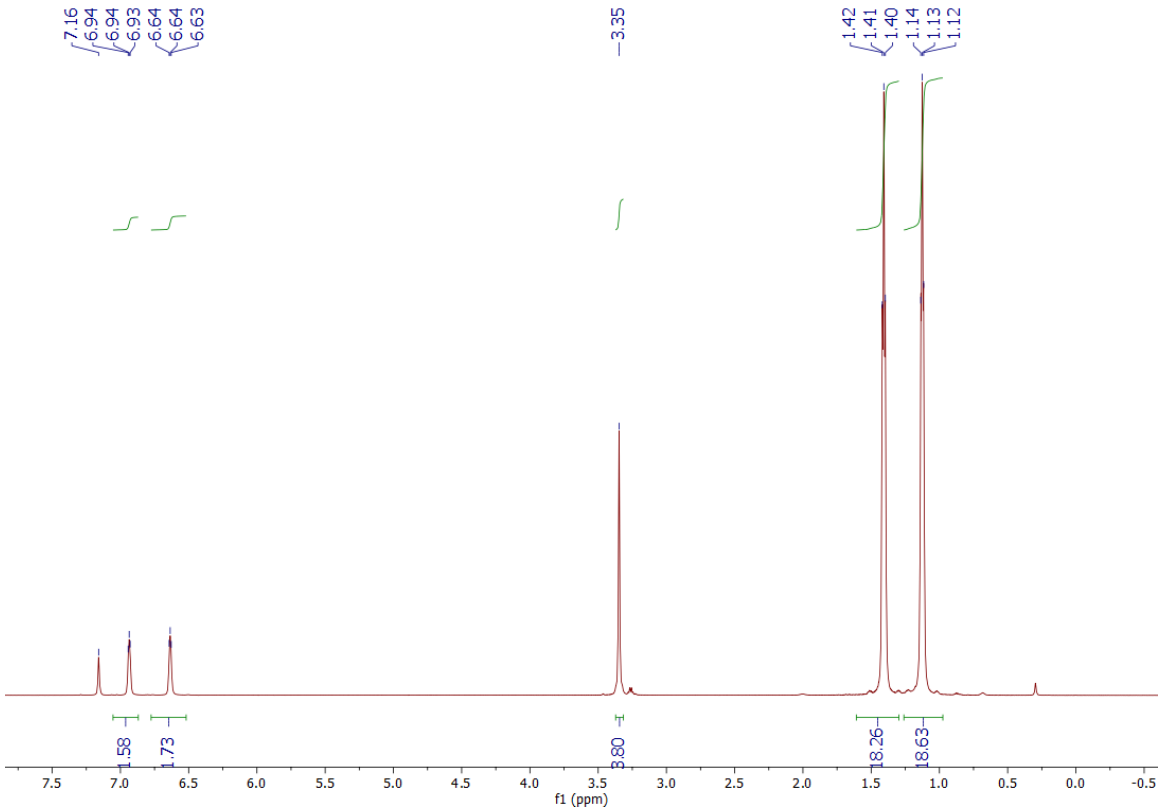

Figure 3.3: ^{1}HNMR of **6** in C_6D_6, 600MHz.

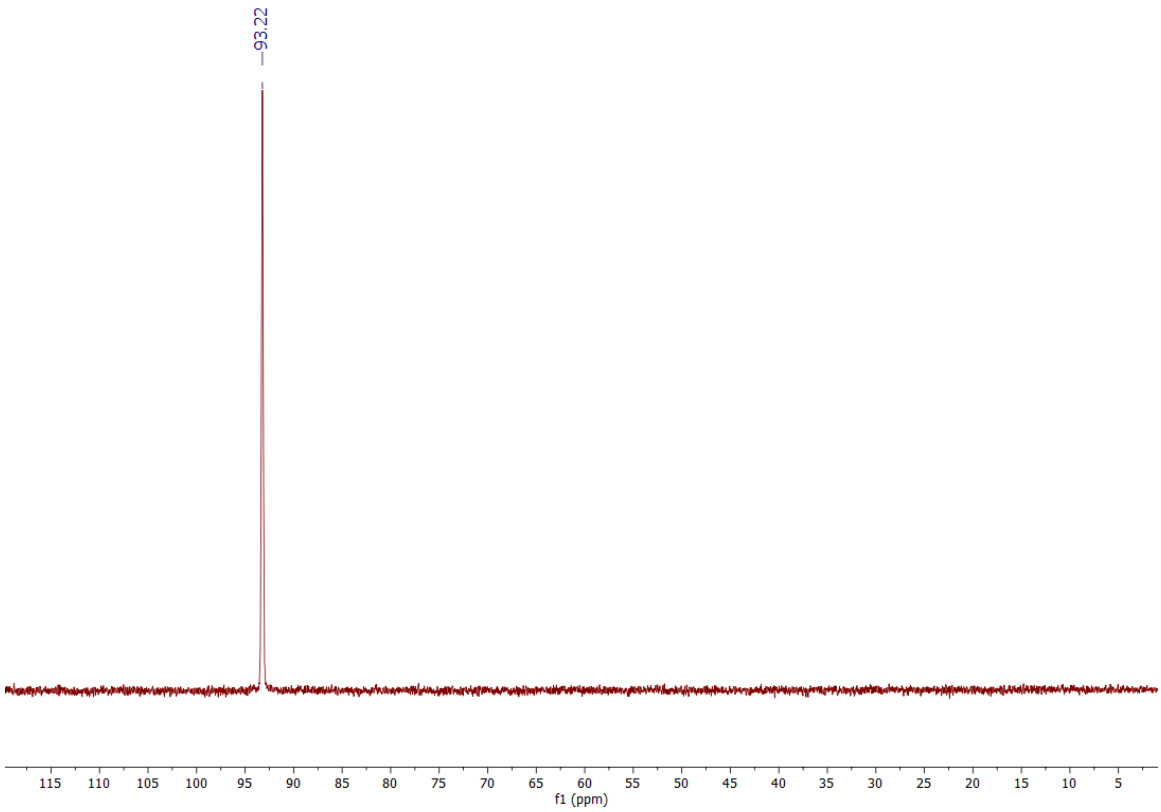

Figure 3.4: ^{31}PNMR of **6** in C_6D_6, 600MHz.

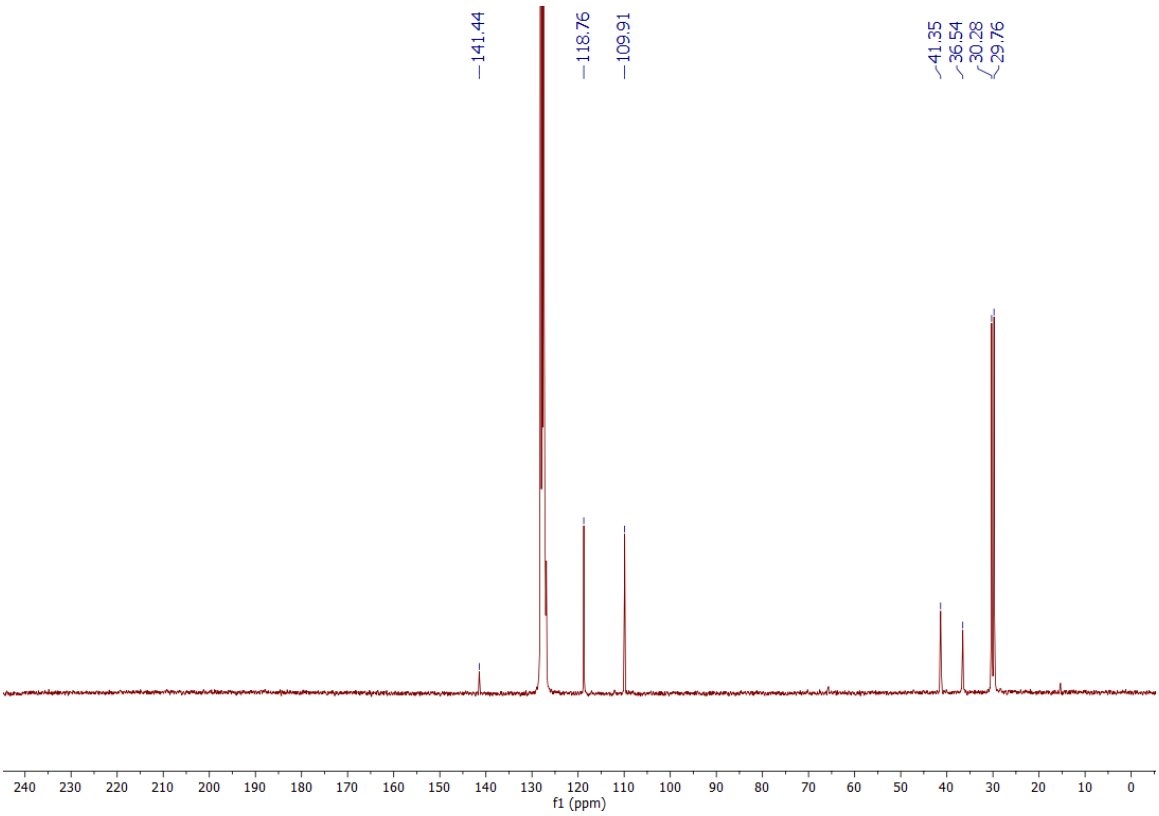

Figure 3.5: ^{13}CNMR of **6** in C_6D_6, 300MHz.

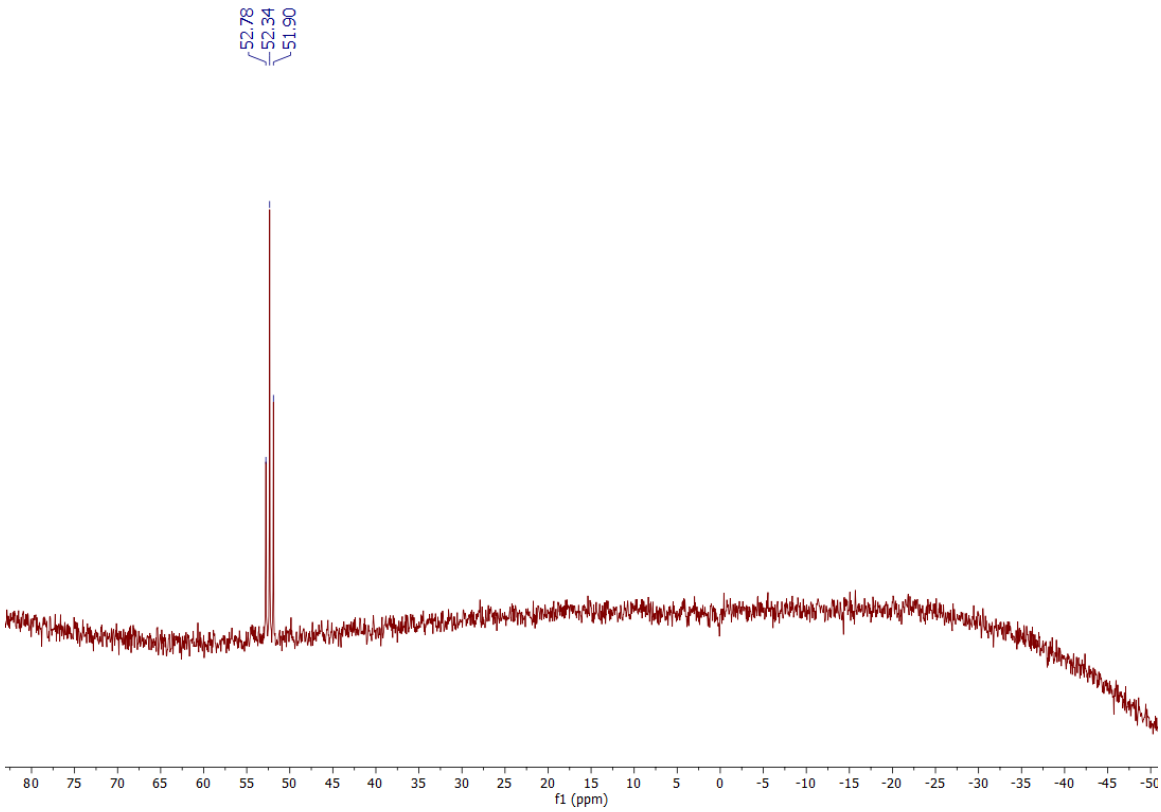

Figure 3.6: ^{29}SiNMR of **6** in C_6D_6, 600MHz.

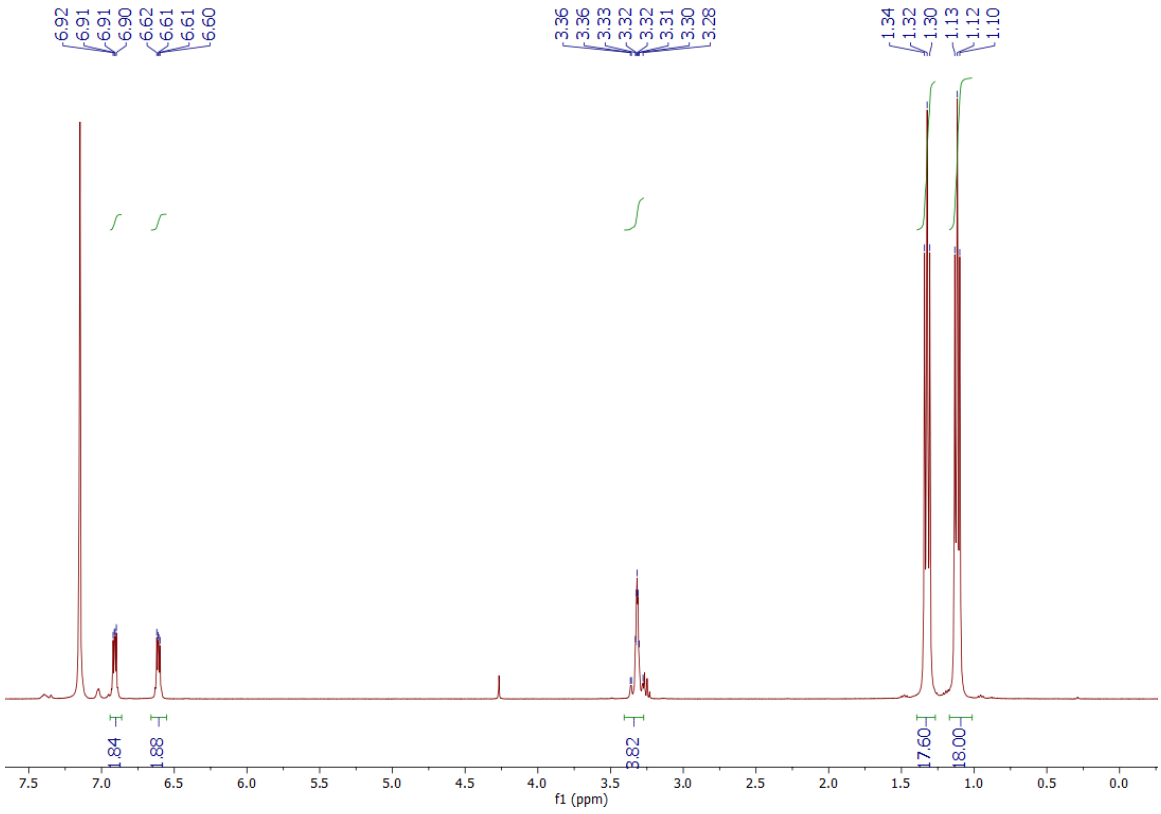

Figure 3.7: ^{1}HNMR of **8** in C_6D_6, 400MHz.

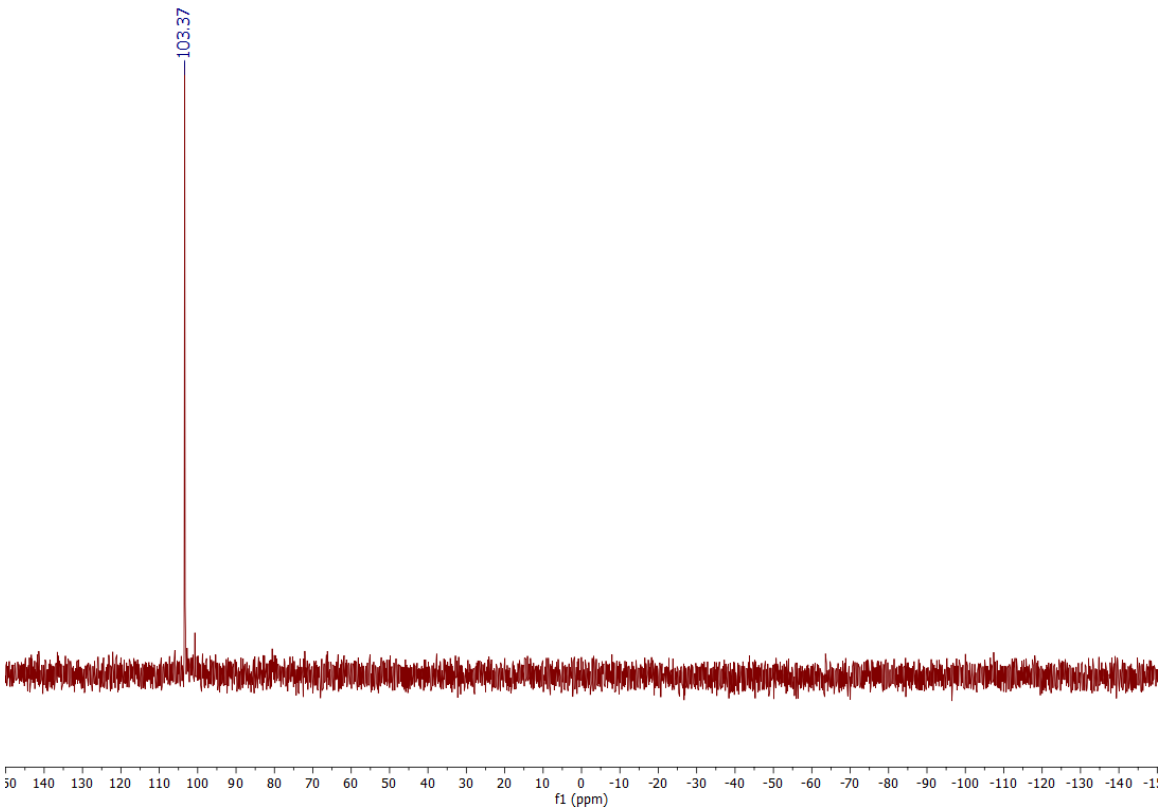

Figure 3.8: ^{31}PNMR of **8** in C_6D_6, 300MHz.

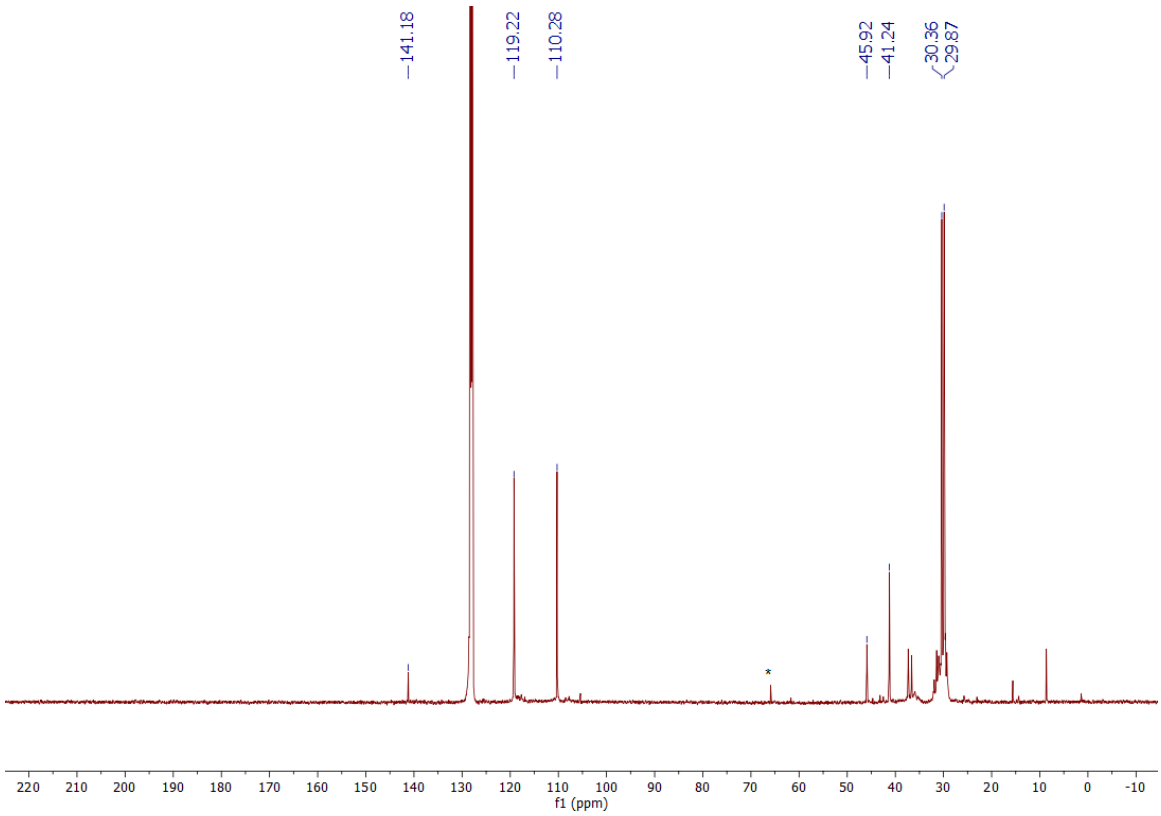

Figure 3.9: ^{13}CNMR of **8** in C_6D_6, 600MHz. Impurities are denoted with a *

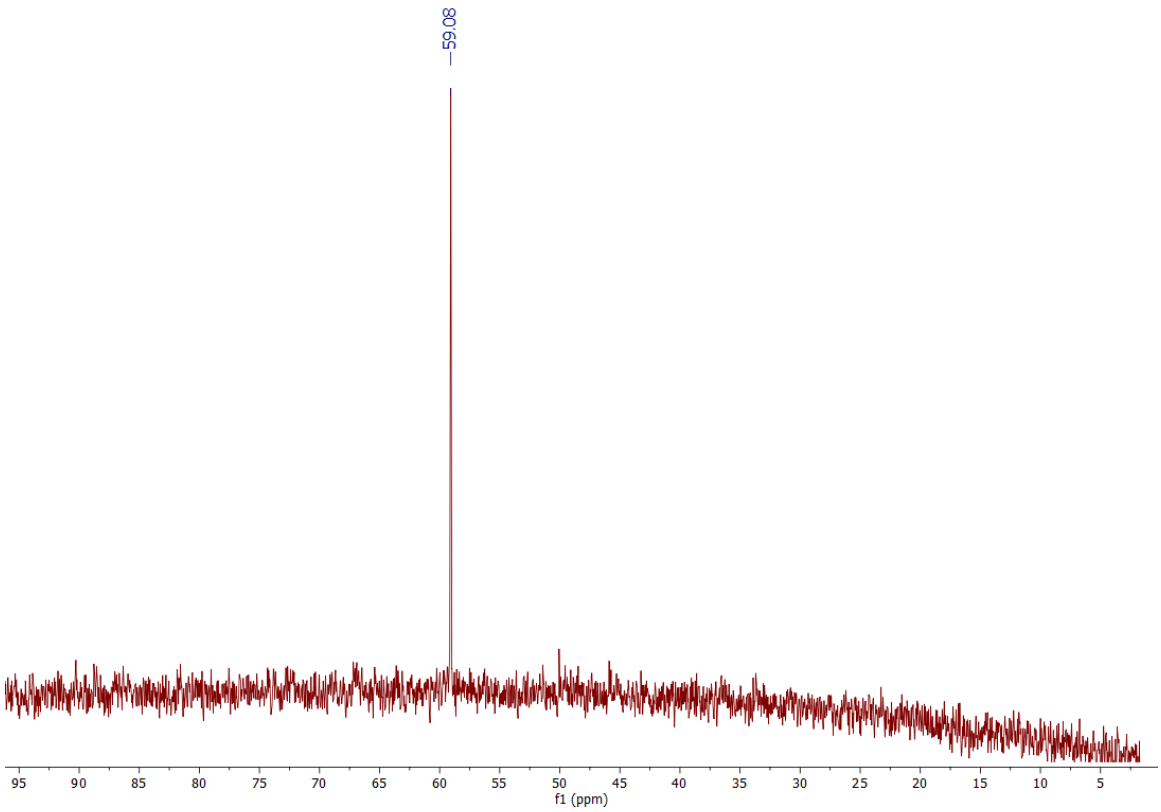

Figure 3.10: ^{29}SiNMR of **8** in C_6D_6, 600MHz.

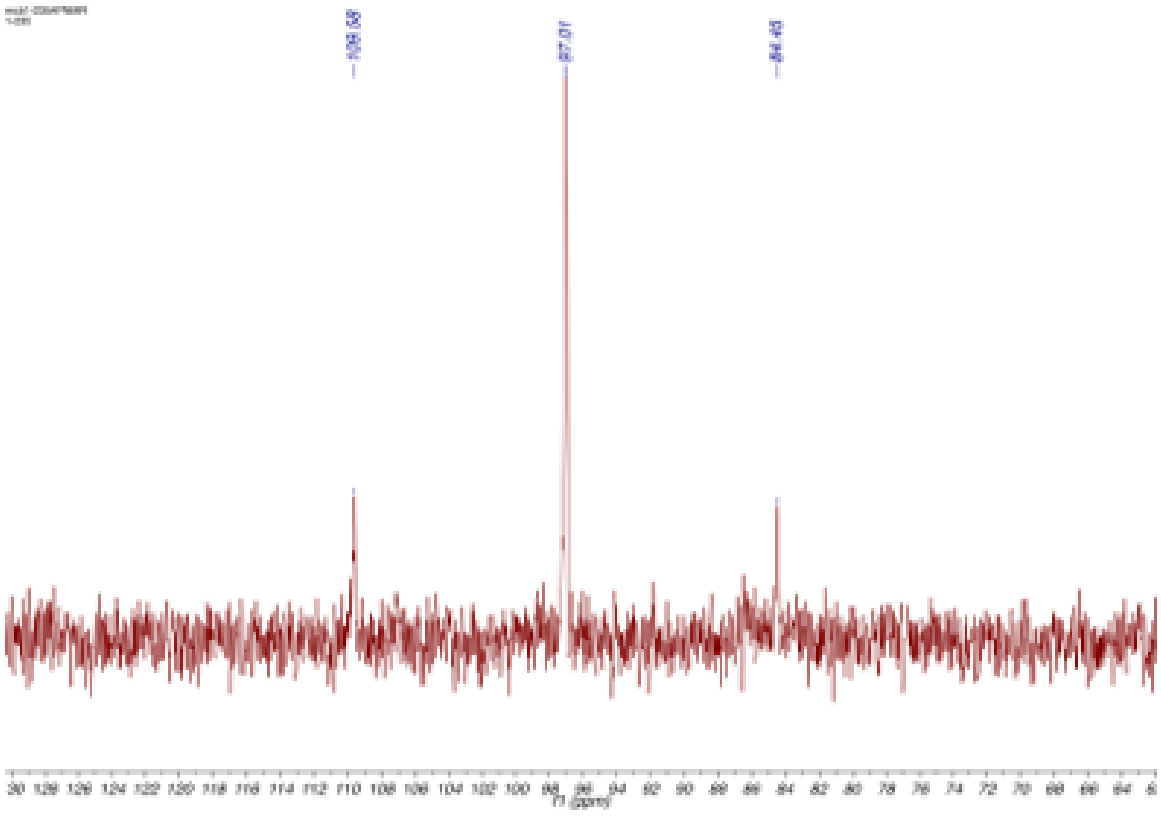

Figure 3.11: ^{31}PNMR of **9** in C_6D_6, 600MHz.

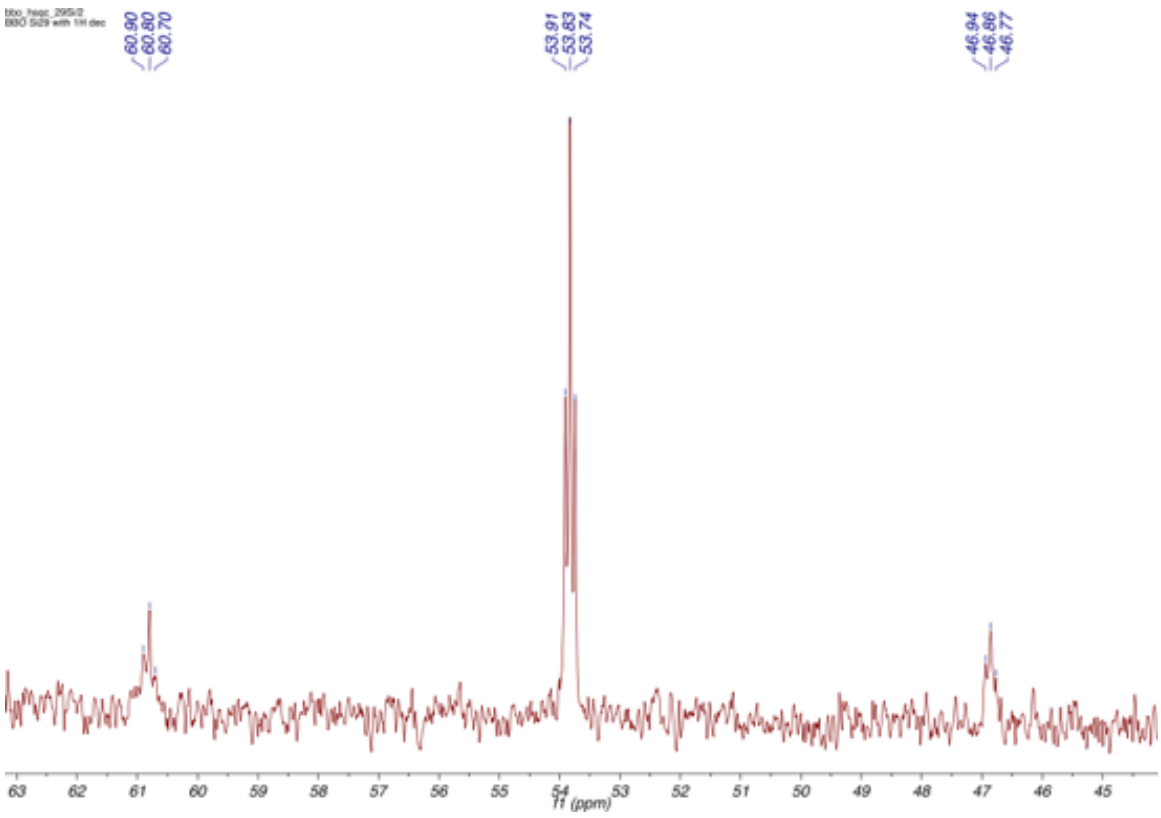

Figure 3.12: ^{29}SiNMR of **9** in C_6D_6, 600MHz.

Chapter 4

Metallation of the Germylene Ligand

4.1 Abstract

After exploring Group 10 metal chemistry, we sought to explore the other first row elements. We initially explored cobalt, but soon found that the germanium pincer framework afforded a variety of bimetallic complexes. This is surprising given that there remain relatively few examples of bimetallic silylene and germylene complexes and few examples of heavier tetrylenes in metal complexes. We were successful in synthesizing a family of cobalt, iron, manganese bimetallic complexes and compared their properties.

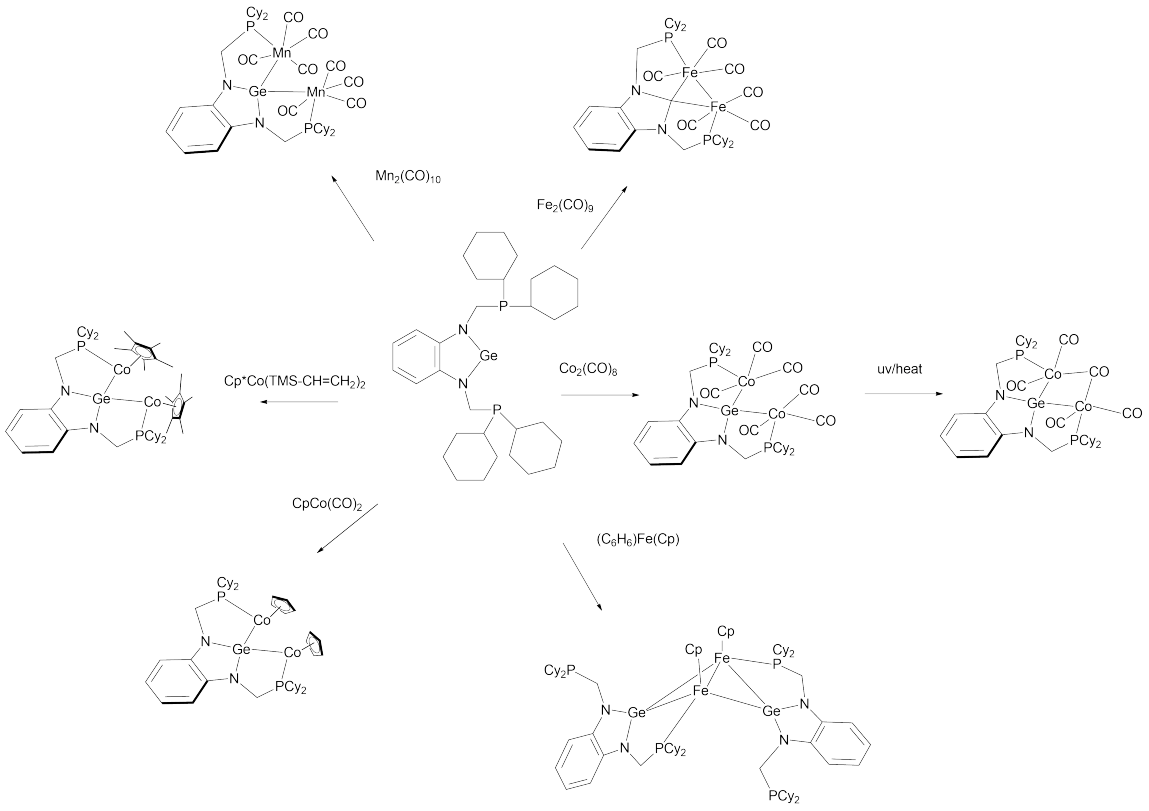

Figure 4.1: Family of Bimetallic Germanium Complexes

4.2 Introduction

When we began the exploration of these complexes the germanium complex **4** and its related metal complexes were unreported in the literature. Since then this area of chemistry has been further explored[1],[2],[3],[4]. Once we discovered that we could produce bimetallic complexes, we sought to exploit a potential for bimetallic reactivity. There have been several instances in the literature of bimetallic reactivity to perform carbene transfers[5],[6]. Furthermore, there existed bimetallic group 14 Ru and Rh complexes, but at the time we began exploring the chemistry, there were very few first row metal complexes[7].

4.3 Results and Discussion

The increased stability of the heavier group 14 elements made exploring the germylene derivative more attractive than attempts to make a silylene ligand precursor. Furthermore the availability of a Ge(II) source, $GeCl_2$-dioxane facilitated the successful synthesis of **5** as described in Chapter 2. Initially the goal was to synthesize a metal-germylene complex. However, we realized the germylene ligand may be unsuitable for supporting monometallic complexes due to the difficulty of coordinating all three donor atoms to the same metal. We therefore examined the synthesis of bimetallic systems.

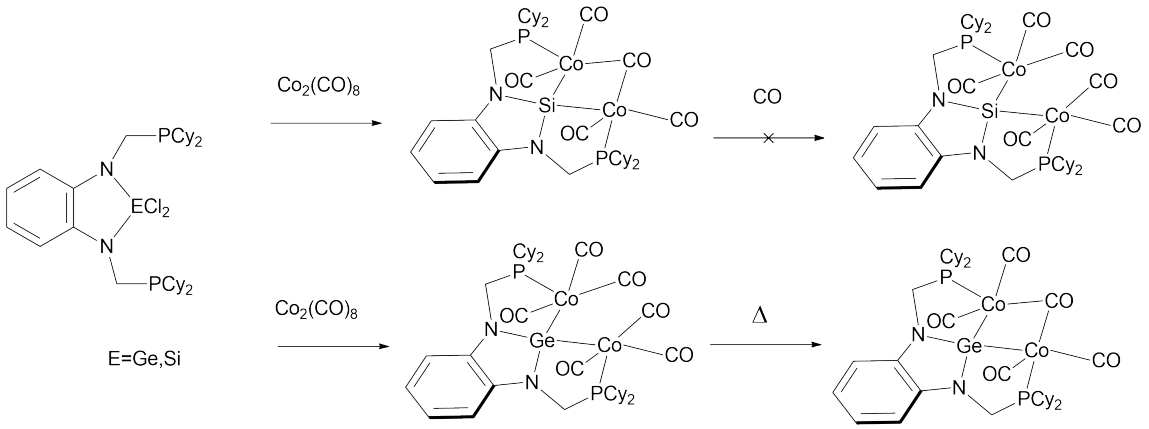

Figure 4.2: Family of Silyl and Germanyl Carbaonyl Complexes

The reaction of $Co_2(CO)_8$ with **5** affords the bimetallic cobalt complex $GeCo_2(CO)_6(NCH_2PCy_2)_2C_6H_4$ (**10**) as an air-sensitive dark red powder after column chromatography. Crystals of **10** for X-ray diffraction were grown from a concentrated solution of pentane and HMDSO and the solid-state structure is shown in **Figure 4.20**. The germanium has a tetrahedral geometry while each cobalt center is in a distored trigonal bipyramidal geometry. There is no direct Co-Co bonds with a Co-Co distance of 4.123Åand no

bridging carbonyl ligands. Our findings are in agreement with the conclusions of Cabeza et al.[1] where they concurrently synthesized the tert-butyl derivative of **10**. We heated **10** at 100° under vacuum in an attempt to liberate some of the CO ligands. This gave rise to a new peak in the ^{31}P NMR spectrum at 99.2 ppm corresponding to the complex $GeCo_2(CO)_5(NCH_2PCy_2)_2C_6H_4$ (**11**)

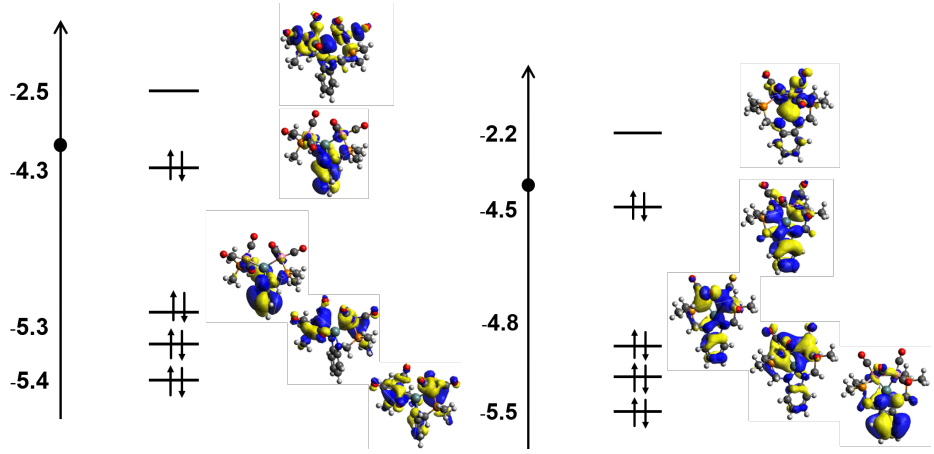

(a) MO of **10** (b) MO of **11**

Figure 4.3: Calculated MO's for **10** and **11** using ORCA Triplet Basis Set FQ OPT

We next sought to synthesize the analogous iron and manganese complexes. Due to the toxicity of $Ni(CO)_4$ we did not attempt to synthesize the analogous nickel complex via the metal carbonyl precursor. We did attempt to synthesize a nickel complex using nickel bis(triphenylphosphine) dicarbonyl but were unsuccessful in isolating a compound with nickel complexed to the ligand framework.

The reaction of $Fe_2(CO)_9$ with **5** affords the bimetallic iron complex $GeFe_2(CO)_5(NCH_2PCy_2)_2C_6H_4$ (**12**) as air-sensitive red crystals after recrystallization from

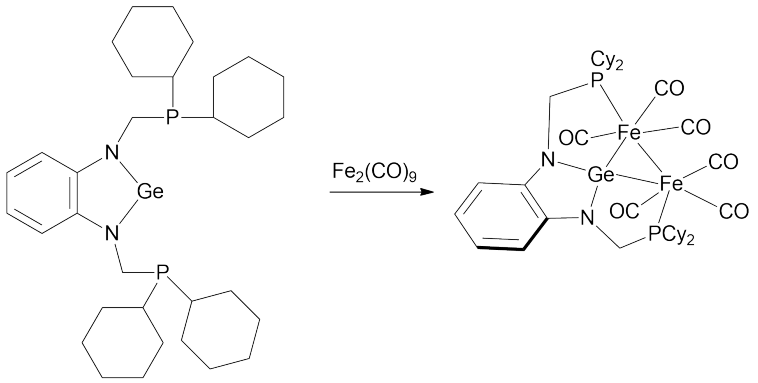

Scheme 4.1: Synthesis of **12**

minmal THF/hexanes. Crystals suitable for X-ray diffraction were from from a concentrated solution of THF/hexanes and the solid-state structure is shown **Figure 4.22**. The germanium has a tetrahedral geometry and each iron center is in a distorted octahedral geometry. The Fe-Fe distance is 2.870Åwhich is slightly above the average Fe-Fe bond length of 2.616Åand suggests there is a iron-iron bond which is in agreement of the NMR data showing **12** to be a diamagnetic compound.

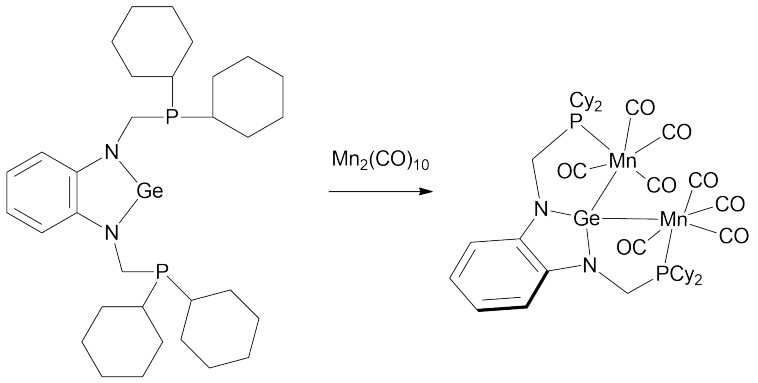

Scheme 4.2: Synthesis of **13**

The reaction of $Mn_2(CO)_{10}$ with **5** affords the analogous manganese complex

$GeMn_2(CO)_8(NCH_2PCy_2)_2C_6H_4$ (**13**). The reaction mixture was purified through column chromotography using silica in the glovebox to give an orange solid. Crystals suitable for X-Ray diffraction were grown from a concentrated solution of THF/hexanes. The solid state structure is similar to **10** with a very long Mn-Mn distance of 4.563Åand indicates there is no metal-metal bond. Interestingly, the analogous tertbutyl complex that was synthesized by Cabeza et al[4] displays very similar Mn-Mn of 4.5162Åand similar characteristics. Of note is The germanium exhibits a tetrahedral geometry and each manganese exhibits a distorted octahedral geometry.

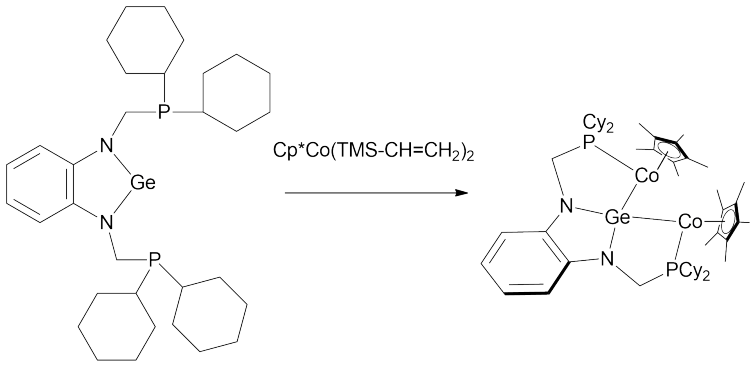

Scheme 4.3: Synthesis of **14**

We next sought routes to access other bimetallic complexes that were not saturtured with carbonyl ligands. We decided upon the known complex cobalt pentamethylcyclopentadiene bis(trimethyl(vinyl)silane) for an accessible low valent metal source with labile trimethyl(vinyl)silyl ligands. The reaction of **5** with pentamethylcyclopentadiene bis(trimethyl(vinyl)silane) affords the compound $GeCo_2(C_5Me_5)_2(NCH_2PCy_2)_2C_6H_4$ (**14**) as a dark purple solid. Crystals suitable for X-Ray diffraction were grown from minimal THF/hexanes. The cobalt-cobalt metal distance is 4.306Å which suggests there is no cobalt-

cobalt bond. This is consistent with the compound being a Co^{1+} $17e^{-}$ complex as supported by the paramagnetic ^{1}H NMR spectrum. Furthermore, we were unable to obtain a $^{31}Pnmr$ which further supports that **14** is paramagnetic. We attempted to explore reactivity with **14**, but it was generally unreactive or the reactions were unproductive.

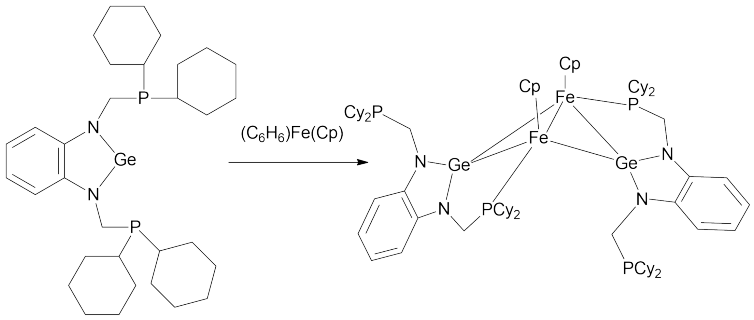

Scheme 4.4: Synthesis of **15**

We then sought to replace the pentamethylcyclopentadiene with a smaller ligand. We then attempted to synthesize the analogous iron cyclopentadiene complex using the starting material iron cyclopentadiene benezene and generating the reduced species insitu and adding **5** to the mixture resulting in a green complex $GeFe_2(C_5H_5)_2(NCH_2PCy_2)_2C_6H_4$ (**15**). The solution was filtered, concentrated and diluted with hexanes to afford dark olive green crystals. However, instead of forming the Fe cyclopentadiene bimetallic complex, we actually isolated a dimer, with one phosphine arm uncoordinated on each ligand. This is consistent with the ^{31}P NMR containing two phosphorus signals. The complex exhibits C2 rotational symmetry. The iron-iron distance is 2.949Å which suggests there is an iron-iron bond. This is consistent with the compound exhibiting a diamagnetic NMR spectrum. The germanium has a tetrahedral geometry and each iron center displays a distorted trigonal bipyramidal geometry.

4.4 Experimental Section

4.4.1 Synthetic Materials and Methods

Unless started otherwise, all compounds were purchased from commercial sources and used without further purification. Solvents were dried and deoxygenated by argon sparge followed by passage through an activated alumina column and were stored over $4\mathring{A}$ molecular sieves. All manipulations were performed under an N_2 atmosphere either in a glovebox or using standard Schlenk techniques. NMR spectra were recorded at 298K using a Varian 300 MHz, 500 MHz, or Bruker 600 MHz instruments. Chemical shifts in ^{1}H NMR are referenced to deuterated solvent. Chemical shifts in ^{31}P NMR are referenced to phosphoric acid. Mass spectra were recorded using either an Agilent LCTOF mass spectrometer or a Waters GCT high-resolution mass spectrometer operating in LIFDI mode. Elemental analysis was performed by Midwest Microlab, LLC; Indianapolis, IN.

4.4.2 $\mathbf{GeCo_2(CO)_6(NCH_2PCy_2)_2C_6H_4}$ (10)

A solution of cobalt octacarbonyl in THF and a solution of **5** in THF were added to a shlenk bomb and heated at 65°C overnight. The volatiles were removed in vacuo. The resulting solid was extracted with hexane, filtered through celite, concentrated, and cooled to -35°C to give dark red crystalline material.

^{1}HNMR:(600 MHz, C_6D_6)δ 6.81 (dd, J=7.8, 3.8 Hz, 2H), 6.73(dd, J=4.4Hz, 2H), 4.13 (dd, J=13.9, 6.8Hz, 2H), 3.08 (t, J=13.5Hz, 2H), 1.92-1.79 (m, 7H), 1.40-1.31 (m, 4H), 1.06 (t, J=12.4 Hz, 7H), 0.99-0.92 (m, 2H), 0.84-0.76 (m, 4H), 0.78-0.67 (m, 4H).

^{31}PNMR (243 MHz, C_6D_6): δ 121.11 (s).

^{13}CNMR (151 MHz, C_6D_6): δ 205.57 (s), 145.03 (s), 118.39 (s), 112.03 (s), 43.98 (s), 37.56 (s), 37.48(s), 36.50 (s), 36.41 (s), 29.93 (s), 29.78 (s), 29.30 (s), 28.74 (s), 27.86 (s), 27.79 (s), 27.71 (s), 27.65 (s), 27.59 (s), 27.50 (s), 27.44 (s), 26.59 (s).

4.4.3 $GeCo_2(CO)_5(NCH_2PCy_2)_2C_6H_4$ (11)

A solution of **10** in THF is placed under static vacuum and heated at 80°C for three days with the vacuum being renewed each day. The volatiles were removed in vacuo and the resulting solid was recrystallized in minimal THF/hexanes.

^{1}HNMR:(600 MHz, C_6D_6)δ 7.12 (s, 2H), 6.93(s, 2H), 3.72 (s, 4H), 1.89 (m, 8H), 1.618 (s, 4H), 1.53 (m, 14H), 1.35 (m, 6H), 1.19 (m, 6H), 1.06 (m, 14H).

^{31}PNMR (243 MHz, C_6D_6): δ 99.99 (s).

^{13}CNMR (151 MHz, C_6D_6): δ 142.0 (s), 118.98 (s), 110.08 (s), 38.39 (s), 38.21 (s), 37.74(s), 37.61 (s), 28.42 (s), 27.94 (s), 29.45 (s), 29.41 (s), 28.35 (s), 26.52 (s).

4.4.4 $GeFe_2(CO)_5(NCH_2PCy_2)_2C_6H_4$ (12)

A solution of iron nonacarbonyl in dioxane and a solution of **5** in dioxane were added to a Straus flask. The flask was then placed under a static vacuum and heated at 86°C for 4 days. The volatiles were removed in vacuo and the resulting solid was recrystallized from minimal THF/hexanes to give red crystals.

^{1}HNMR:(600 MHz, C_6D_6)δ 7.12 7.08 (m, 2H), 6.92 6.87 (m, 2H), 3.27 (s, 4H), 2.08 (d, J = 10.0 Hz, 4H), 1.93 (d, J = 12.9 Hz, 5H), 1.84 (d, J = 12.9 Hz, 5H), 1.60 (d, J = 13.7 Hz, 9H), 1.47 (d, J = 11.8 Hz, 5H), 1.35 (q, J = 13.0 Hz, 4H), 1.24 (q, J = 12.5 Hz, 4H), 1.06 (dt, J = 22.3, 12.0 Hz, 11H).

^{31}PNMR (243 MHz, C_6D_6): δ 88.28 (s).

^{13}CNMR (151 MHz, C_6D_6): δ 214.86 (s), 143.65 (s), 118.98 (s), 110.00 (s), 39.15 (s), 38.96 (s), 38.83 (s), 29.29 (s), 28.95 (s), 27.80 (s), 27.73 (s), 27.66 (s), 26.27 (s). Anal. Cald for $C_{38}H_{52}Fe_2GeN_2O_6P_2$: C: 51.92, H: 5.96, N: 3.19, Found: C: 52.40, H: 6.13, N: 2.92

4.4.5 $GeMn_2(CO)_8(NCH_2PCy_2)_2C_6H_4$ (13)

A solution of dimanganese decacarbonyl in tetrahydrofuran and a solution of **5** in tetrahydrofuran were added to a Straus flask. The flask was then placed under a static vacuum and heated 80C for 3 days. The volatiles were removed in vacuo. The resulting solid was then purified by column chromatography in a nitrogen glovebox using a mixture of THF/hexanes. The product was then further purified by recrystallization from minimal THF/hexanes to give orange crystals.

^{1}HNMR:(600 MHz, C_6D_6)δ 6.82 (dd, J = 5.8, 3.2 Hz, 2H), 6.75 6.71 (m, 2H), 4.12 (dd, 2H), 3.04 (dd, 2H), 2.21 (s, 1H), 2.10 (d, J = 9.4 Hz, 2H), 1.94 (d, J = 11.8 Hz, 7H), 1.86 (d, J = 15.0 Hz, 5H), 1.71 1.66 (m, 3H), 1.62 (d, J = 12.3 Hz, 3H), 1.54 (t, J = 15.6 Hz, 9H), 1.44 (dtd, J = 17.0, 10.5, 8.8, 4.6 Hz, 7H), 1.36 (s, 3H), 1.20 1.01 (m, 10H), 0.99 0.94 (m, 4H), 0.86 (s, 1H), 0.84 (s, 5H).

^{31}PNMR (243 MHz, C_6D_6): δ 108.8

^{13}CNMR (151 MHz, C_6D_6): δ 147.13 (s), 117.70 (s), 110.12 (s), 42.65 (s), 42.55 (s), 39.66 (s), 39.57 (s), 39.29 (s), 39.21 (s), 31.16 (s), 30.99 (s), 30.26 (s), 30.13 (s), 27.97 (s), 27.91 (s), 27.80 (s), 27.74 (s), 27.68 (s), 26.56 (s), 26.47 (s).

Anal. Cald for $C_{40}H_{52}Mn_2GeN_2O_8P_2 + \frac{1}{2}(C_6H_{12})$: C: 52.89, H: 6.09, N: 2.87, Found: C: 52.91, H: 6.20, N: 2.90

4.4.6 $GeCo_2(C_5Me_5)_2(NCH_2PCy_2)_2C_6H_4$ (14)

A solution of cobalt pentamethylcyclopentadiene bis(trimethyl(vinyl)silane) in pentane was added to a slurry of **5** in pentane. The reaction was stirred overnight and the precipitated solids were collected by filtration and washed with small portions of pentane. The crude product was then recrystallized in minimal THF/hexanes to give dark purple crystals.

4.4.7 $GeFe_2(C_5H_5)_2(NCH_2PCy_2)_2C_6H_4$ (15)

This compound can be prepared by two different methods.

Method A: A solution of iron cyclopentadiene benzene hexafluorophosphate in THF is added to an excess amount of sodium. The reduction proceeds for approximately 20-30 minutes resulting in a dark green solution. The reaction mixture is then filtered through celite into a solution of **5** in THF and stirred overnight. The volatiles were removed in vacuo and the resulting solid was recrystalized from minimal THF/hexanes giving dark olive green crystals.

Method B: A solution of **5** in THF is added to a solution of iron cyclopentadienyl benzene hexafluorophosphate in THF and a stochiometric amount of sodium metal. The reaction is stirred overnight. The volatiles were removed in vacuo and the resulting solid was recrystalized from minimal THF/hexanes.

4.5 References

Bibliography

[1] lvarez Rodrguez, L.; Brugos, J.; Cabeza, J. A.; Garca-lvarez, P.; Prez-Carreo, E.; Polo, D. *Chem. Commun.* **2017**, *53*, 893–896.

[2] Álvarez-Rodríguez, L.; Brugos, J.; Cabeza, J. A.; García-Álvarez, P.; Pérez-Carreño, E.; Polo, D. *Chem. Commun.* **2017**,

[3] Brugos, J.; Cabeza, J. A.; Garca-lvarez, P.; Prez-Carreo, E.; Polo, D. *Dalton Trans.* **2018**, *47*, 4534–4544.

[4] Brugos, J.; Cabeza, J.; Garca-lvarez, P.; Prez Carreo, E. *Organometallics* **2018**, *37*.

[5] Dai, X.; Warren, T. H. *Journal of the American Chemical Society* **2004**, *126*, 10085–10094, PMID: 15303885.

[6] Maity, A. K.; Zeller, M.; Uyeda, C. *Organometallics* **2018**, *37*, 2437–2441.

[7] Balch, A. L.; Hope, H.; Wood, F. E. *Journal of the American Chemical Society* **1985**, *107*, 6936–6941.

4.6 Figures, Schemes, and Tables

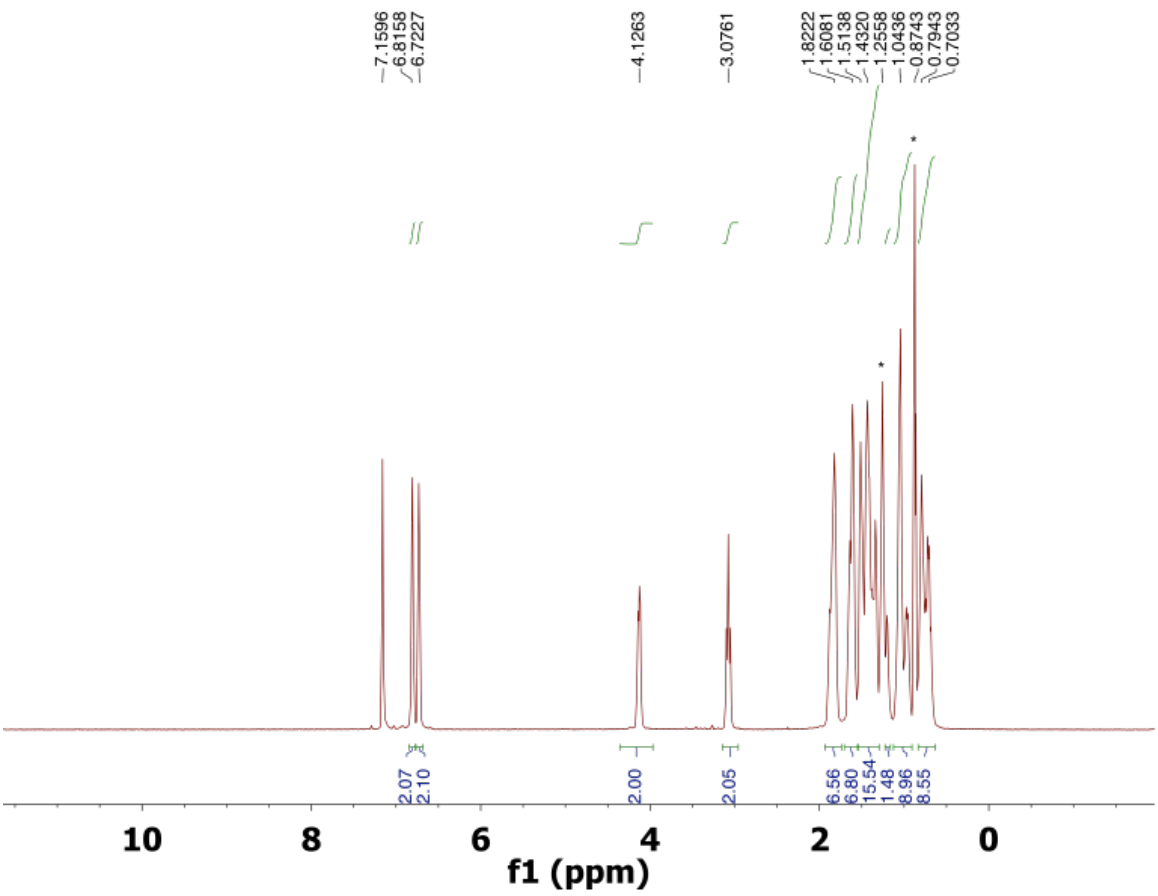

Figure 4.4: ^{1}HNMR of **10** in C_6D_6, 600MHz Residual hexane is designated with a *.

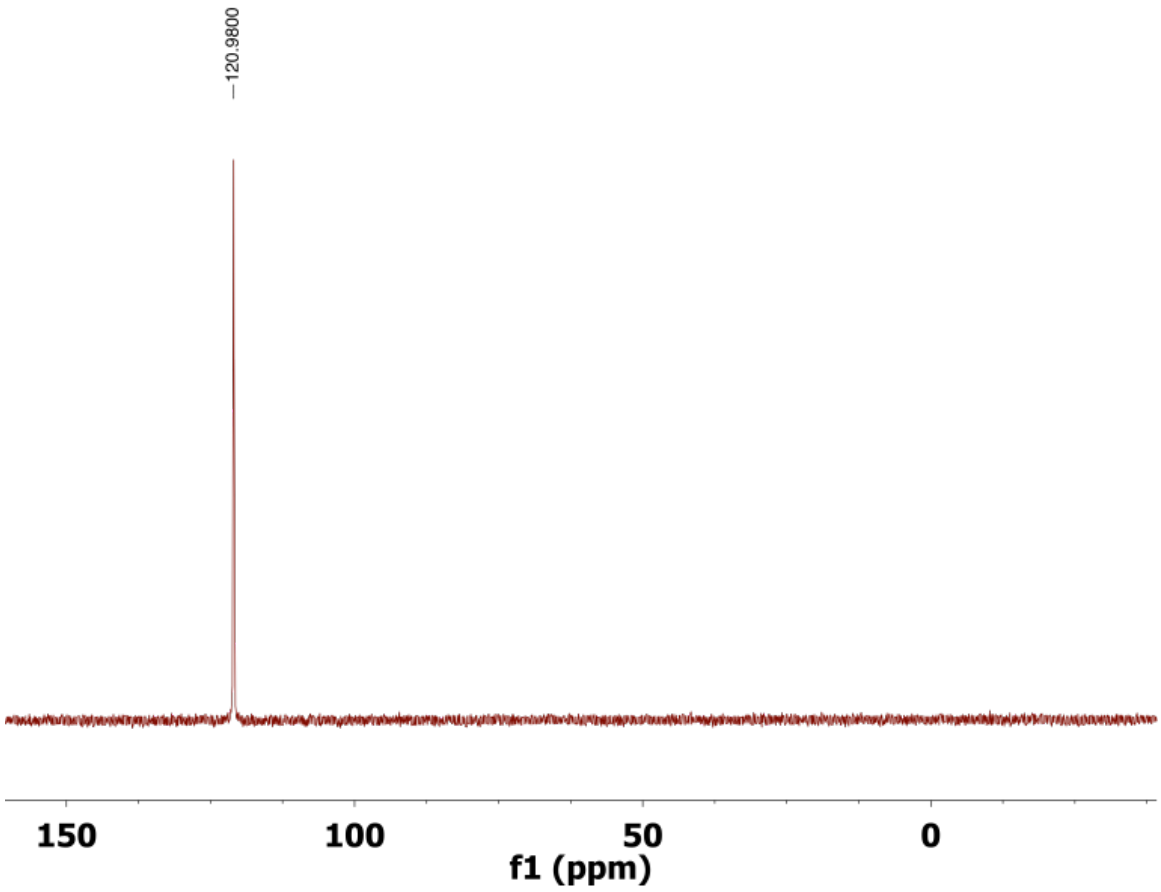

Figure 4.5: ^{31}PNMR of **10** in C_6D_6, 600MHz

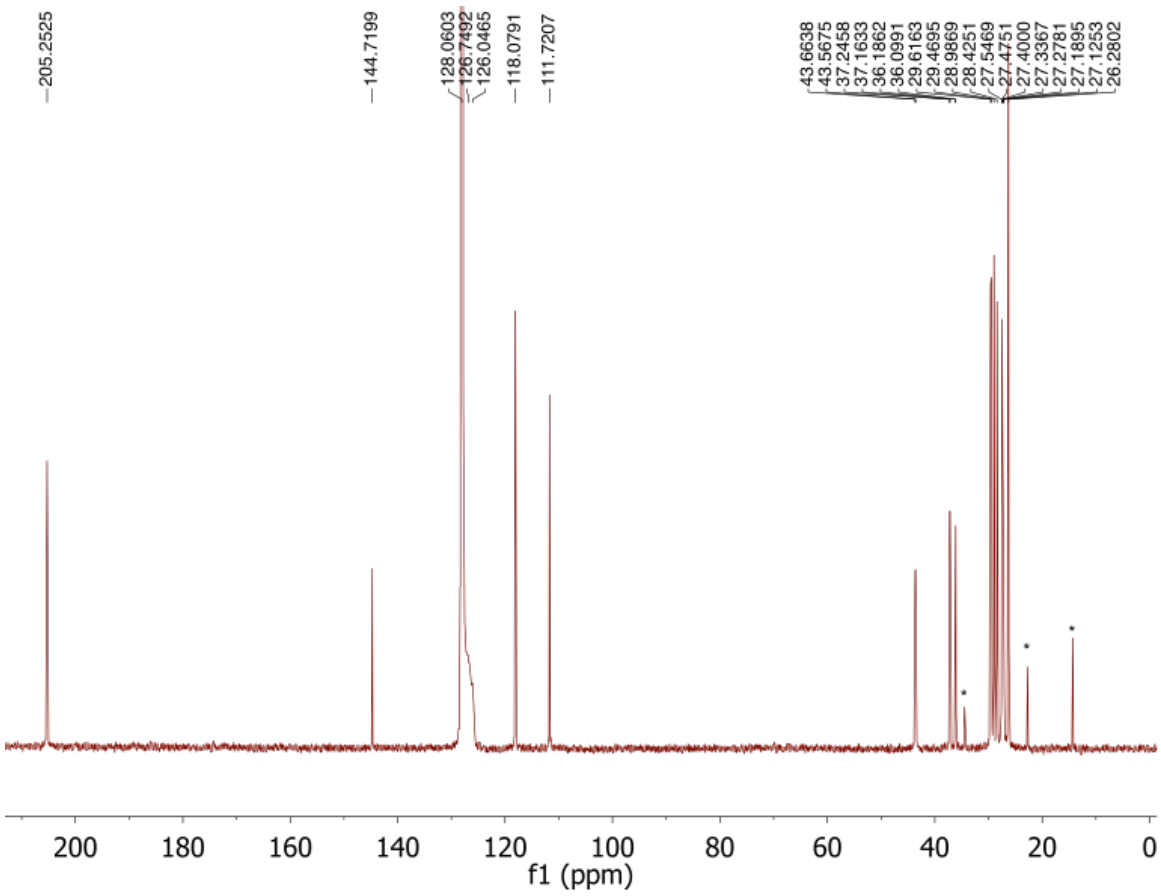

Figure 4.6: ^{13}CNMR of **10** in C_6D_6, 600MHz Residual hexane is designated with a *.

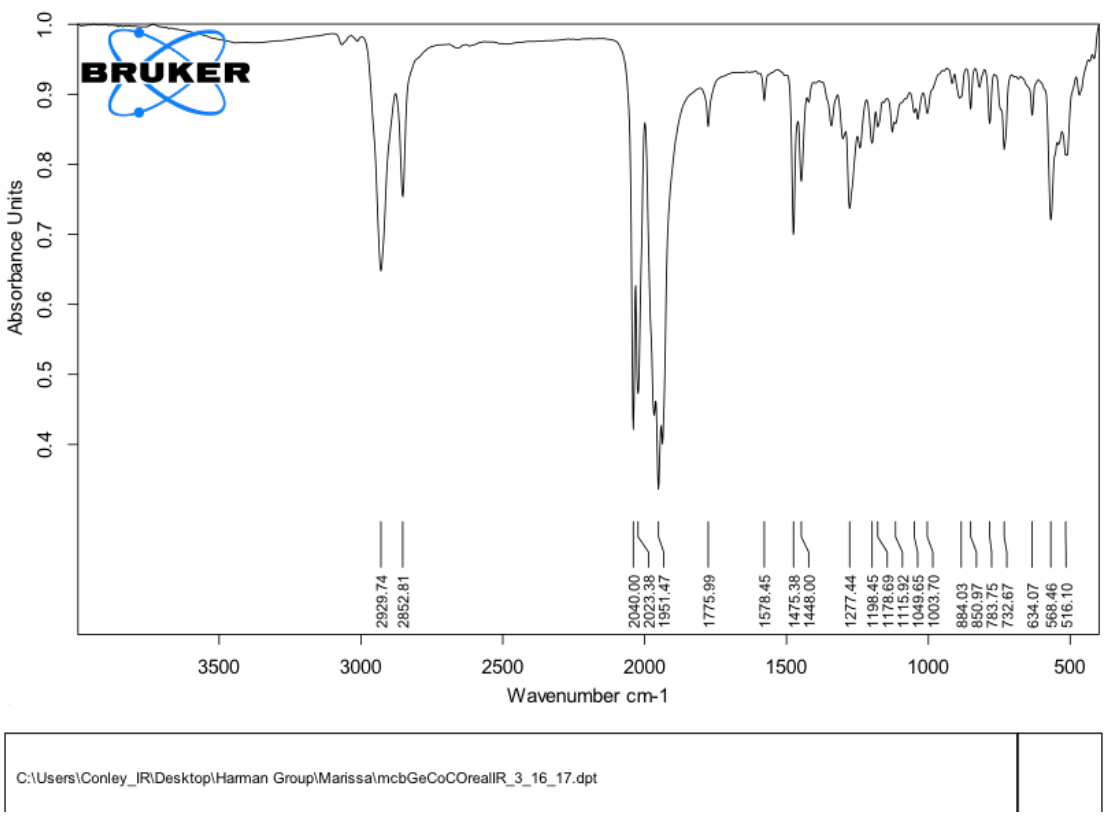

Figure 4.7: FTIR spectrum of **10**

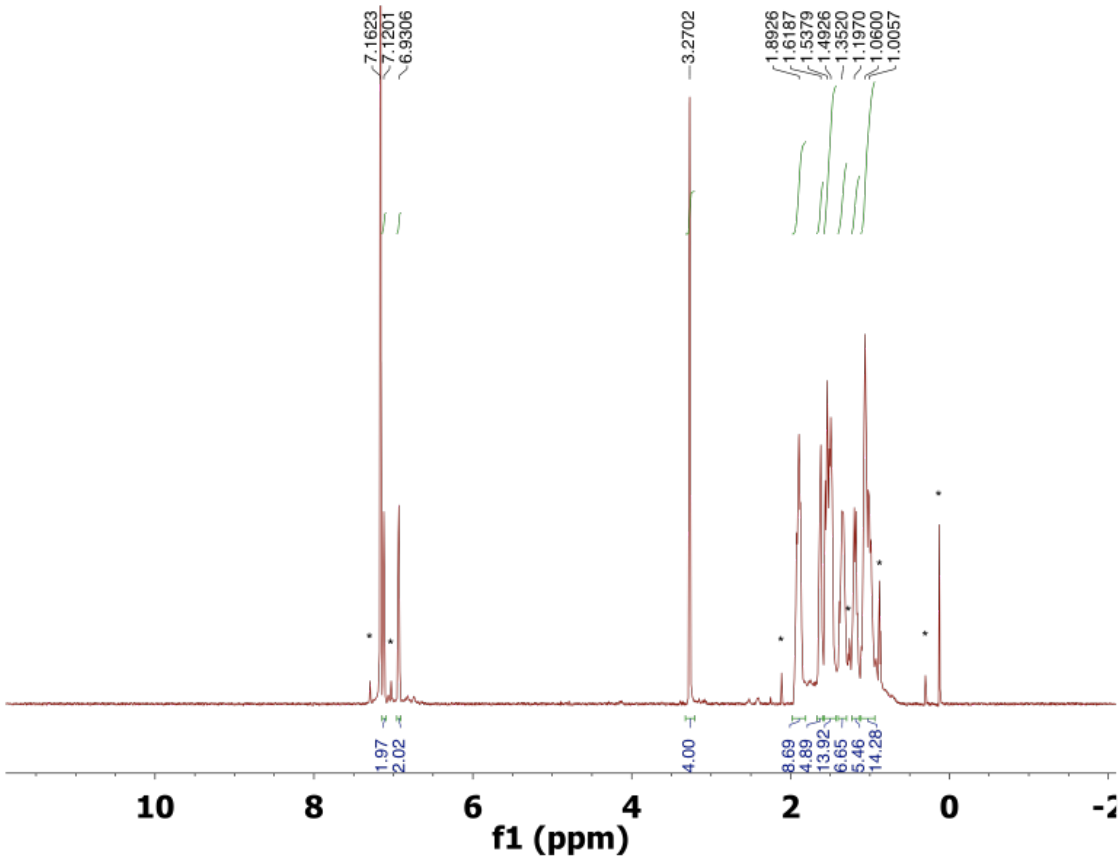

Figure 4.8: ^{1}HNMR of **11** in C_6D_6, Impurities and residual solvent is denoted with a *.

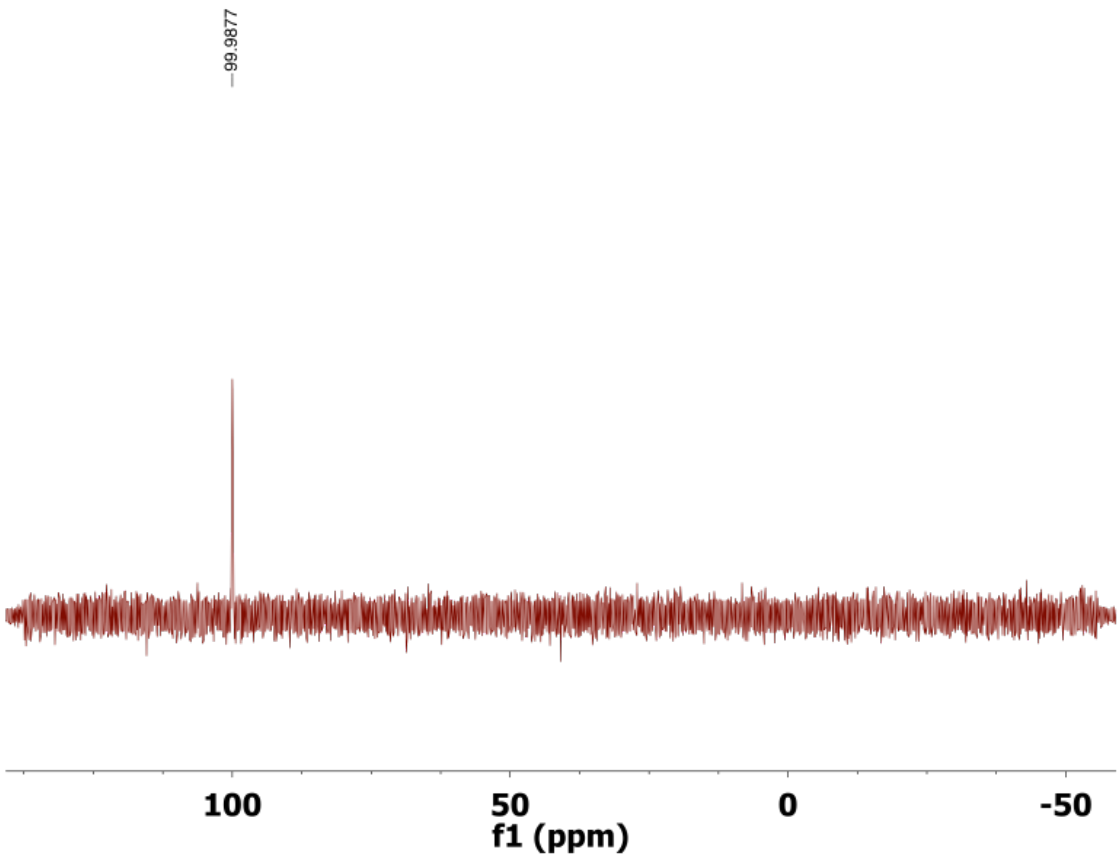

Figure 4.9: ^{31}PNMR of **11** in C_6D_6.

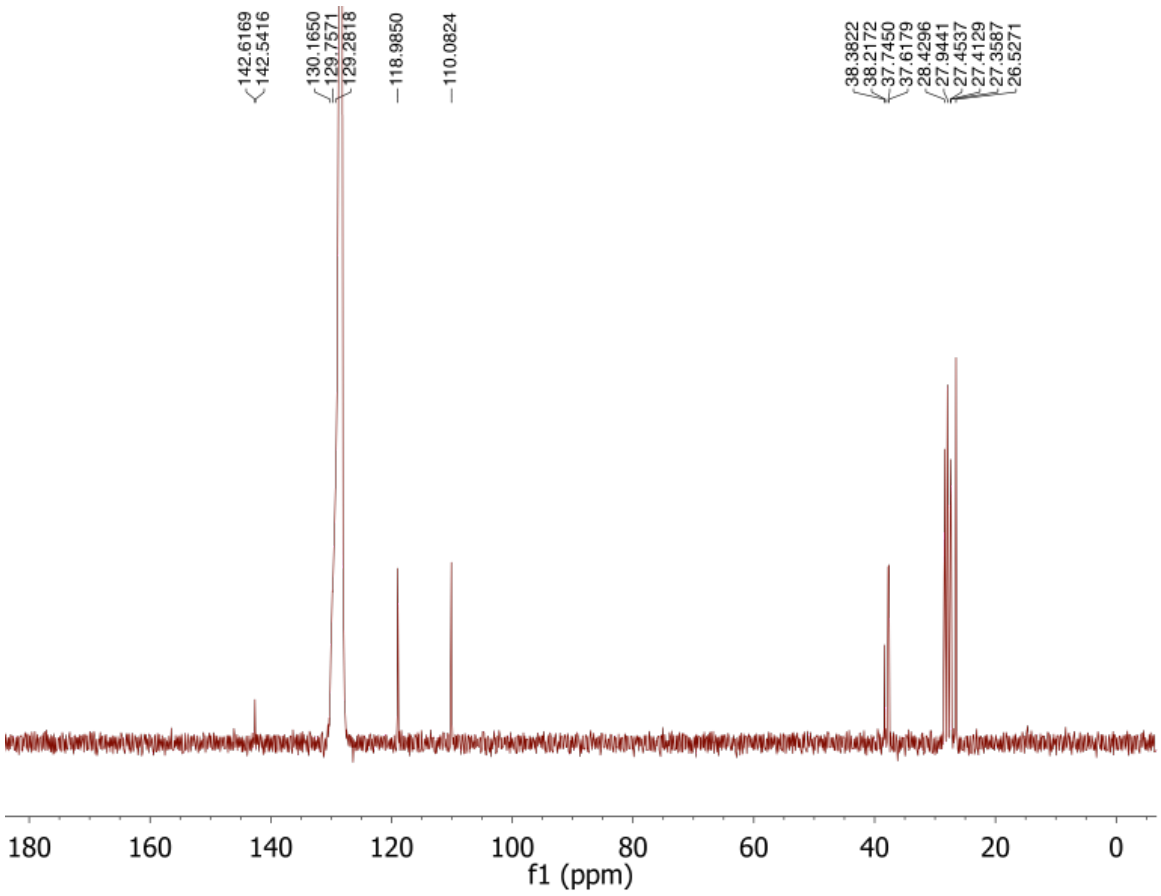

Figure 4.10: ^{13}CNMR of **11** in C_6D_6.

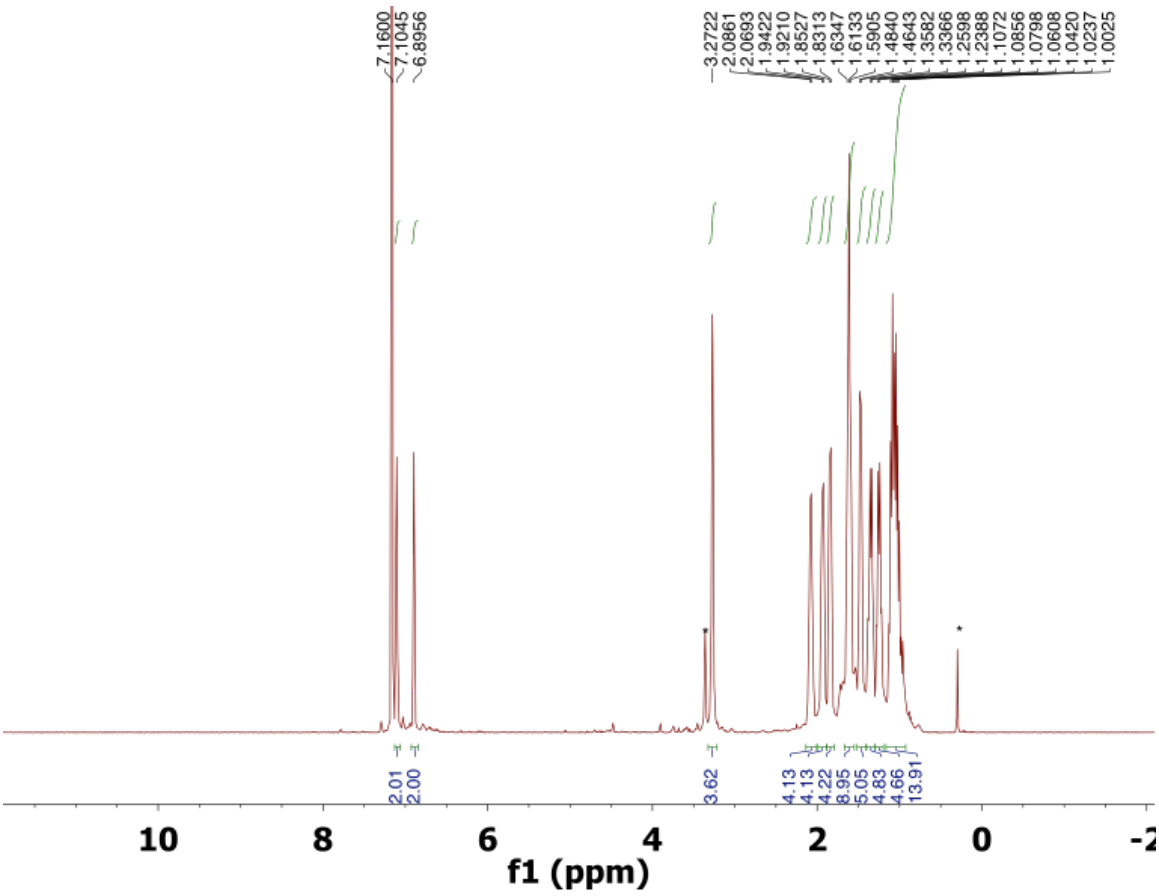

Figure 4.11: ^{1}HNMR of **12** in C_6D_6 Residual dioxane and silicon grease is denoted with a *.

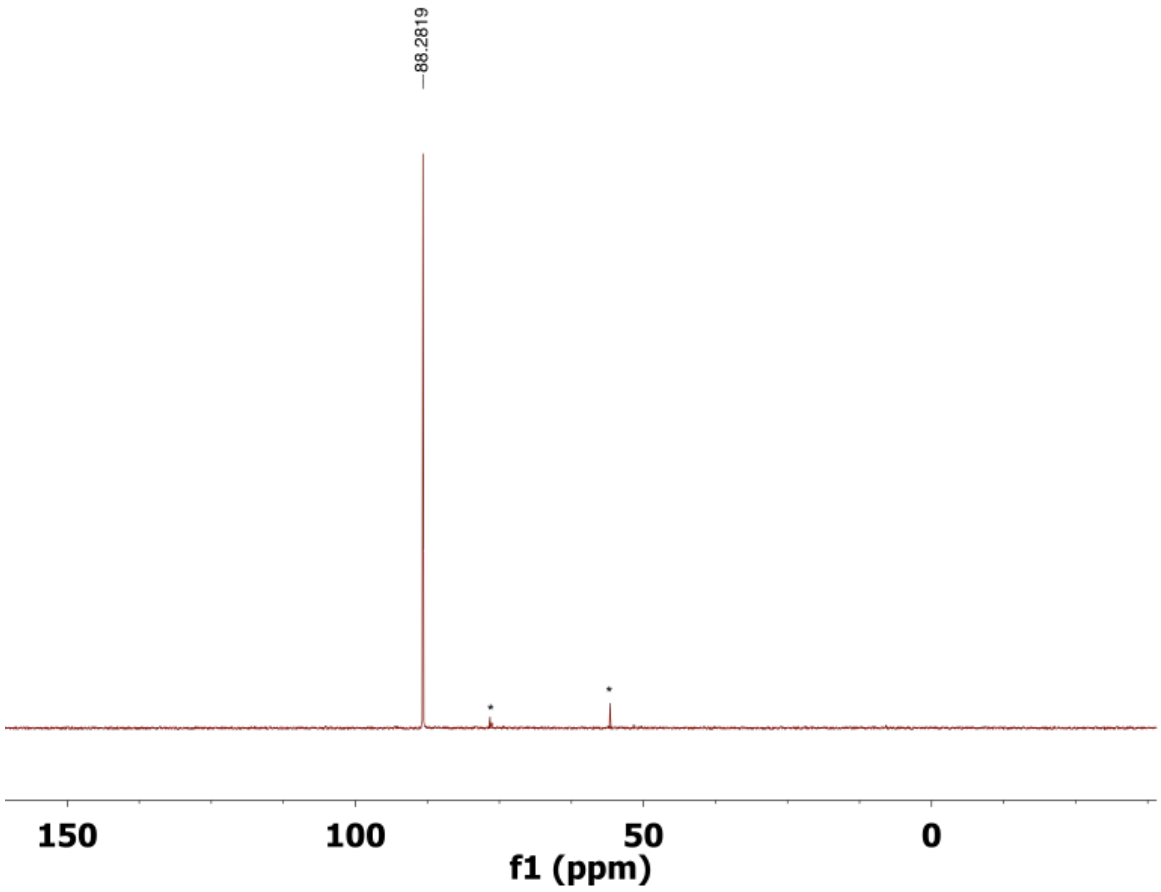

Figure 4.12: ^{31}PNMR of **12** in C_6D_6 Impurities are denoted with a *

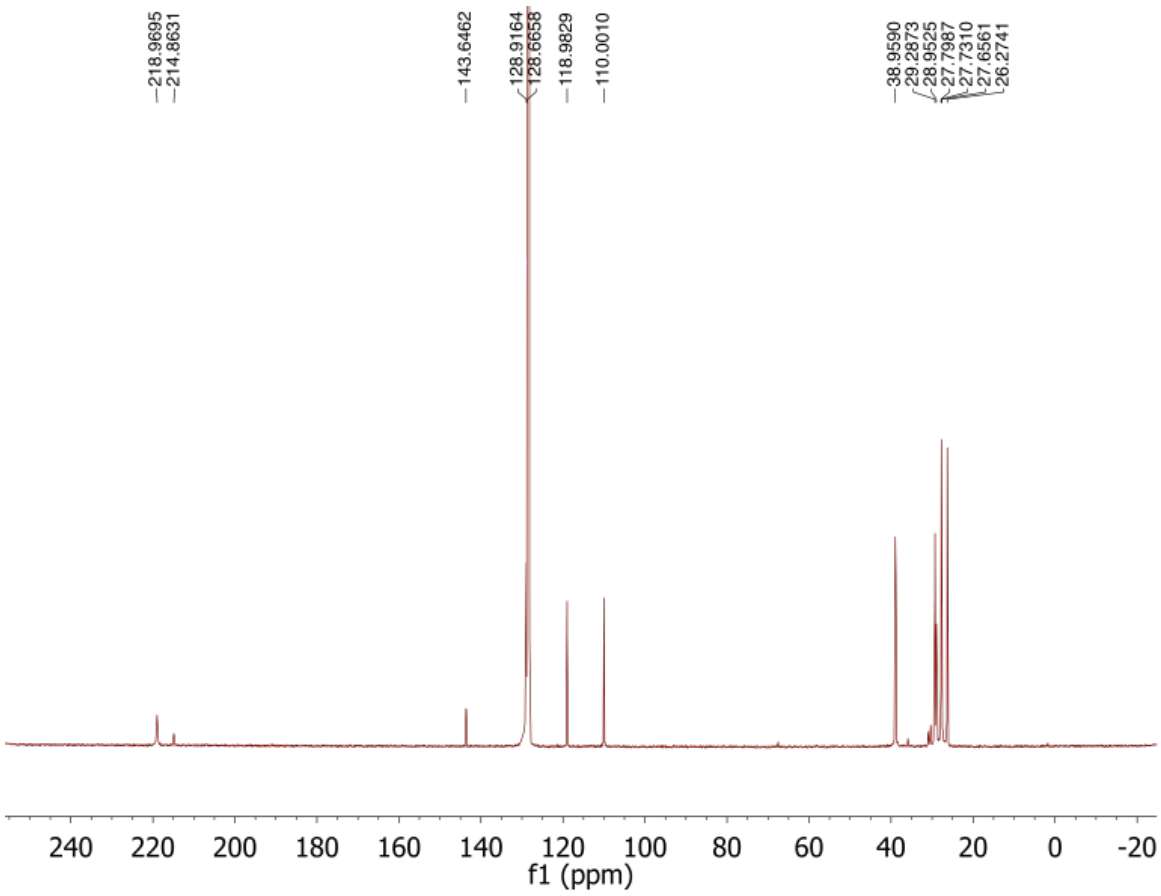

Figure 4.13: ^{13}CNMR of **12** in C_6D_6 Impurities are denoted with a *

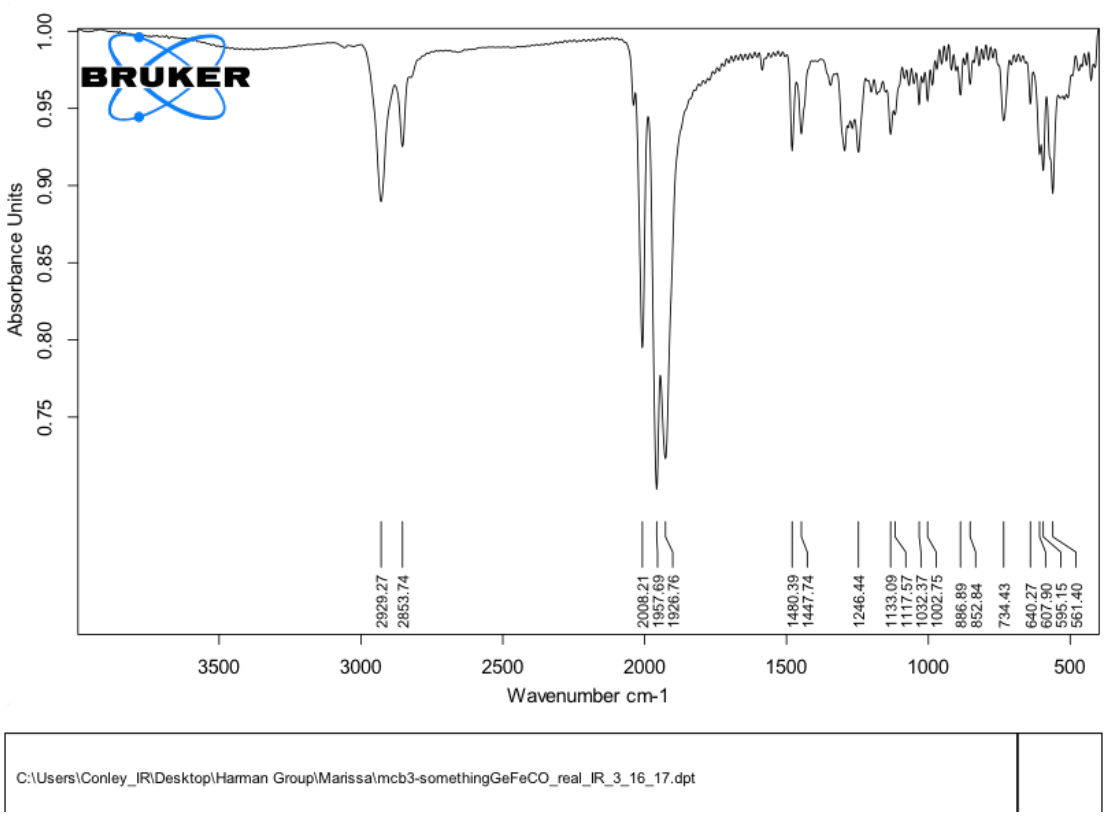

Figure 4.14: FTIR of **12**

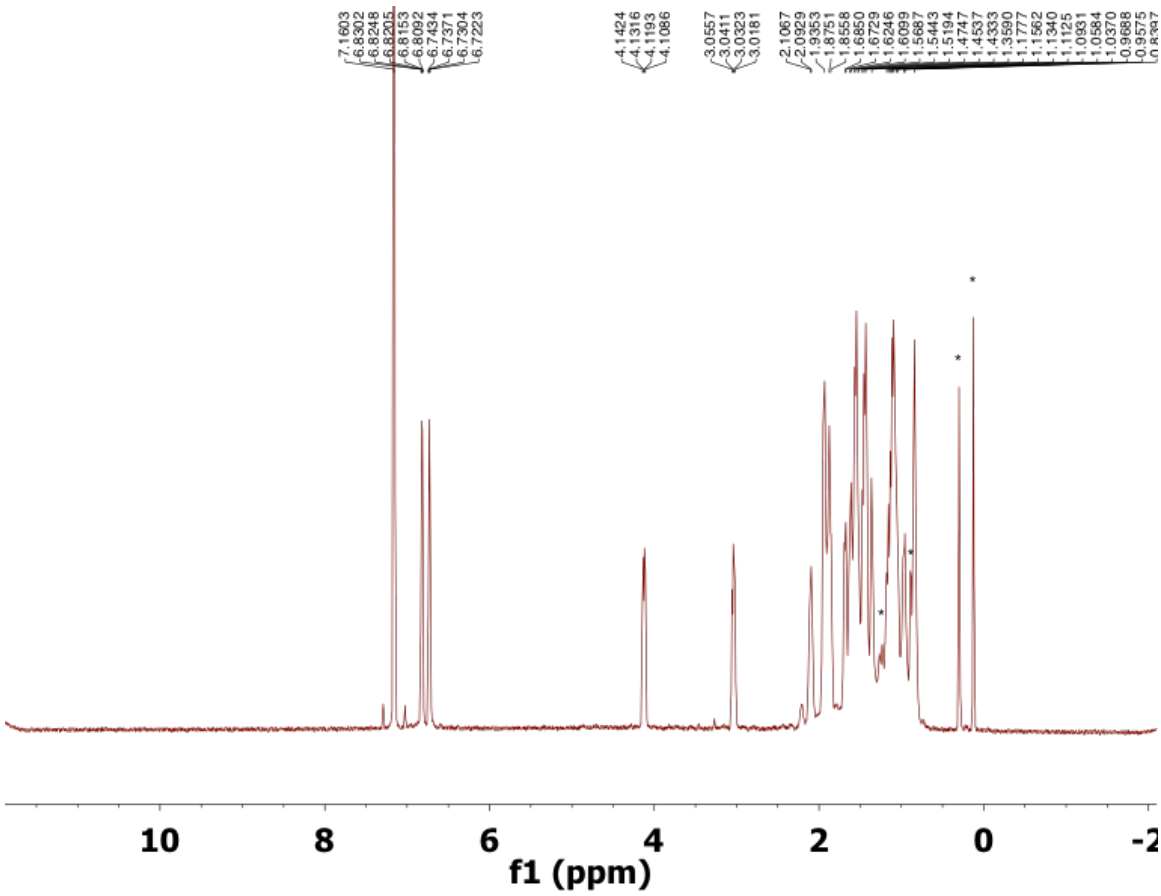

Figure 4.15: ^{1}HNMR of **13** in C_6D_6 Residual HMDSO, silicon grease and pentane are denoted with a *.

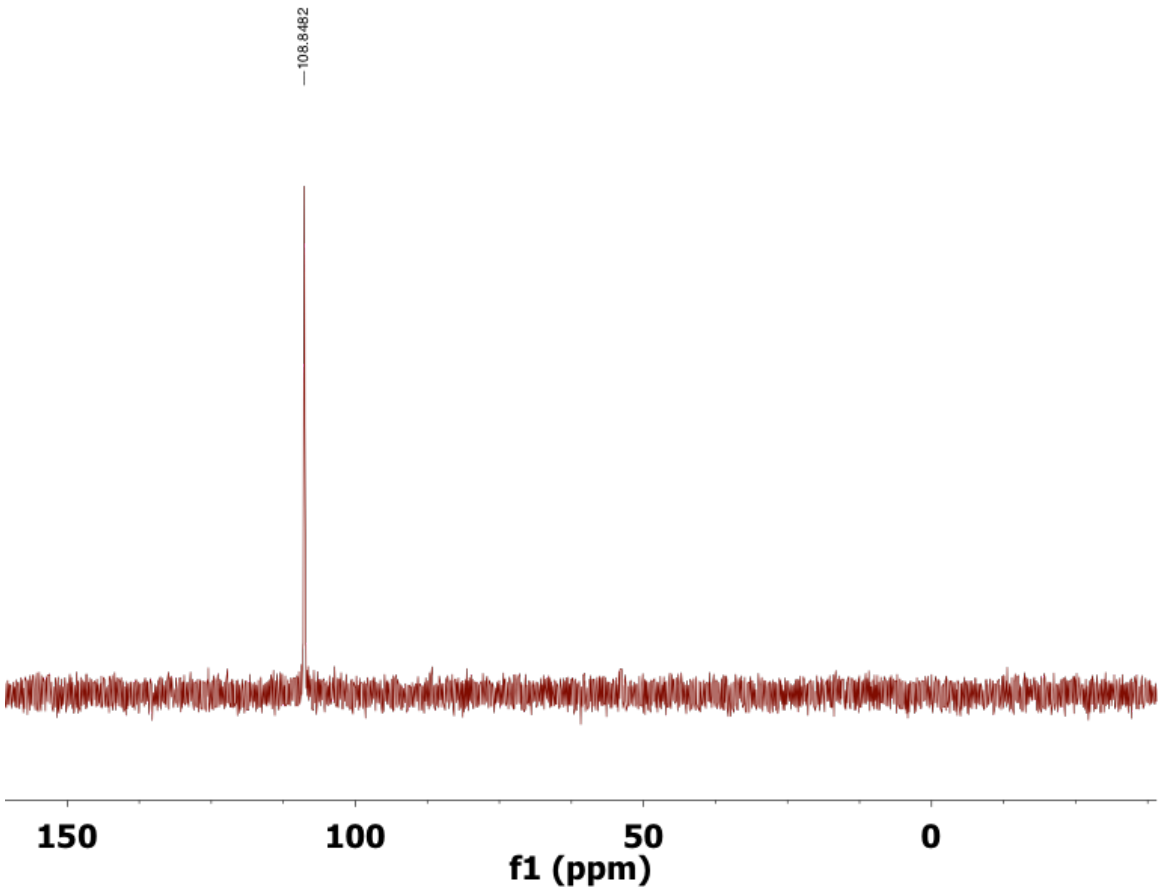

Figure 4.16: ^{31}PNMR of **13** in C_6D_6

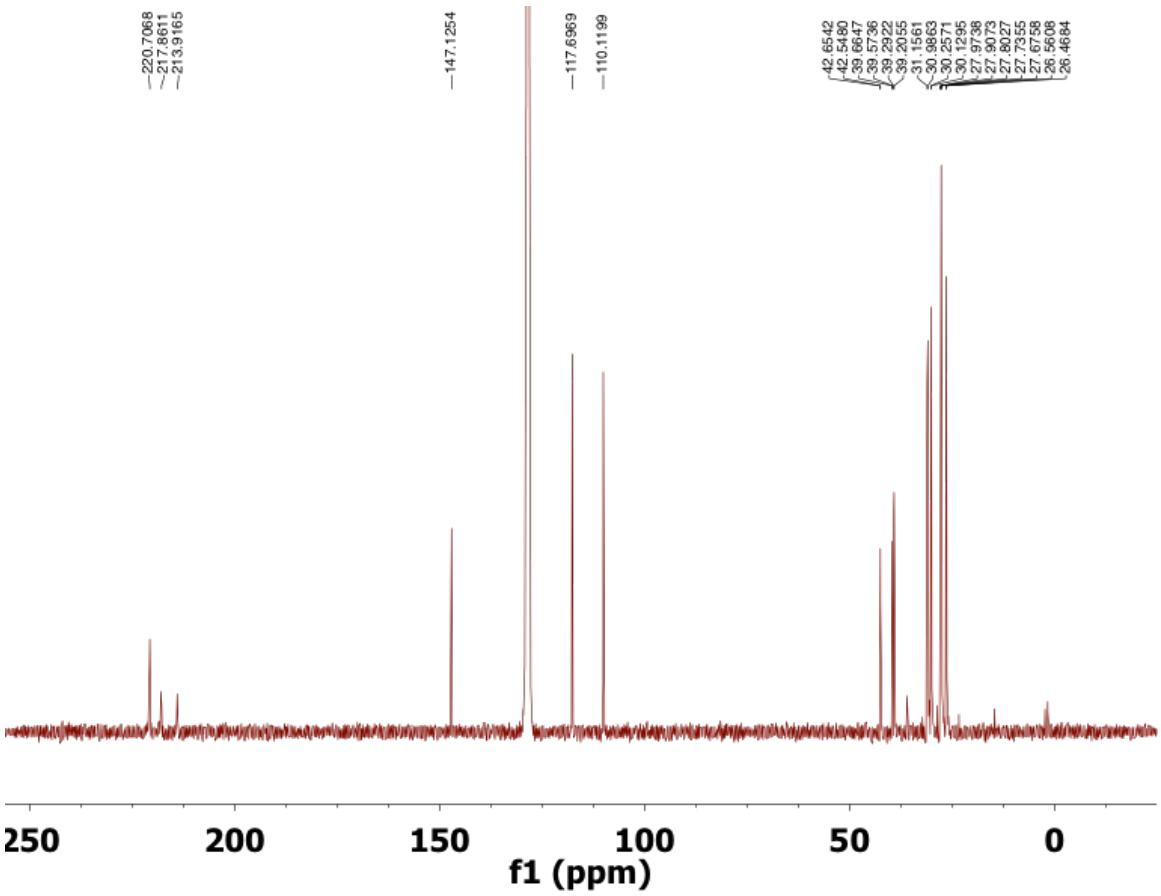

Figure 4.17: ^{13}CNMR of **13** in C_6D_6

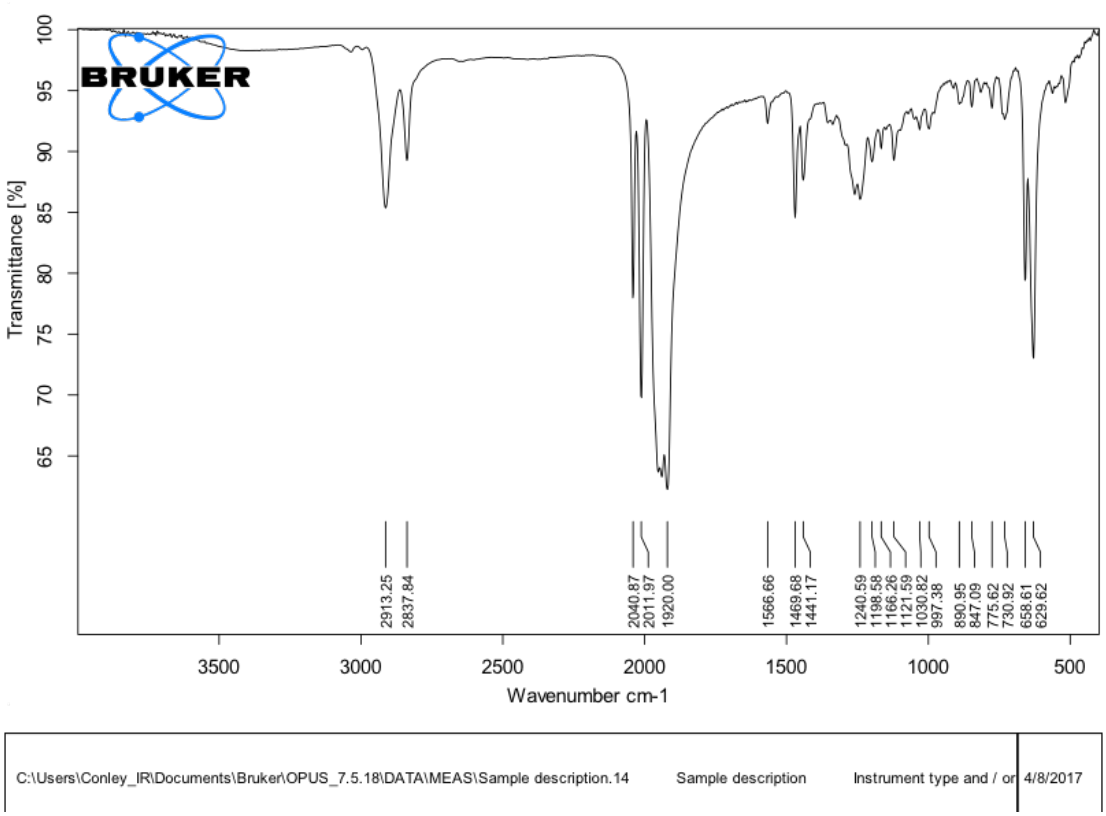

Figure 4.18: FTIR of **13**

	10	**11**	**12**
chemical formula	$C_{38}H_{52}Co_2GeN_2O_6P_2$	$C_{37}H_{52}Co_2GeN_2O_5P_2$	$C_{38}H_{52}Fe_2GeN_2O_6P_2$
formula weight	885.20	857.19	879.04
T (K)	100	100	100
l (Å)	0.71073	0.71073	0.72073
crystal system	monoclinic	monoclinic	monoclinic
space group	P 21/c (#14)	P21/n	P 21/c (#14)
a (Å)	15.2631(2)	14.8753(3)	13.8066(4)
b (Å)	14.6858(2)	16.5205(3)	16.7541(5)
c (Å)	18.7496(3)	15.5405(3)	17.1755(6)
α **(deg)**	90	90	90
β **(deg)**	107.9143(5)	98.4187(10)	92.3893(5)
γ **(deg)**	90	90	90
V (Å^3)	3998.98(10)	3777.89(13)	3969.5(2)
Z	4	4	4
$\mathbf{r}_{calcd}$ **(g/cm^3**	1.470	1.507	1.471
$\mathbf{R}_1$**,** $\mathbf{R}_{W2}$	0.0319, 0.0615	0.0468, 0.0650	0.0330, 0.0666
GOF	1.067	1.036	1.033

Table 4.1: Crystallographic Data for Complex **10**, **12**

	13	**14**	**15**
chemical formula	$C_{45.08}H_{63.86}GeMn_2N_2O_8P_2$	$C_{52}H_{82}Co_2GeN_2P_2$	$C_{82}H_{113}Fe_2Ge_2N_4P_4$
formula weight	1006.27	987.58	1555.68
T (K)	100	100	100
l (Å)	0.71073	0.71073	0.71073
crystal system	triclinic	triclinic	triclinic
space group	P -1 (2)1	P -1 (2)	P -1 (2)
a (Å)	13.4157(5)	12.2765(3)	14.9894(8)
b (Å)	13.8194(5)	14.5534(4)	17.1562(9)
c (Å)	14.842(6)	15.0356(4)	17.8246(9)
α **(deg)**	94.2153(6)	84.5532(4)	113.5344(9)
β **(deg)**	110.3228(6)	88.6096(4)	102.0215(9)
γ **(deg)**	110.5939(6)	65.5674(4)	97.3694(9)
V (Å^3)	2355.37(16)	2434.39(11)	39994.5(4)
Z	2	2	2
$\mathbf{r}_{calcd}$ **(g/cm^3**	1.419	1.347	1.293
$\mathbf{R}_1$**,** $\mathbf{R}_{W2}$	0.0377, 0.0986	0.0268, 0.0637	0.0521, 0.0889
GOF	1.108	1.045	1.022

Table 4.2: Crystallographic Data for Complex **13**, **14**, **15**

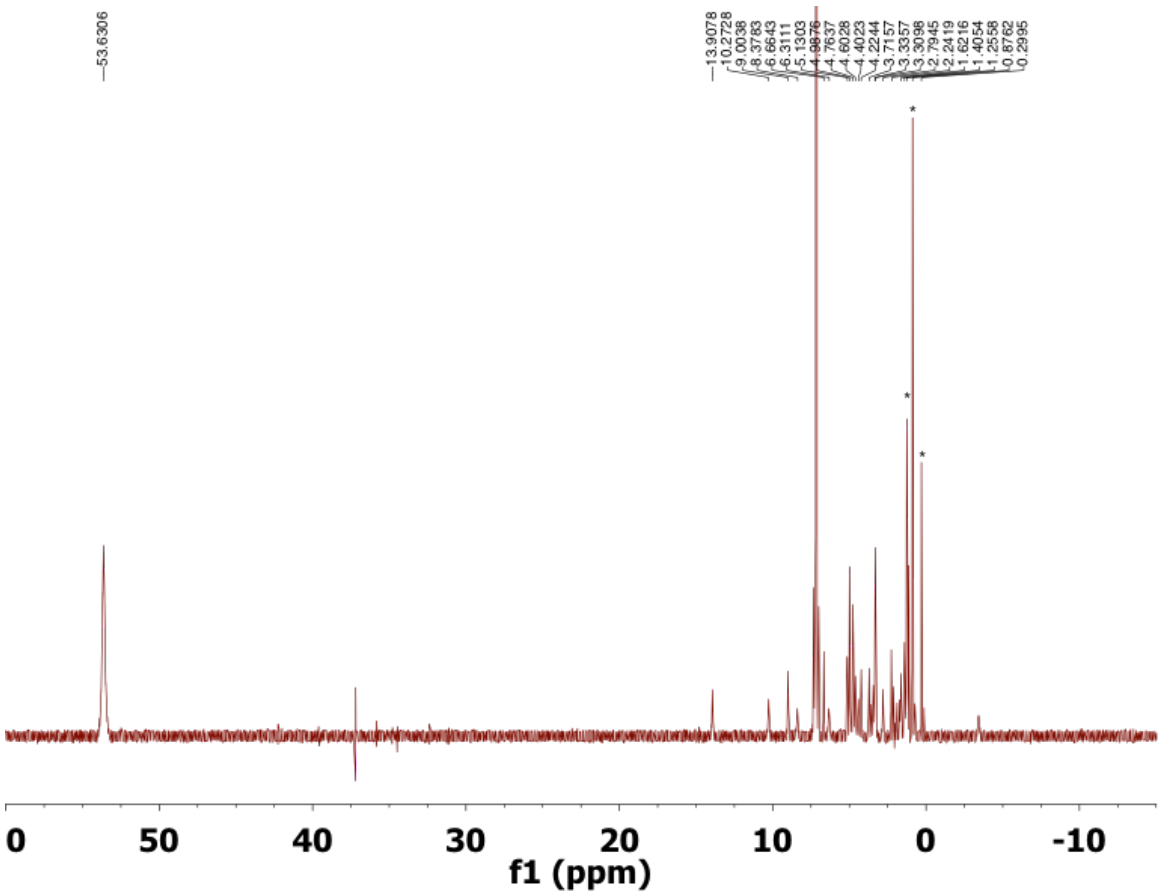

Figure 4.19: ^{1}HNMR of **14** in C_6D_6 Residual HMDSO, silicon grease and pentane are denoted with a *.

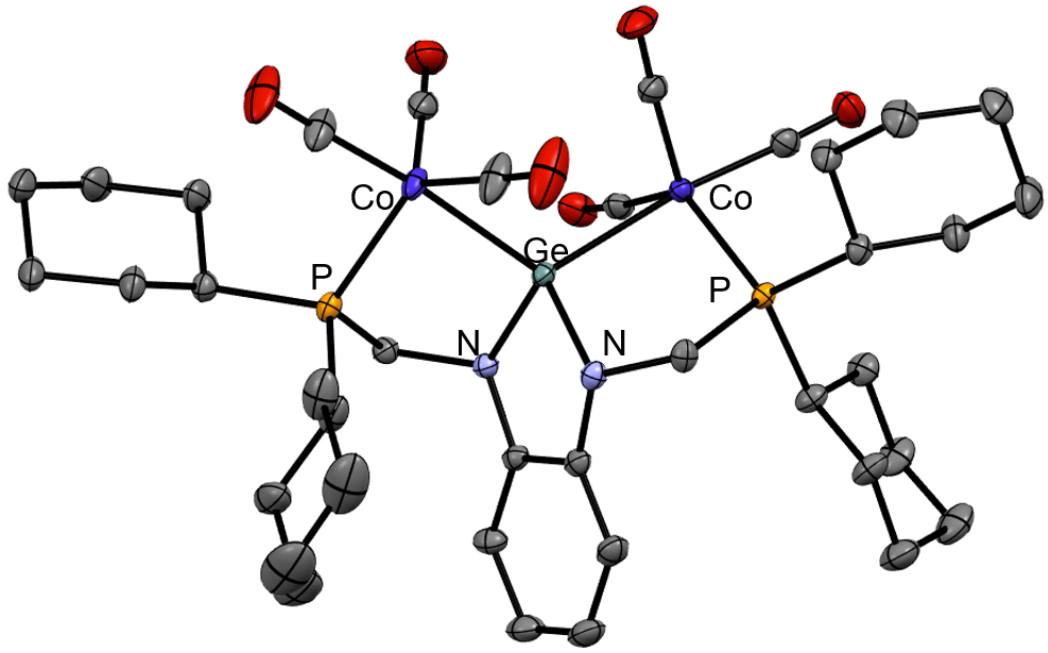

Figure 4.20: Thermal ellipsoid plot at 50% probability of the bimetallic cobalt carbonyl complex **10**. Orange, gray blue, teal, blue, red and grey ellipsoids correspond to phosphorus, nitrogen, germanium, cobalt, oxygen and carbon atoms, respectively. Hydrogen atoms bonded to carbon have been omitted for clarity.

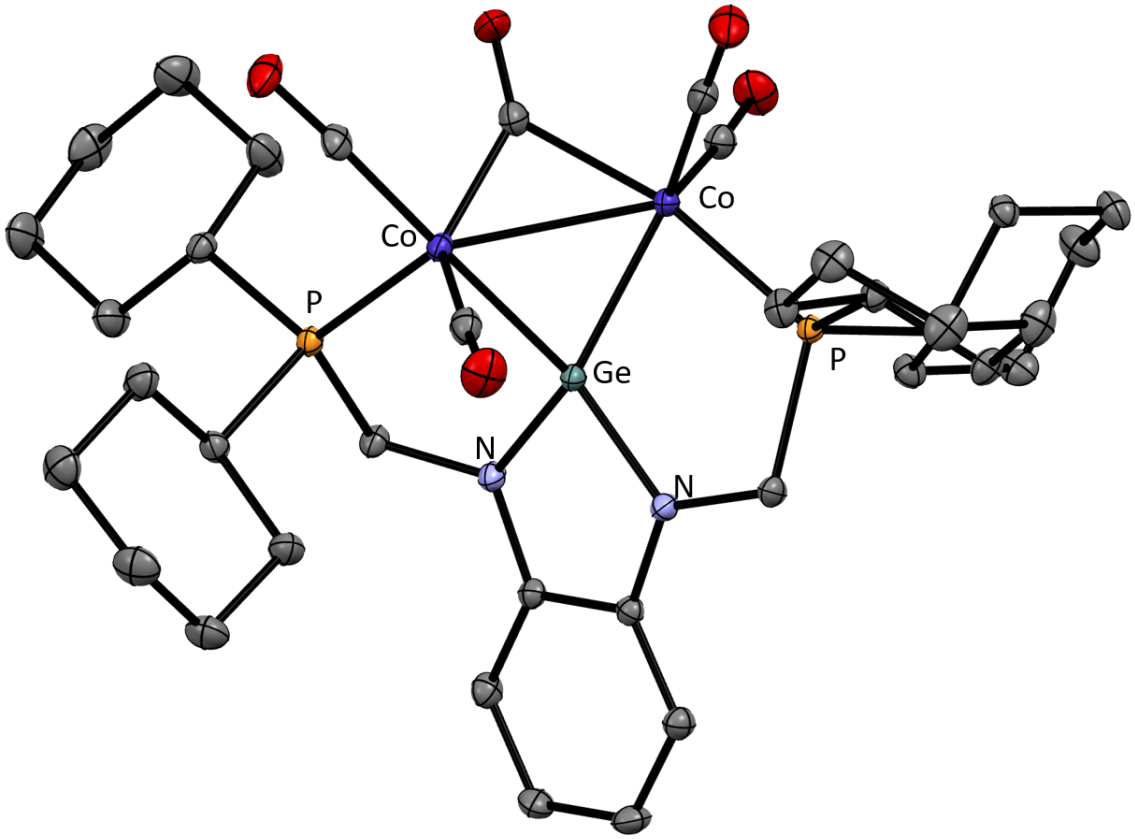

Figure 4.21: Thermal ellipsoid plot at 50% probability of the bimetallic cobalt carbonyl complex **11**. Orange, gray blue, teal, blue, red and grey ellipsoids correspond to phosphorus, nitrogen, germanium, cobalt, oxygen and carbon atoms, respectively. Hydrogen atoms bonded to carbon have been omitted for clarity.

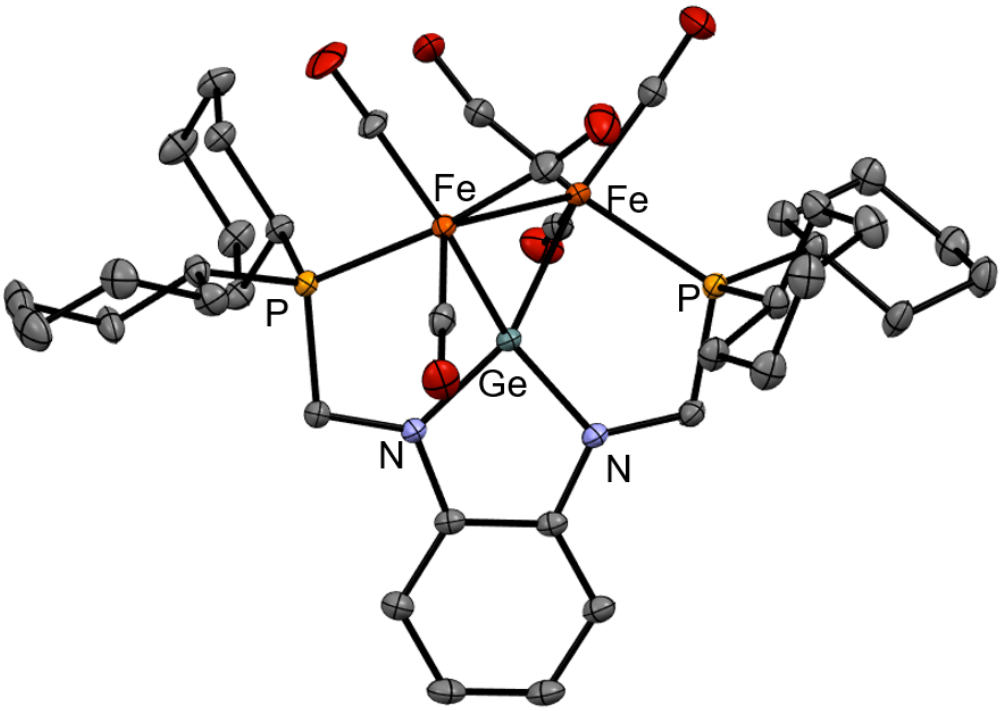

Figure 4.22: Thermal ellipsoid plot at 50% probability of the bimetallic iron carbonyl complex **12**. Light orange, gray blue, teal, orange, red and grey ellipsoids correspond to phosphorus, nitrogen, germanium, iron, oxygen and carbon atoms, respectively. Hydrogen atoms bonded to carbon have been omitted for clarity.

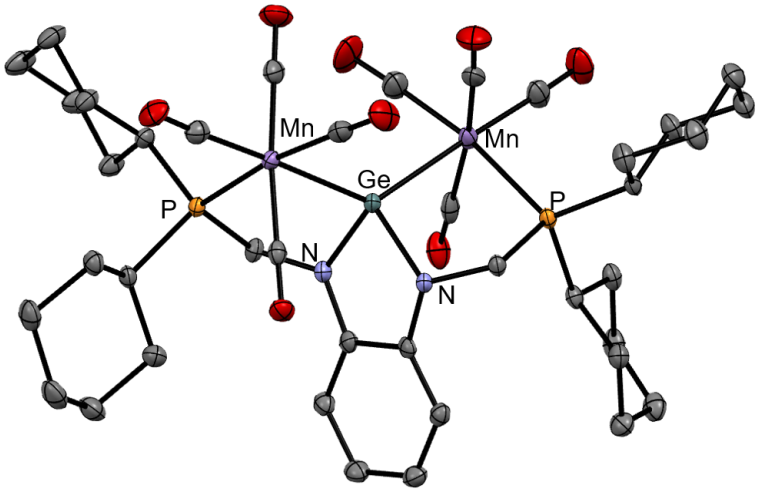

Figure 4.23: Thermal ellipsoid plot at 50% probability of the bimetallic manganese carbonyl complex **13**. Light orange, gray blue, teal, purple, red and grey ellipsoids correspond to phosphorus, nitrogen, germanium, manganese, oxygen and carbon atoms, respectively. Hydrogen atoms bonded to carbon have been omitted for clarity.

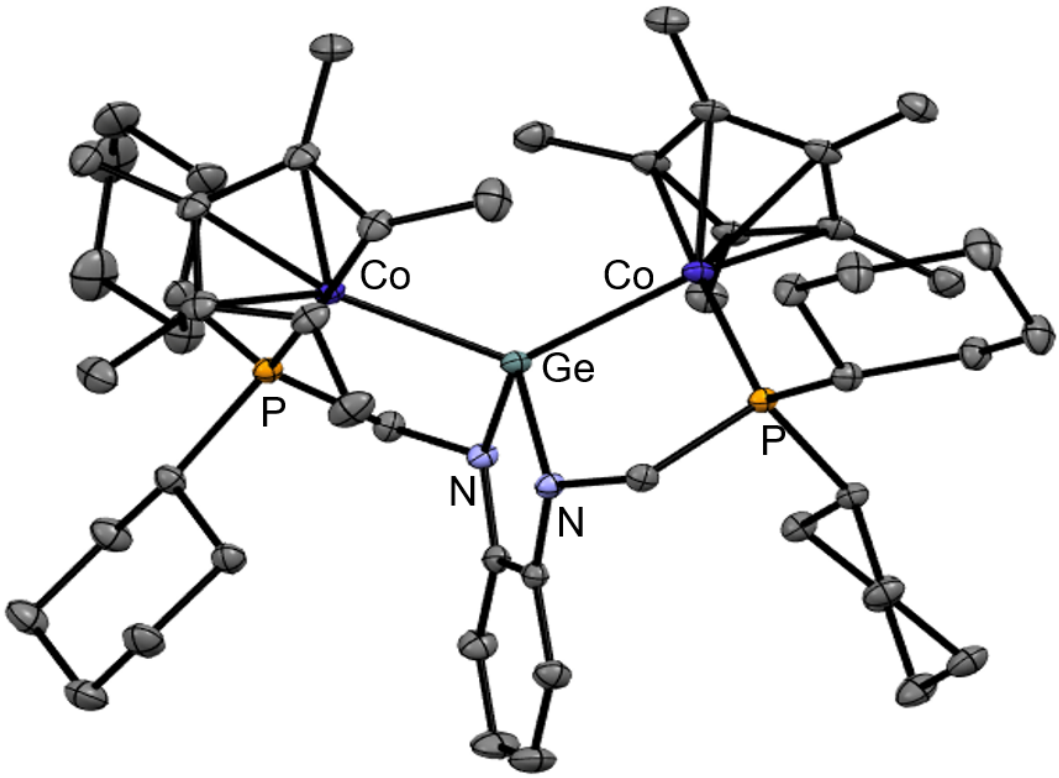

Figure 4.24: Thermal ellipsoid plot at 50% probability of the bimetallic cobalt complex **14**. Light orange, gray blue, teal, blue and grey ellipsoids correspond to phosphorus, nitrogen, germanium, cobalt, and carbon atoms, respectively. Hydrogen atoms bonded to carbon have been omitted for clarity.

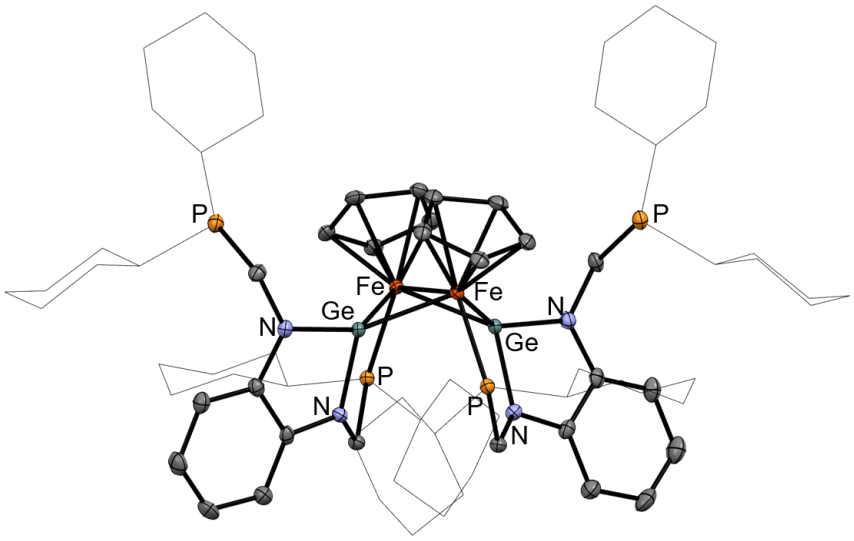

Figure 4.25: Thermal ellipsoid plot at 50% probability of the bimetallic iron complex **15**. Light orange, gray blue, teal, orange and grey ellipsoids correspond to phosphorus, nitrogen, germanium, iron, and carbon atoms, respectively. Hydrogen atoms bonded to carbon have been omitted for clarity.

Chapter 5

Reactivity with Carbon Dioxide

5.1 Abstract

We were successful in synthesizing a reduced Pd silylene dimer capable of small molecule activation. The Pd(0) dimer complexes was shown to be reactive with carbon dioxide to form a carbonate adduct. The complex also reacted with water and various O-atom sources. While these processes are not catalytic, they still provide fundamental insight on the reactivity of this class of Pd silylene dimers.

5.2 Introduction

With the beginning of the industrial revolution, there seems to be a rise in the level of atmospheric carbon dioxide as a result of anthropogenic activities. As levels of carbon dioxide rise, scientists turn towards carbon neutral based approaches to energy by seeking ways to capture CO_2 from the atmosphere and convert it into methanol and other fuels

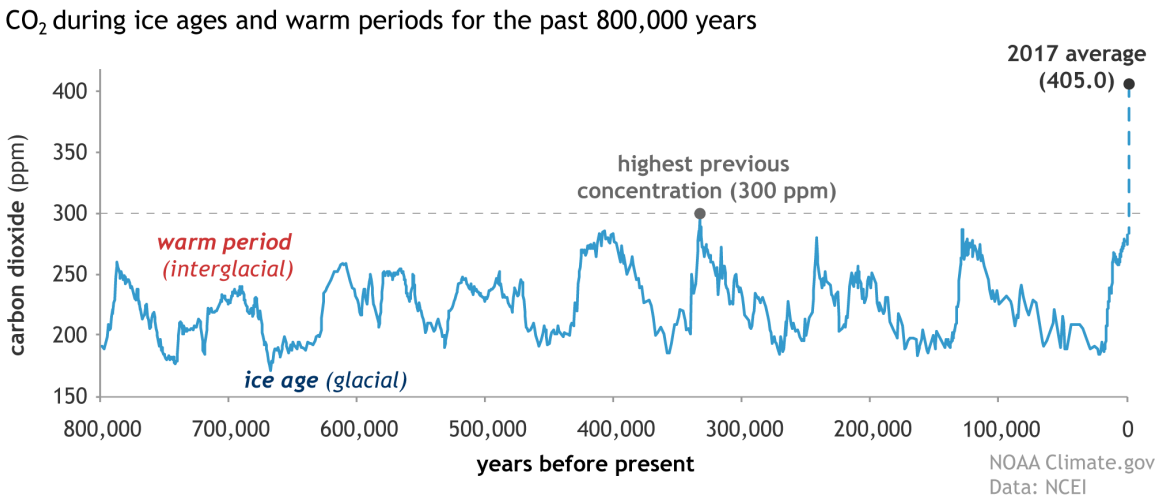

Figure 5.1: Rising Levels of Carbon Dioxide: Climate.gov "Climate Change: Atmospheric Carbon Dioxide"

photocatalytically. However there are many challenges associated with this process[1][2].

If we begin to examine the different reactions necessary to convert carbon dioxide to fuel, we see that many of these processes are multi-electron involving 4, 6, and up to 8 electrons. One major challenge is that many metal oxidation/reduction processes involve only 1 or 2 electron processes, so finding a system capable of multi-electron processes is a challenge. Furthermore, there are also competitive reactions which make this difficult such as the completing H+ to hydrogen reduction which occurs at a higher potential.

To solve this issue, nature has created enzymes, carbon monoxide dehydrogense, capable of converting carbon dioxide to carbon monoxide. These enzymes contain bimetallic

	E°(v)	
$CO_2 + e^- \longrightarrow CO_2^{-\cdot}$	-1.9	(5.1)
$CO_2 + 2e^- + 2H^+ \longrightarrow CO + H_2O$	-0.53	(5.2)
$CO_2 + 2e^- + 2H^+ \longrightarrow HCOOH$	-0.61	(5.3)
$CO_2 + 4e^- + 4H^+ \longrightarrow H_2CO + H_2O$	-0.48	(5.4)
$CO_2 + 6e^- + 6H^+ \longrightarrow H_3COH + H_2O$	-0.38	(5.5)
$CO_2 + 8e^- + 8H^+ \longrightarrow CH_4 + 2H_2O$	-0.24	(5.6)
$H^+ + 2e^- \longrightarrow H_2$	-0.41	(5.7)

metal ceters, one being Fe-Ni based, the other Mo-Cu. Taking inspiration from these bimetallic catalysts, we hoped to explore similar reactivity with our bisphosphino Pd silylene dimer. We also sought to pursue late group 10 transition metals since another challenge of carbon dioxide activation is breaking the M-O bond once formed. However group 10 M-O bonds are weaker making potential catalytic transformations more facile[3].

In the literature, there exists relatively few examples of group 10 bimetallic silylene complexes. There is a diiron (I) complex that reacts with CO_2 to give a carbonate adduct and CO[4]. However, there is precedent for group 10 reactivity with carbon dioxide. The first nickel-CO_2 adduct was isolated in 1975[5], and more recently in an analogous compound was isolated in 2010 by Hillhouse[6]. In attempts to mimic the CODH active site, Lee et al, synthesized a Ni-Fe bimetallic complex by adding an iron fragment to a Ni-CO_2 adduct[7].

5.3 Results and Discussion

While we were unable to isolate a reduced species of **6**, a co-worker, Amy Bartrom Jehl, had sucess in reducing the analogous compound with cyclohexyl phosphine arm substituents as opposed to tert-butyl substituents. The reduction of this compound resulted in a nickel silylene dimer. We suspect that the tert-butyl substituents are too bulky and

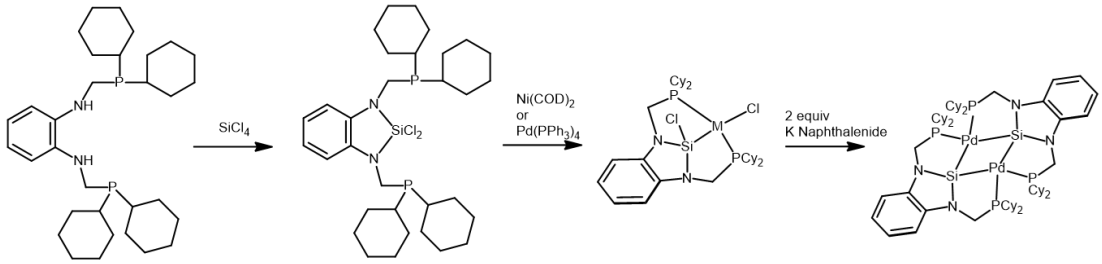

Scheme 5.1: Reduction of **19** to **16**

prevent the reduced species from dimerizing. Without this dimerization, we have been otherwise unable to isolate a stable reduced species[8]. This discovery led us to explore whether the palladium cyclohexyl compound, **19** could also be reduced. We began by using the same procedures previously established by Amy, and found that reduction of **19** using 2.2 equivalents of KC_8 in benzene resulted in a dark green compound. This compound is very similar spectroscopically to its nickel analog. At room temperature, we observe a very broad ^{31}PNMR around 73 ppm. After performing VT experiments, we concluded this broad signal is due to fluctional behavior. Based off of calculations using the VT spectrum in 5.5 we estimated the energy difference between the two conformers to be approximately .22kJ/mol. At low temperatures, we see two phosphine signals consistant with C2 rotational symmetry as there are a total of 4 phosphines. At high temperatures the fluctional behavior makes all phosphines equivalent as indicated by a single PNMR peak around 73ppm. This dynamic behavior is similar to that observed in the nickel silylene cyclohexylphosphine dimer.

We next sought to explore reactivity. Interestingly, in our hands, we were unable to get **16** to react with H_2. We did have success in reacting **16** with 2 equivalents of carbon

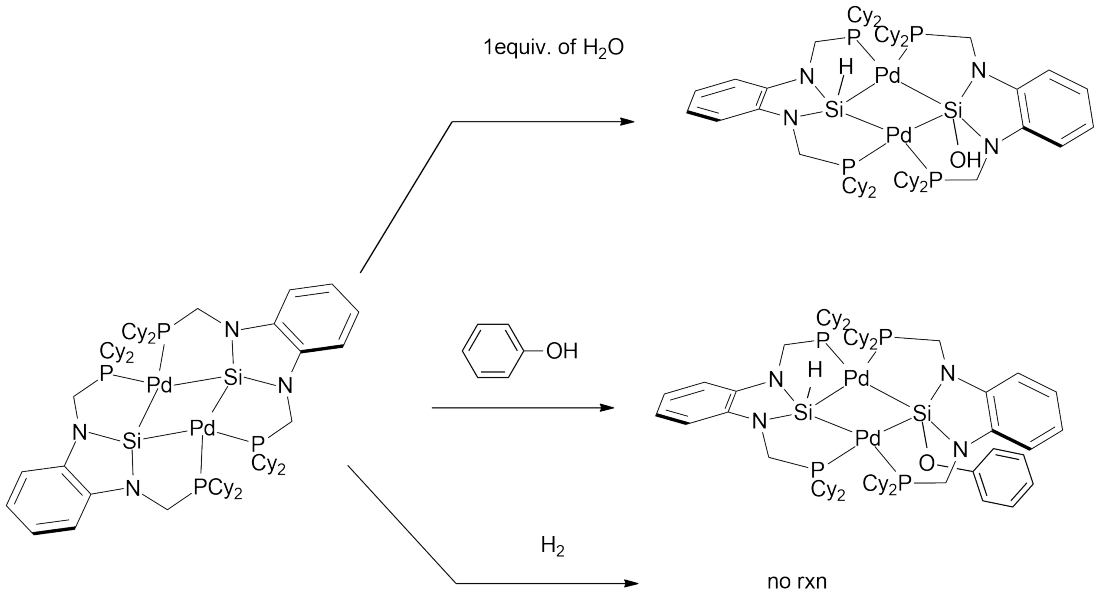

Figure 5.2: E-H Activation with **16**

dioxide to form **17** and releasing an equivalent of carbon monoxide. When we react **16** with one equivalent of carbon dioxide, we get a new compound, but we have been unsuccessful in isolating the compound. From the phosphorus NMR, we know it is a product that has C2 rotational symmetry, but further studies are needed in this area. The carbonate is added across the silicon with silicon being 5 coordinate, but formally Si(IV) with one of the palladium's acting as an L type ligand to support one silicon. This difference in types of bond to each silicon from the palladium is supported by the differences in bond lengths. Each silicon center has one bond length of 2.6 $\AA$ to one Pd center and 2.4 $\AA$ to the other Pd.

We also explore the reactivity of **16** with various oxygen atom sources such as oxygen, pyridine n-oxide, and nitrous oxide. Each reaction gave a consistent product **18** as most easily characterized by two ^{31}PNMR signals at 52 and 45.8 ppm 5.14. This also

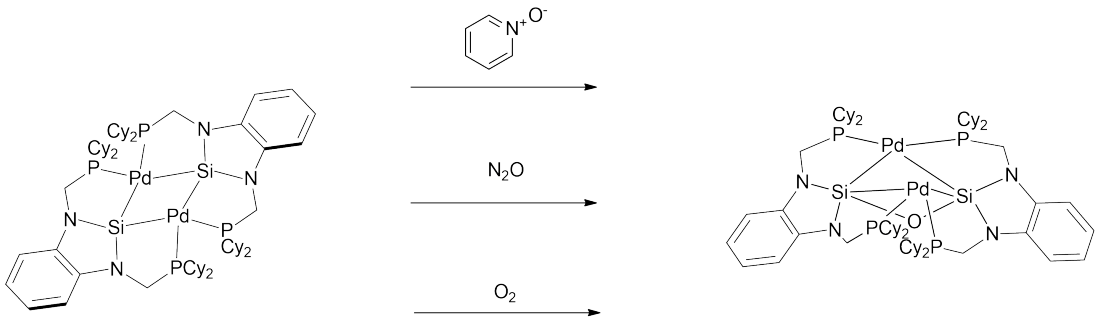

Figure 5.3: Various routes to **18**

indicates that the molecule posses C2 symmetry. These results are also consistent with results from co-workers in the lab on the analogous nickel oxygen bridged compound.

5.4 Experimental Section

5.4.1 Synthetic Materials and Methods

Unless started otherwise, all compounds were purchased from commercial sources and used without further purification. Solvents were dried and deoxygenated by argon sparge followed by passage through an activated alumina column and were stored over $4\mathring{A}$ molecular sieves. All manipulations were performed under an N_2 atmosphere either in a glovebox or using standard Schlenk techniques. NMR spectra were recorded at 298K using a Varian 300 MHz, 500 MHz, or Bruker 600 MHz instruments. Chemical shifts in ^{1}H NMR are referenced to deuterated solvent. Chemical shifts in ^{31}P NMR are referenced to phosphoric acid. Mass spectra were recorded using either an Agilent LCTOF mass spectrometer or a Waters GCT high-resolution mass spectrometer operating in LIFDI mode. Elemental analysis was performed by Midwest Microlab, LLC; Indianapolis, IN.

5.4.2 $Si_2Pd_2((NCH_2PCy_2)_2C_6H_4)_2$ (16)

19 was dissolved in a solution of minimal benzene. A suspension of potassium naphthalenide in benzene was added to this solution with mixing. The reduction was monitored by ^{31}PNMR and after approximatley one hour the reaction was determined to by done as characterized by a broad peak at 72.54 ppm in the ^{31}PNMR as shown in 5.5. The reaction mixture was filtered through a pad of celite and the volatiles were evaporated under reduced pressure. The resulting solid was recrystalized from a concentrated solution of ether to give dark green crystals.

^{1}HNMR:(600 MHz, C_6D_6)δ 6.96 (dt, J = 6.2, 3.0 Hz, 4H), 6.86 (dt, J = 6.2, 3.0 Hz, 4H), 3.91 (d, J = 13.0 Hz, 4H), 3.24 (d, J = 13.1 Hz, 4H), 2.02 (d, J = 13.2 Hz, 4H), 1.85 (d, J = 13.0 Hz, 4H), 1.77 (t, J = 12.8 Hz, 8H), 1.72 (d, J = 15.2 Hz, 7H), 1.65 (q, J = 14.1, 13.6 Hz, 21H), 1.55 (d, J = 12.4 Hz, 7H), 1.44 (t, J = 12.6 Hz, 4H), 1.28 (d, J = 12.6 Hz, 8H), 1.24 (d, J = 8.3 Hz, 7H), 1.23 1.06 (m, 14H), 1.06 0.95 (m, 5H).

^{31}PNMR (243 MHz, C_6D_6): δ 72.54 (s).

^{13}CNMR (151 MHz, C_6D_6): δ 142.43, 127.77, 127.61, 127.45, 117.26, 107.66, 38.86, 38.78, 37.84, 35.44, 29.56, 29.09, 27.72, 27.59, 27.31, 27.23, 27.12, 26.58, 26.46. ^{29}SiNMR (119 MHz, C_6D_6): δ 173.33 (s).

5.4.3 $Si_2Pd_2CO_2((NCH_2PCy_2)_2C_6H_4)_2$ (17)

16 was dissolved in benzene. The solution underwent three freeze, pump, cycles using liquid nitrogen. After the final thawing cycle, the solution was exposed to a flow of

UHP carbon dioxide. The mixture was stirred and turned orange immediately. The solvent was reduced in vacuo and the solid was recrystalized from minimal hexanes/THF to give yellow crystals.

^{1}HNMR:(600 MHz, C_6D_6)δ 7.17 (s, 1H), 7.03 (dd, J = 7.8, 3.0 Hz, 1H), 6.89 (dd, J = 7.8, 3.1 Hz, 1H), 4.14 (t, J = 10.4 Hz, 1H), 3.86 3.79 (m, 1H), 3.54 (dq, J = 12.9, 4.2 Hz, 1H), 2.99 (d, J = 12.7 Hz, 1H), 2.26 (t, J = 12.0 Hz, 1H), 1.98 (d, J = 12.5 Hz, 1H), 1.91 (t, J = 12.3 Hz, 5H), 1.80 (s, 1H), 1.73 (q, J = 14.4, 13.6 Hz, 5H), 1.63 (d, J = 12.8 Hz, 4H), 1.57 (d, J = 12.9 Hz, 4H), 1.52 (d, J = 11.7 Hz, 3H), 1.46 (s, 1H), 1.43 (d, J = 13.8 Hz, 2H), 1.39 (s, 1H), 1.34 1.29 (m, 3H), 1.26 (d, J = 12.8 Hz, 2H), 1.20 1.14 (m, 2H), 1.12 (d, J = 14.0 Hz, 3H), 1.08 (s, 2H), 1.03 (dt, J = 24.8, 10.8 Hz, 6H), 0.93 (ddd, J = 25.9, 13.4, 3.6 Hz, 3H).

^{31}PNMR (243 MHz, C_6D_6): δ 52.02, 45.84.

^{13}CNMR (151 MHz, C_6D_6): δ 146.52, 141.46, 139.76, 128.06, 127.90, 127.74, 118.73, 116.74, 108.93, 107.61, 43.00, 41.21, 41.04, 36.68, 36.53, 34.87, 34.67, 33.76, 30.68, 30.44, 30.35, 28.69, 28.04, 27.92, 27.60, 27.42, 27.35, 27.25, 27.20, 27.16, 26.76, 26.57, 26.27, 25.98.

^{29}SiNMR (119 MHz, C_6D_6): δ 23.04 (m), 21.37 (m).

5.4.4 $Si_2Pd_2CO_2((NCH_2PCy_2)_2C_6H_4)_2$ (17)

16 was dissolved in benzene. The solution underwent three freeze, pump, cycles using liquid nitrogen. After the final thawing cycle, the solution was exposed to a flow of UHP carbon dioxide. The mixture was stirred and turned orange immediately. The solvent was reduced in vacuo and the solid was recrystalized from minimal hexanes/THF to give

yellow crystals.

^{1}HNMR:(600 MHz, C_6D_6)δ 7.17 (s, 1H), 7.03 (dd, J = 7.8, 3.0 Hz, 1H), 6.89 (dd, J = 7.8, 3.1 Hz, 1H), 4.14 (t, J = 10.4 Hz, 1H), 3.86 3.79 (m, 1H), 3.54 (dq, J = 12.9, 4.2 Hz, 1H), 2.99 (d, J = 12.7 Hz, 1H), 2.26 (t, J = 12.0 Hz, 1H), 1.98 (d, J = 12.5 Hz, 1H), 1.91 (t, J = 12.3 Hz, 5H), 1.80 (s, 1H), 1.73 (q, J = 14.4, 13.6 Hz, 5H), 1.63 (d, J = 12.8 Hz, 4H), 1.57 (d, J = 12.9 Hz, 4H), 1.52 (d, J = 11.7 Hz, 3H), 1.46 (s, 1H), 1.43 (d, J = 13.8 Hz, 2H), 1.39 (s, 1H), 1.34 1.29 (m, 3H), 1.26 (d, J = 12.8 Hz, 2H), 1.20 1.14 (m, 2H), 1.12 (d, J = 14.0 Hz, 3H), 1.08 (s, 2H), 1.03 (dt, J = 24.8, 10.8 Hz, 6H), 0.93 (ddd, J = 25.9, 13.4, 3.6 Hz, 3H).

^{31}PNMR (243 MHz, C_6D_6): δ 52.02, 45.84.

^{13}CNMR (151 MHz, C_6D_6): δ 146.52, 141.46, 139.76, 128.06, 127.90, 127.74, 118.73, 116.74, 108.93, 107.61, 43.00, 41.21, 41.04, 36.68, 36.53, 34.87, 34.67, 33.76, 30.68, 30.44, 30.35, 28.69, 28.04, 27.92, 27.60, 27.42, 27.35, 27.25, 27.20, 27.16, 26.76, 26.57, 26.27, 25.98.

^{29}SiNMR (119 MHz, C_6D_6): δ 23.04 (m), 21.37 (m).

5.4.5 $Si_2Pd_2O((NCH_2PCy_2)_2C_6H_4)_2$ (18)

This compound can be prepared by two methods.

Method A: **16** was dissolved in minimal benzene. To a stirring solution was added pyridine n-oxide in a solution of benzene. The reaction was allowed to go overnight with stirring. The dark-green solution became an orange solution overnight. The volatiles were reduced.and the compound was crashed out with ether. The parcipitate was washed with ether to remove excess pyridine n-oxide. **18** was recrystallized from minimal hexanes/THF.

Method B: **16** was dissolved in minimal benzene and subjected to three freeze, pump, thaw cycles. The solution was then exposed to UHP nitrous oxide. The solution turned orange immediately. The volatiles were reduced.and the compound was crashed out with ether. The parcipitate was washed with ether to remove excess pyridine n-oxide. **18** was recrystallized from minimal hexanes/THF. ^{1}HNMR:(600 MHz, C_6D_6)δ 7.19 7.13 (m, 4H), 6.89 (dd, J = 7.5, 1.3 Hz, 2H), 6.84 (dd, J = 7.5, 1.3 Hz, 2H), 3.98 (dd, J = 12.6, 10.4 Hz, 2H), 3.60 (dd, J = 12.6, 4.9 Hz, 2H), 3.50 (dt, J = 12.2, 3.1 Hz, 2H), 3.41 (dt, J = 12.4, 4.7 Hz, 2H), 2.26 (d, J = 13.2 Hz, 4H), 2.17 2.00 (m, 8H), 1.96 (t, J = 14.8 Hz, 2H), 1.88 (s, 8H), 1.86 1.78 (m, 4H), 1.75 (d, J = 12.6 Hz, 3H), 1.69 (d, J = 14.8 Hz, 2H), 1.63 1.56 (m, 12H), 1.56 1.50 (m, 2H), 1.50 (d, J = 11.1 Hz, 2H), 1.49 (s, 12H), 1.46 (d, J = 15.8 Hz, 4H), 1.38 1.08 (m, 18H), 1.08 1.01 (m, 4H), 1.01 0.92 (m, 2H). ^{31}PNMR (243 MHz, C_6D_6): δ 55.10, 44.34.

^{13}CNMR (151 MHz, C_6D_6): δ 13C NMR (151 MHz, Benzene-d6) 142.88, 134.29, 118.97, 115.97, 109.83, 106.48, 44.92, 44.76, 42.65, 38.57, 37.57, 35.86, 33.69, 31.72, 31.03, 30.74, 29.11, 29.01, 28.82, 28.68, 28.32, 27.81, 27.39, 27.13, 26.98, 26.85, 26.82, 26.53. ^{29}SiNMR (119 MHz, C_6D_6): δ 6.60 (m), 5.40 (m)

5.5 References

Bibliography

[1] Lackner, K. S.; Brennan, S.; Matter, J. M.; Park, A.-H. A.; Wright, A.; van der Zwaan, B. *Proceedings of the National Academy of Sciences* **2012**, *109*, 13156–13162.

[2] Bolton, J. R. *Science* **1978**, *202*, 705–711.

[3] Hazari, N.; Heimann, J. E. *Inorganic Chemistry* **2017**, *56*, 13655–13678, PMID: 29115825.

[4] Sadique, A. R.; Brennessel, W. W.; Holland, P. L. *Inorganic Chemistry* **2008**, *47*, 784–786, PMID: 18171059.

[5] Aresta, M.; Nobile, C. F.; Albano, V. G.; Forni, E.; Manassero, M. *J. Chem. Soc., Chem. Commun.* **1975**, 636–637.

[6] Anderson, J. S.; Iluc, V. M.; Hillhouse, G. L. *Inorganic Chemistry* **2010**, *49*, 10203–10207, PMID: 20883021.

[7] Yoo, C.; Lee, Y. *Chem. Sci.* **2017**, *8*, 600–605.

[8] Jehl, A. B. N-Heterocyclic Silyl and Silylene Metal Complexes with a PSiP Framework: Synthesis, Structure, and Reactivity. Ph.D. thesis, University of California at Riverside, 2019.

5.6 Figures, Schemes, and Tables

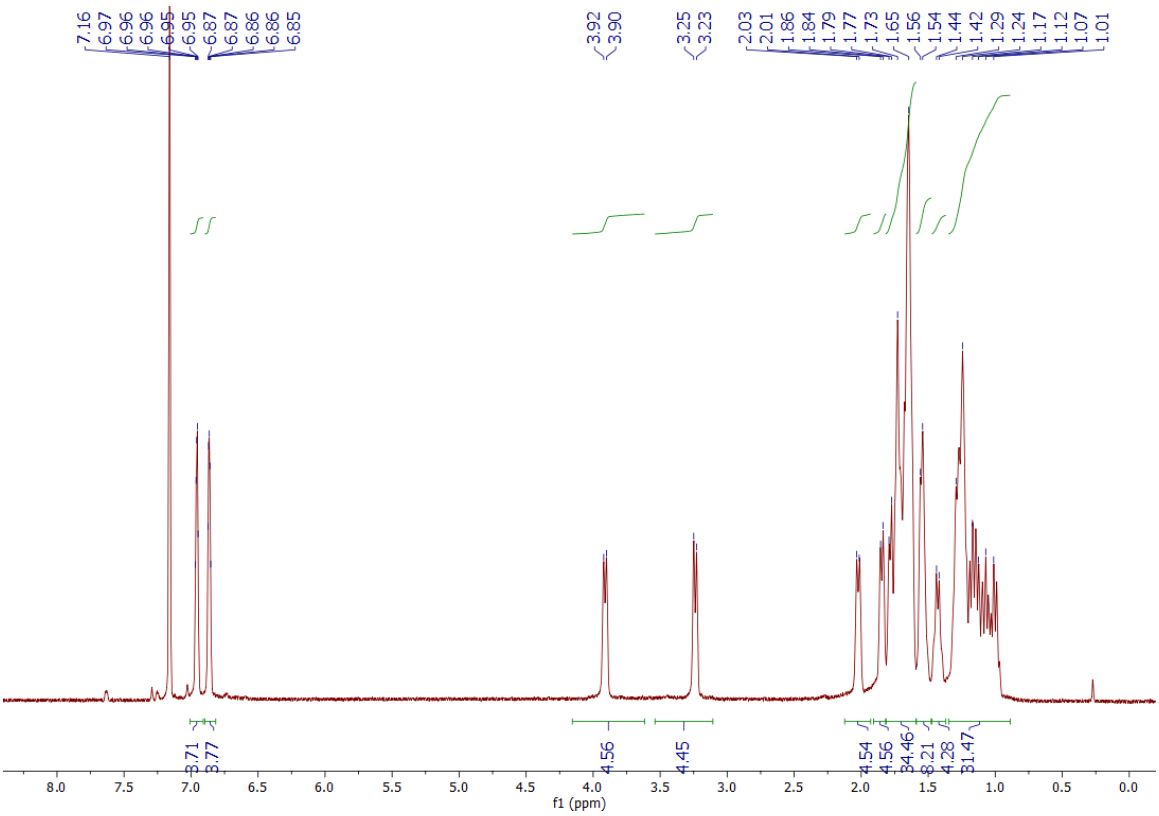

Figure 5.4: ^{1}HNMR spectrum of **16** at 65°C in C_6D_6, 600MHz.

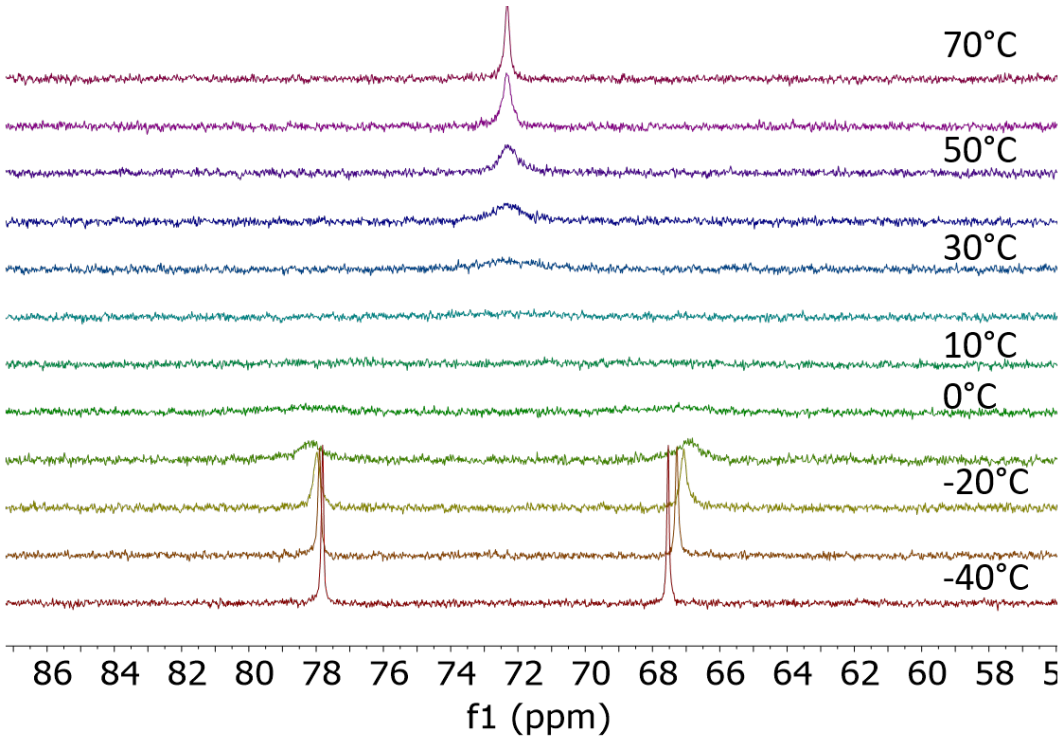

Figure 5.5: Variable Temperature ^{31}PNMR spectrum of **16** from -40°C to 70°C in C_6D_6, 600MHz.

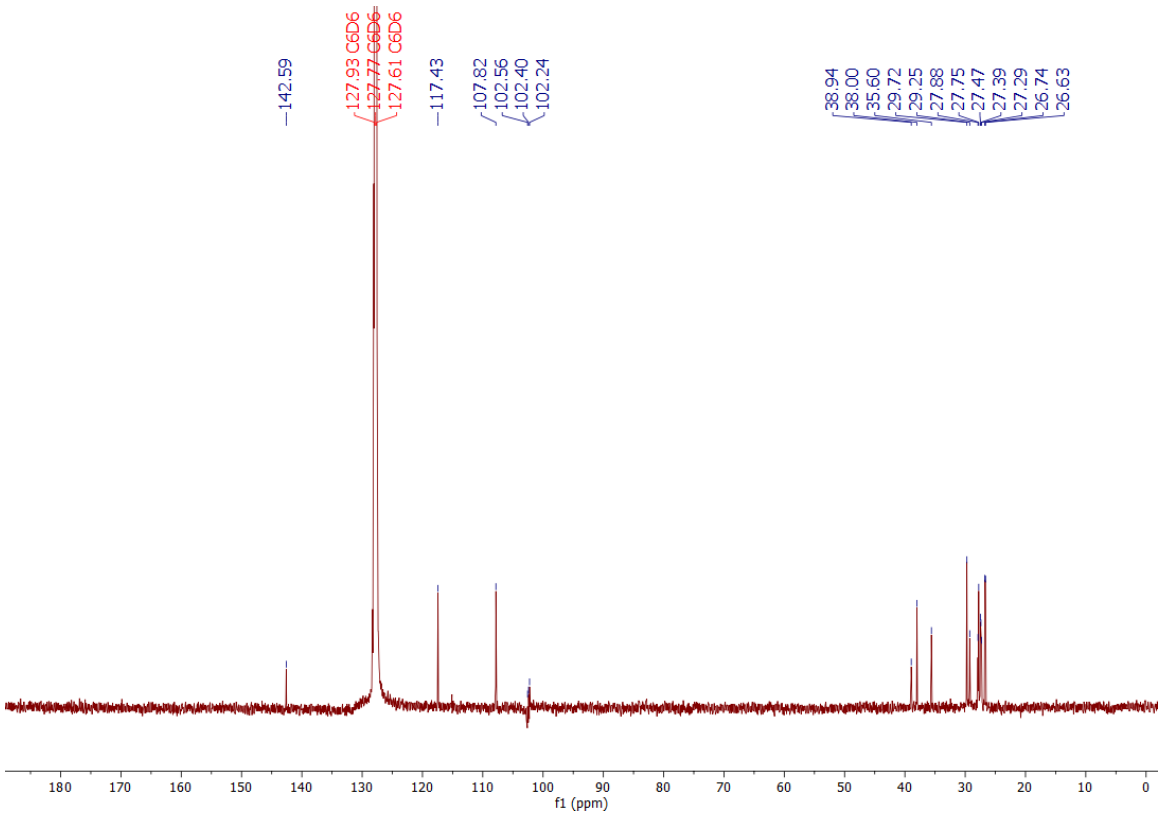

Figure 5.6: ^{13}CNMR spectrum of **16** at 65°C in C_6D_6, 600MHz.

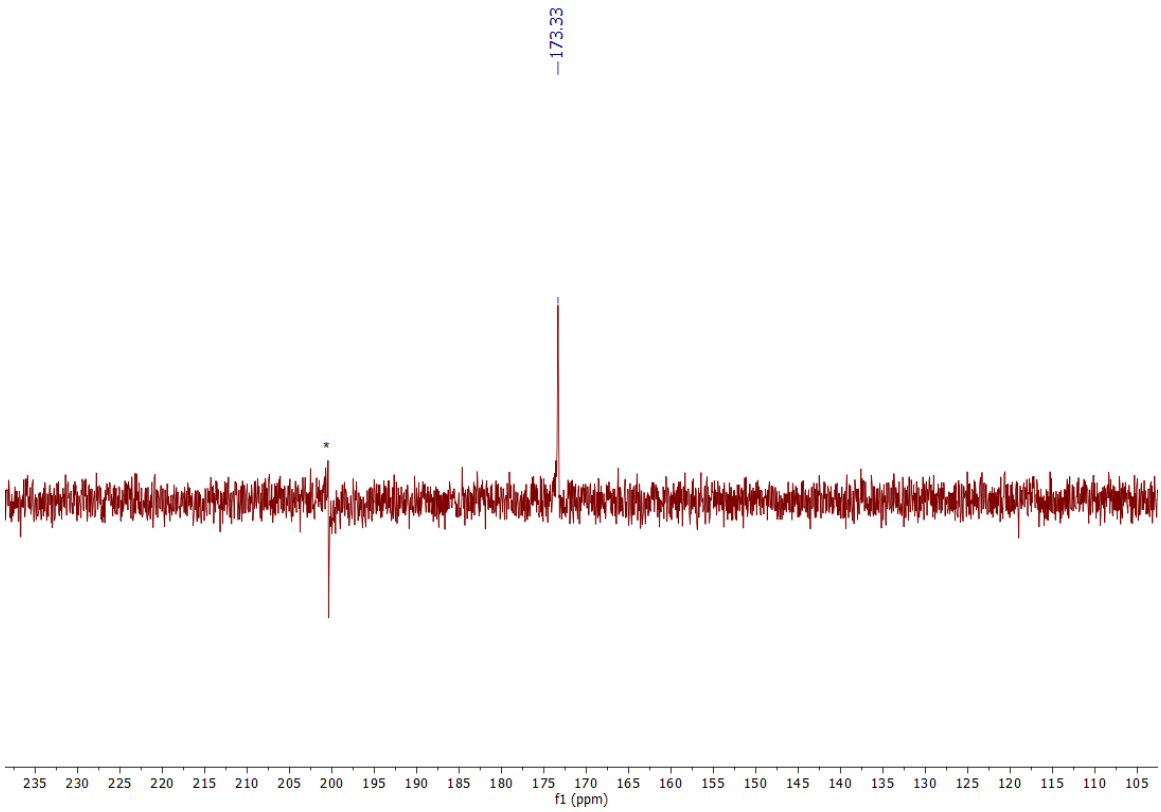

Figure 5.7: ^{29}SiNMR spectrum of **16** at 65°C in C_6D_6, 600MHz. Spectrum was centered at 200ppm resulting in an artifact noted with an *

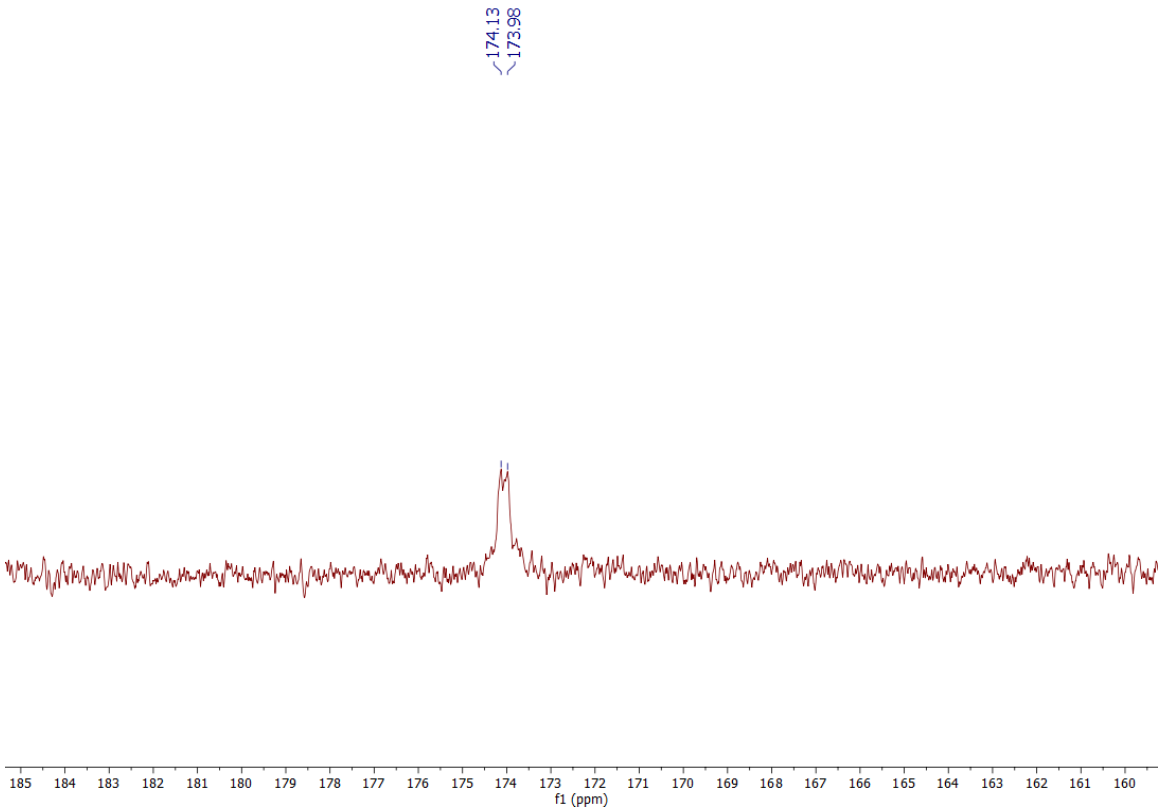

Figure 5.8: ^{29}SiNMR spectrum of **16** at -40°C in C_6D_6, 600MHz.

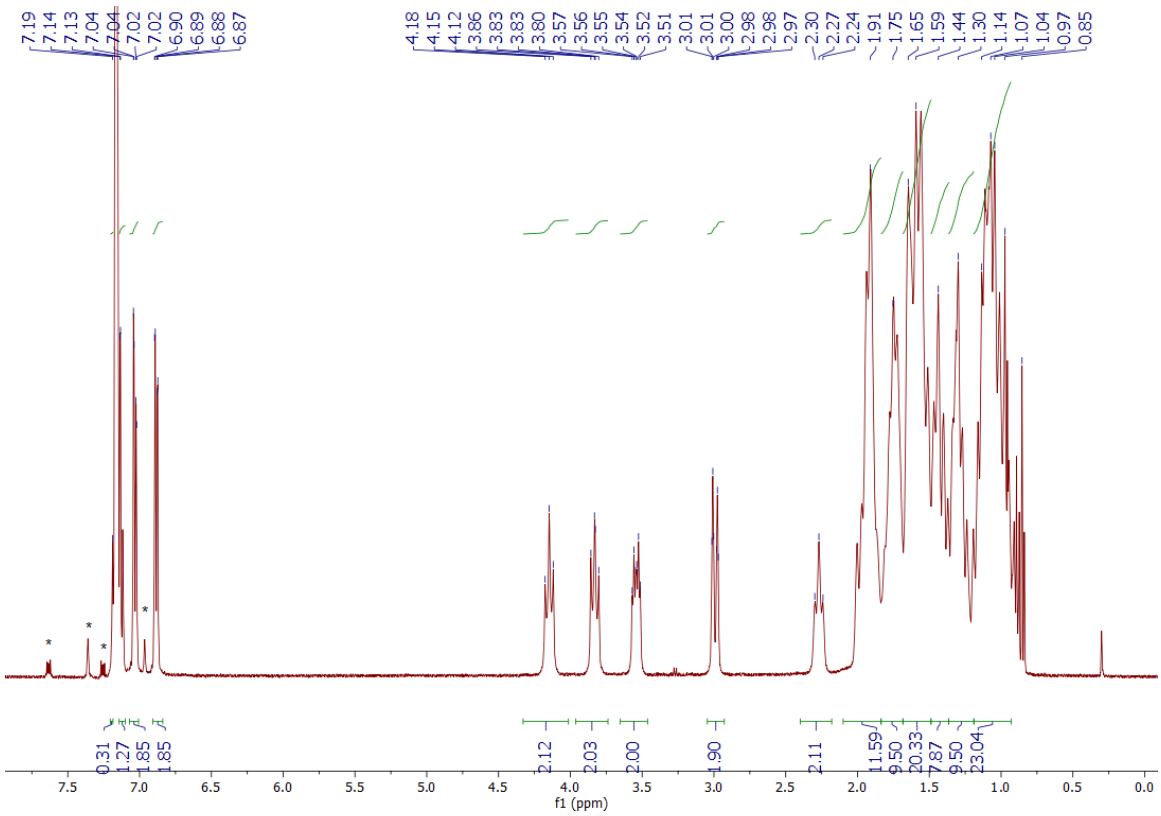

Figure 5.9: ^{1}HNMR spectrum of **17** in C_6D_6, 600MHz.

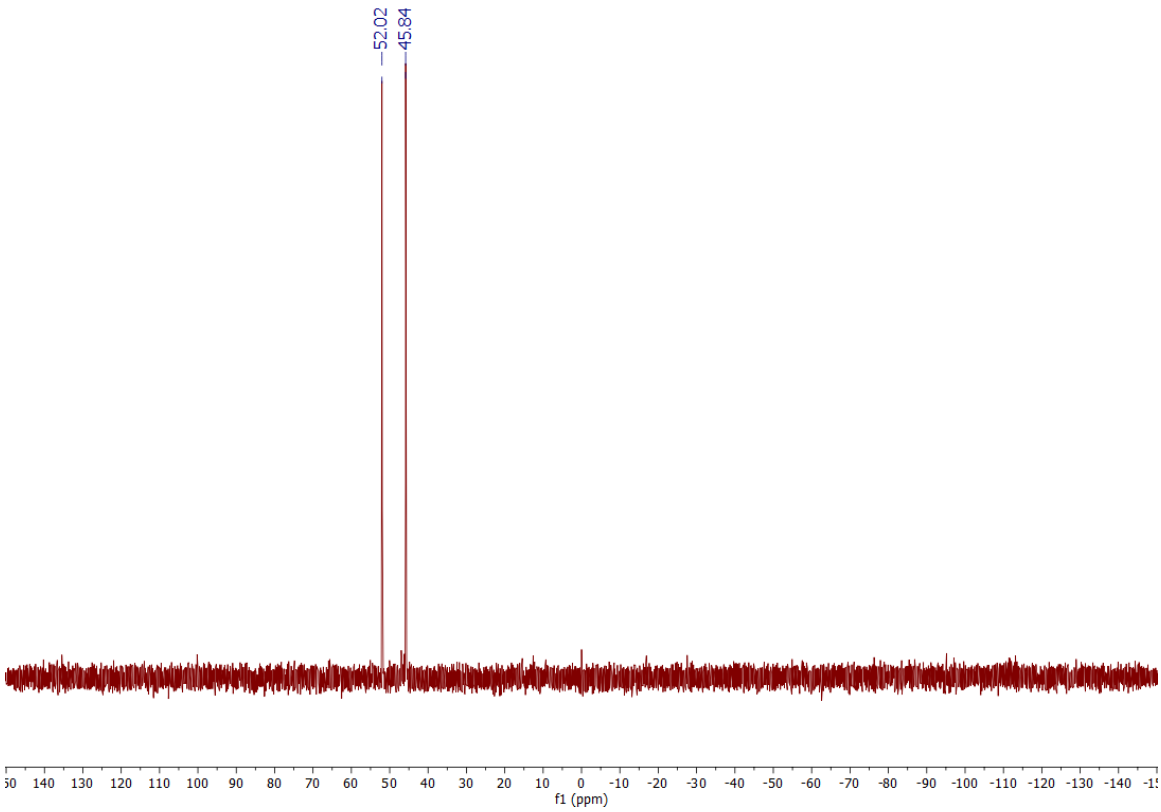

Figure 5.10: ^{31}PNMR spectrum of **17** in C_6D_6, 600MHz.

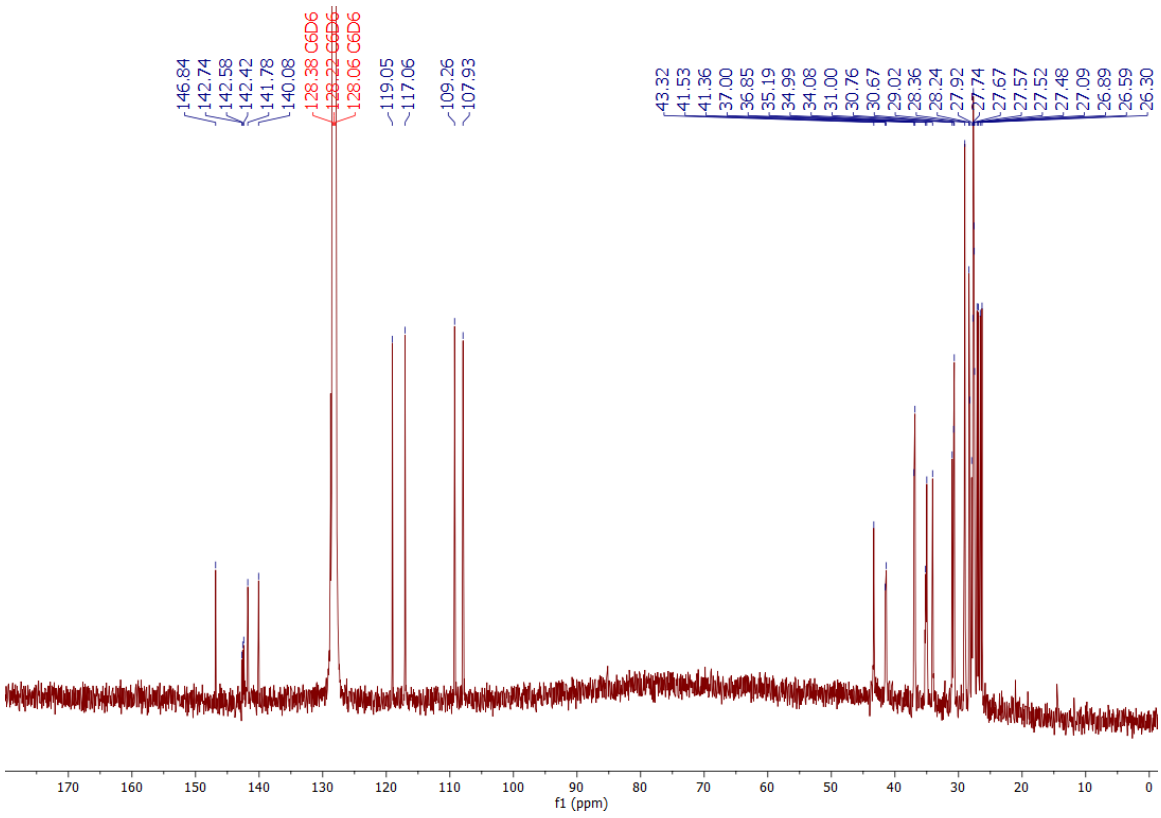

Figure 5.11: ^{13}CNMR spectrum of **17** in C_6D_6, 600MHz.

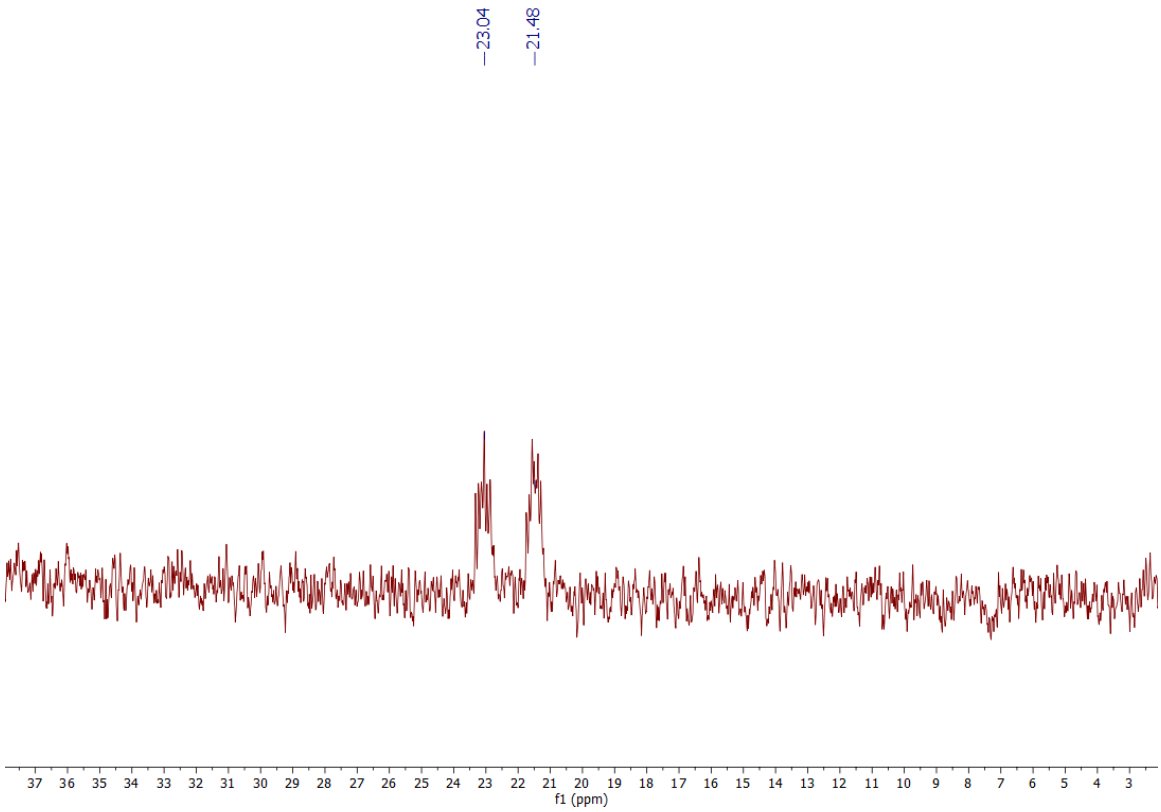

Figure 5.12: ^{29}SiNMR spectrum of **17** in C_6D_6, 600MHz.

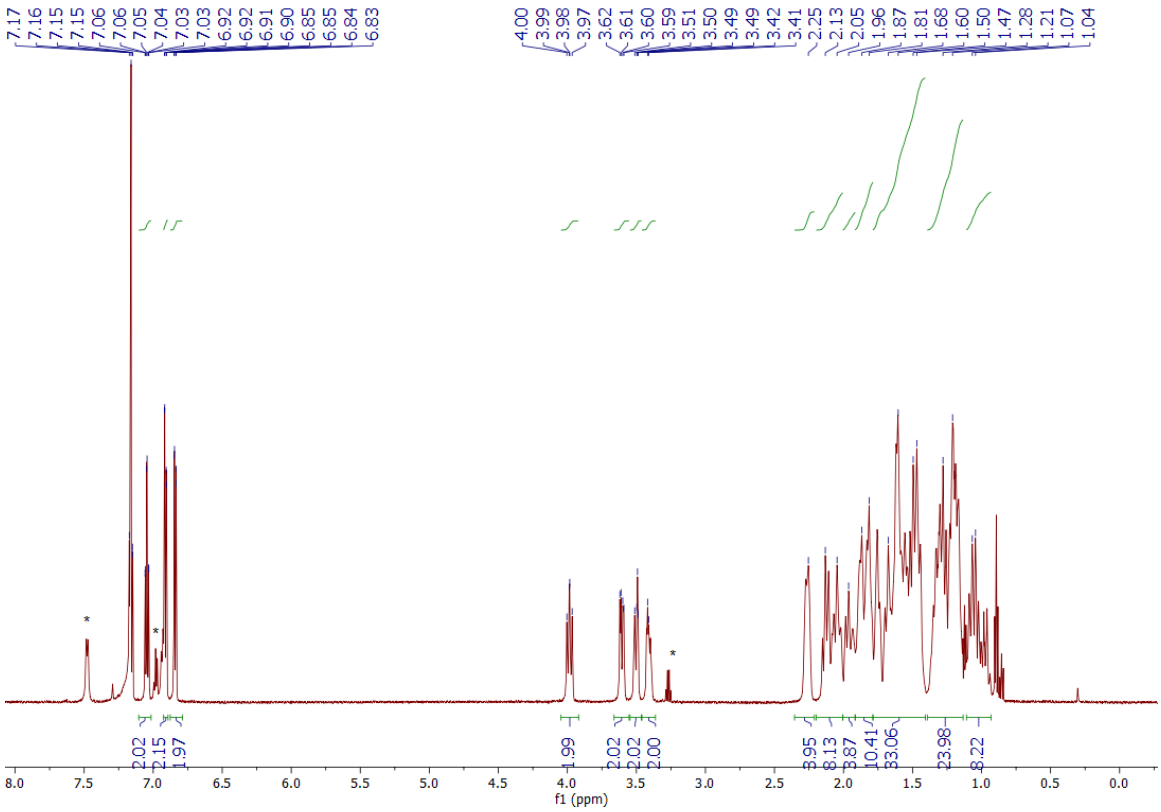

Figure 5.13: ^{1}HNMR spectrum of **18** in C_6D_6, 600MHz.

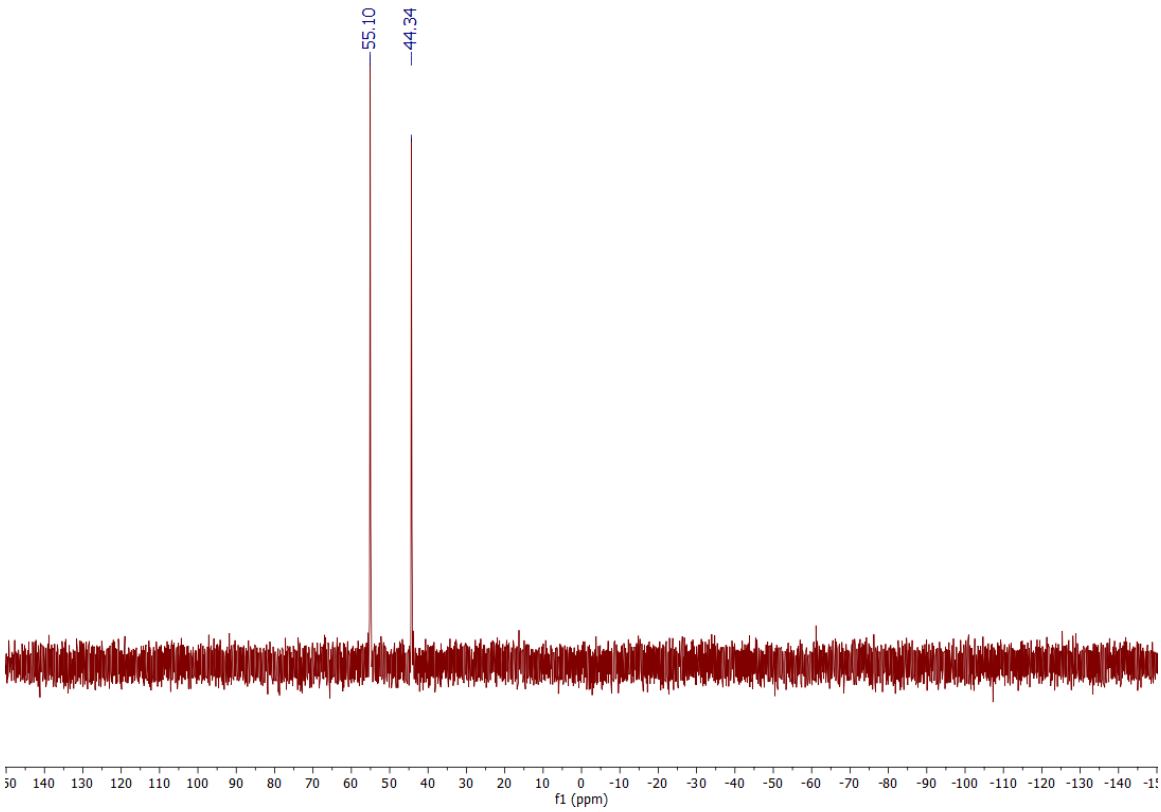

Figure 5.14: ^{31}PNMR spectrum of **18** in C_6D_6, 600MHz.

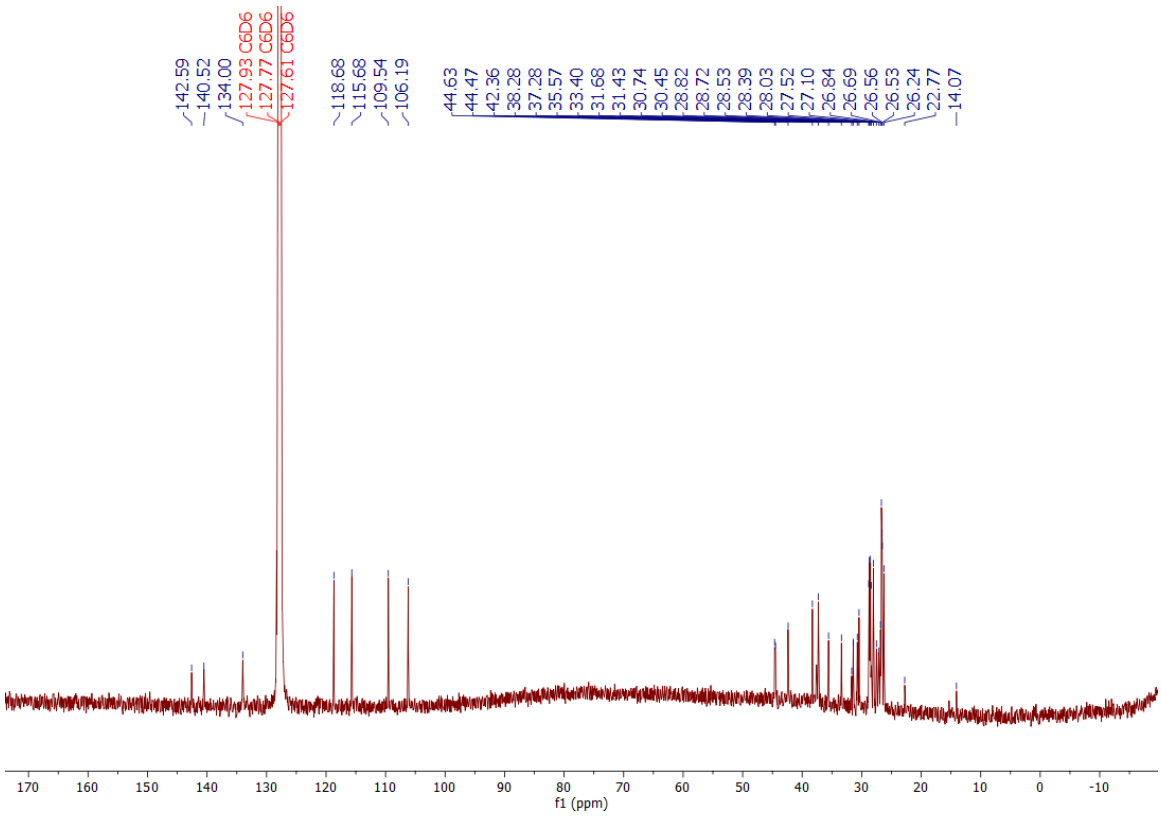

Figure 5.15: ^{13}CNMR spectrum of **18** in C_6D_6, 600MHz.

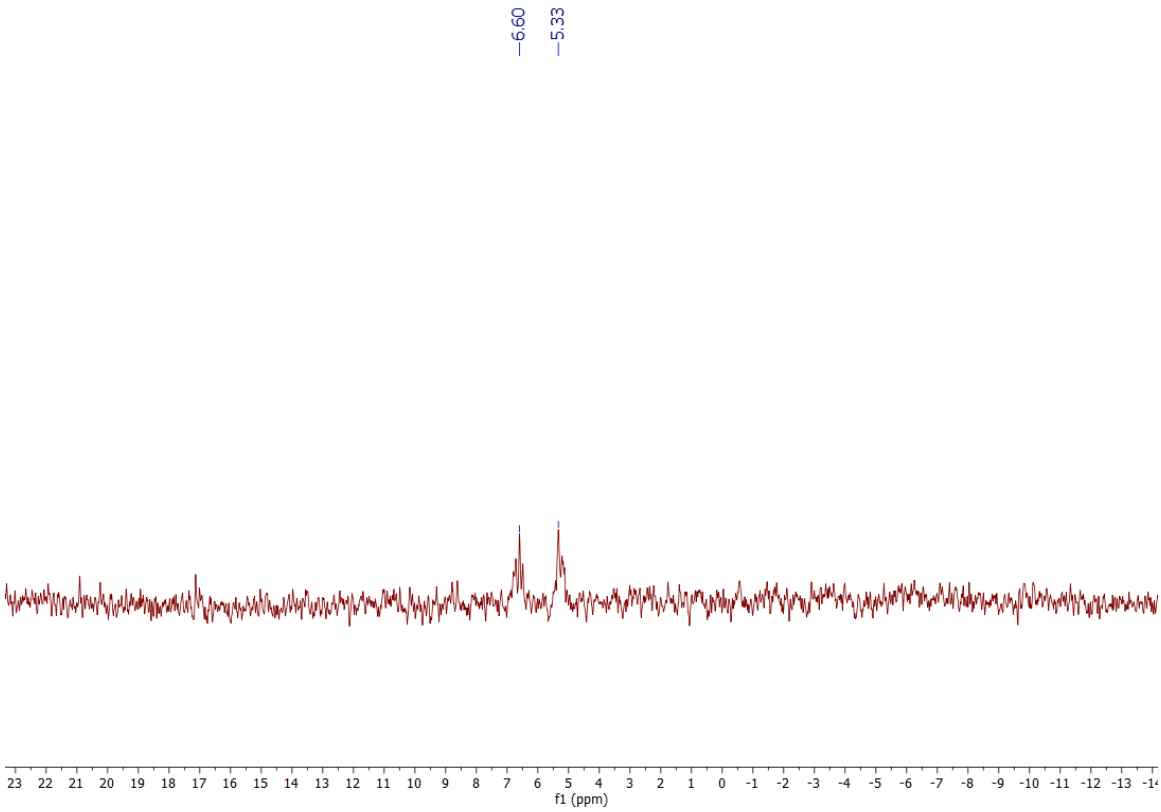

Figure 5.16: ^{29}SiNMR spectrum of **18** in C_6D_6, 600MHz.

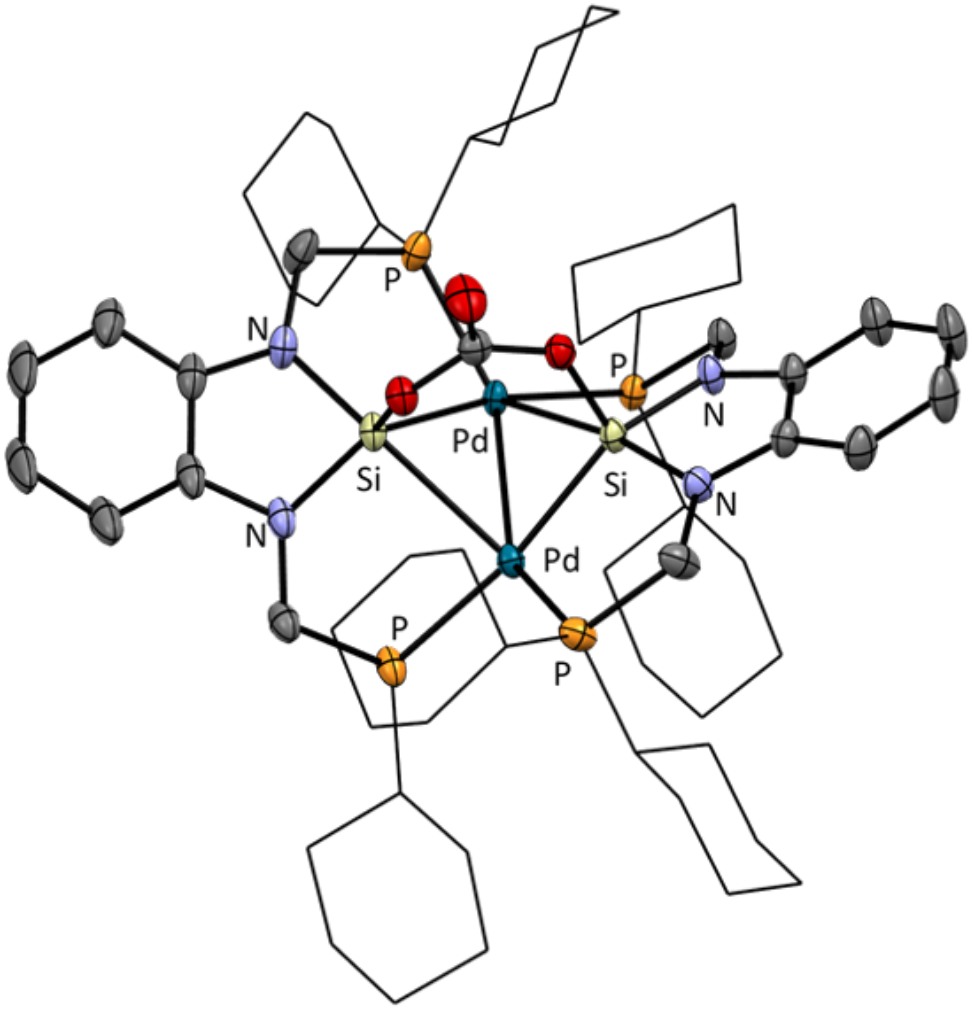

Figure 5.17: Thermal ellipsoid plot at 50% probability of the palladium silyl carbonate complex. **17**. Light orange, gray blue, aqua blue, red, light yellow and grey ellipsoids correspond to phosphorus, nitrogen, palladium, oxygen, silicon, and carbon atoms, respectively. Hydrogen atoms bonded to carbon have been omitted for clarity.